UNIVERSITY OF WARMIA AND MAZURY IN OLSZTYN

Technical Sciences

20(2) 2017

PUBLISHER UWM

OLSZTYN 2017

The Technical Sciences is indexed and abstracted in BazTech (http://baztech.icm.edu.pl) and in IC Journal Master List (http://journals.indexcopernicus.com)

The Journal is available in electronic form on the web sites
http://www.uwm.edu.pl/techsci (subpage Issues)
http://wydawnictwo.uwm.edu.pl (subpage Czytelnia)

The electronic edition is the primary version of the Journal

PL ISSN 1505-4675
e-ISNN 2083-4527

Address
ul. Jana Heweliusza 14
10-718 Olsztyn-Kortowo, Poland
tel.: +48 89 523 36 61
fax: +48 89 523 34 38
e-mail: wydawca@uwm.edu.pl

Ark. wyd. 7,4, ark. druk. 6,0, nakład 85 egz.
Druk – Zakład Poligraficzny UWM w Olsztynie
zam. nr 362

Contents

Technical Sciences, 2017, 20(2), 111–129

UNIWERSYTET WARMIŃSKO-MAZURSKI W OLSZTYNIE

Quarterly peer-reviewed scientific journal

ISSN 1505-4675

e-ISSN 2083-4527

TECHNICAL SCIENCES

Homepage: www.uwm.edu.pl/techsci/

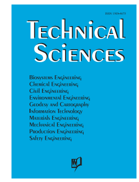

LIDAR AND GROUND PENETRATING RADAR DATA IN DETERMINING ROAD SURFACE CONDITIONS AND GEOLOGICAL CHARACTERISTICS OF UNSTABLE SOILS

***Artur Plichta*[1], *Adam Piasecki*[2]**

[1] Department of Surveying,
Poznan University of Technology
[2] Apex Geoservices Ltd.,
Gorey, Republic of Ireland

Received 31 March 2016, accepted 23 February 2017, available online 27 February 2017

Key words: road investment, laser scanning, geophysics, ground penetrating radar.

Abstract

Within the road investments the very important element determining repeatedly the success of the whole project is an adequate information about the characteristics of the site, its load capacity, stability and the possible impact of geological characteristics that may interfere with subsequent service life, not only for the road surface itself, but also for the surrounded objects. The surface is incessantly influenced by geological characteristics, determining its durability and functional usefulness. The main aim of this paper is to answer the question how by the usage of modern technics for obtaining data it is possible to find a link confirming the characteristics of land on which the specific road projects are supposed to be carried out, or where these projects have already been accomplished, concerning their requirements with high accuracy of location and also the stability and durability of the ground. This article makes also an attempt to answer not only the question how to identify the construction of road surface, but also how to locate underground cavities, created or influenced by the flow of water, or due to geological structures characterized as an inconsistent ground. The results were supported with geophysical researches using GPR method, and also data collected with laser scanners.

Correspondence: Artur Plichta, Zakład Geodezji, Instytut Inżynierii Lądowej, Wydział Budownictwa i Inżynierii Środowiska, Politechnika Poznańska, Piotrowo 5, 60-965 Poznań, phone: 61 6652419, e-mail: artur.plichta@put.poznan.pl

Introduction

Due to rapid development of remote methods of obtaining data for certain areas and the imagery from the aerial and satellite altitude, and also further development of digital technologies of their processing, integration and visualization, the possibilities of generating the various sets of results are still growing. Every day they are becoming more useful for creation of various databases and information systems, thereby causing a steady growth of range of their users. A completely new situation arose upon the occurrence of airborne laser scanning methods with very high resolution. In terms of basic performance parameters, these methods slowly but steadily and quite effectively find the right place in market applications (KURCZYŃSKI, WOLNIEWICZ 2002, 2005, KURCZYŃSKI 2005, Spaceimaging.com.). LIDAR data, obtained on the basis of the results of the scan area provide rich and real information about the interested areas, and it may be also a valuable component of information systems, and due to their combination of geophysical methods can create an interdisciplinary space for their adoption (HOWARD 2009, SANDERS 2000). An example of such use is the collection of data about the terrain model, which, together with geophysical data, provide information and evidence of existence of variety of geological structures, and thus the heterogeneous characteristics of the land. These techniques also give an opportunity to achieve information about changes and defects in the structural layers. In addition, the efficiency and quality of such kind of data made them one of the basic methods of assessing the structural condition of road surface, together with providing data about the terrain profiles and their physico-chemical composition. This in turn gives an opportunity to create geo-referenced GIS databases that allow to conduct multivariate and multi-criteria statistical and space analysis.

Aim of the study

The lack of adequate investment for safety in area of geological protection quite often results with the inappropriate quality parameters of the implemented project, both during construction stage and during its operating time. The overall aim of strengthening the subsoil is adjusting its parameters to the operational requirements of installed facilities. Before we determine the necessity of strengthening the ground we should acquire an adequate engineering-geological conditions introduced by the study of the inconsistent ground presented i.e. in the form of geological and engineering documentation of the interested area. As the contrast to typical practice, the range of research should also include investigation of layers properties usually and generally referred as unstable – these effectively always should be strengthened. Their physical and mechanical properties (before and after amplification) are, after all, not only the basis for the design or a choice of how to strengthen the ground, but also the choice of how to implement the entire project and its cost calculation (JERMOŁOWICZ 2013). Some of the European legislation in terms of designing routes imposes very specific conditions. If it is possible, it should be avoided to project driving routes through the areas of peat bogs, silt and other highly irrigated unstable soils. These are constantly wet, hard and poorly penetrable surfaces, covered with marsh and marshy-meadow plant communities, extremely valuable in terms of natural heritage. Apart from aspects of nature, the construction of roads through the area of wetlands always brings increased costs because of the use of very expensive engineering solutions. The costs of maintaining such a route are usually much higher than the route carried out in normal water and groundwater circumstances. The unstable grounds are not suitable for direct foundation of engineering structures. Road embankments, in turn, set on weak soil grounds may be affected by the significant deformations due to its compressibility and plastic deformations. Methods of road designing on unstable soils are extremely invasive and can be used only on land of low thickness and playing no significant role from the point of view of natural heritage. Setting roads over peat bogs and other wetlands or high ground water level should be preceded by a thorough examination of geological and geophysical terms (SISKOM, http://www.siskom.waw.pl).

Second approach taken in this article, is the quality checking of the correctness and "honesty" of the execution of the road surface, which must deal not only with the requirements of quality, but also must contain a cross-section of all (required by the regulations) layers of road, in addition with complying the project thicknesses. It is, or rather should be, in a way a control parameter, not only during the construction phase of the road, but also as a part of control measurements, giving a rise to the approval by the client the correctness of the execution of works. Lack of adequate quality information, both in respect of the surface layers and the land can seriously interfere with the subsequent service life of not only for the same road, but also for the objects within its course. The paper presents a case study how by the usage of modern techniques for obtaining data is it possible to find a link confirming the characteristics of land on which the specific road projects are supposed to be carried out or were already carried out, concerning their requirements in high accuracy in regards of location and also the stability and durability of the ground and secondly correctly identify the structure of the road surface. Both factors play a significant role in determining a possible opportunity to perform (in a given place) the planned investment or later to affect its durability. Complementing the LIDAR – detailed information together with the Ground

Penetrating Radar (GPR) technique data, we are able to get a reliable image of the geological structures and road layers running through the site, which allows, for example to choose correct location of future roads, or to indicate incorrect location of future structure.

Methods

Point cloud gathered with LiDAR gives information about the topography of the terrain, what is also the most common reason to use scanning technology. Analysis of LIDAR signal, reflecting from various surfaces, allows us to do more. Special raw data processing algorithms are able to determine the physical properties of these surfaces or their movement. When the surface is covered with objects partially transparent for the laser beam (eg. vegetation or snow) it can also gather information about their structure. The signal emitted during the measurement is partially disturbed by the atmosphere – in connection with the LIDAR data it also gives information on its characteristics. LIDAR has already found its place in optimizing the use of wind energy with for example control system (built by engineers from Stuttgart) that measures wind speed and direction before it reaches the turbine blades (Optic.org. The business of photonics. http://optics.org/news/3/6/16).

The base for correct interpretation of the obtained measurement data is the clarity of the resulting material. The raw data without proper processing cannot meet its role, if chosen (depending on the usage) accuracy is poor – the obtained image clarity is also not satisfying. It is necessary to consider each point obtained with LIDAR technology, so the capacity of data required equipment with high computing power. For example, in an area of about 100 hectares are collected more than 4 million laser points (in *.xyz format), of which nearly 2,5 million are points containing valuable information. Selection of the suitable GRID resolution is also very important in the process of interpretation. Figure 1 shows one of developed mosaic of established GRID with resolution of 0.5×0.5 m with usage of the "Surfer" software. It enables to distinguish changes in topography, providing the potential risks of instability and incoherence of the ground (Fig. 2). "Surfer" allows to create grids of values used to produce maps of land surface, three-dimensional representation of triplets (*XYZ*) type of data, which can be exported to several different formats (*.dxf, *.kmz, *.kml etc). It allows both creating simple maps of the baseline, as well as more complex spatial maps of the surface, also vector maps, relief shaded maps, map of single points, overlaid maps and others. The program has a rich computing capabilities, enabling an automatic calculation of surface projected data using *XY* plane, the curve surface, volumes and distance between points. Specialized procedures allow to generate cross-sections along an arbitrary broken line. The data is calculated by a regular grid of values, on the basis of which the special type of map can be created. Thanks to its capabilities this program is used to visualize data in various fields, including geophysical data and geography. The built-in wide range of interpolation methods for generating regular grid of values, allows to choose the optimal algorithm "gridding" to the nature of the input data (Gambit Centrum Oprogramowania i Szkoleń Sp. z o.o. http://www. gambit.net.pl).

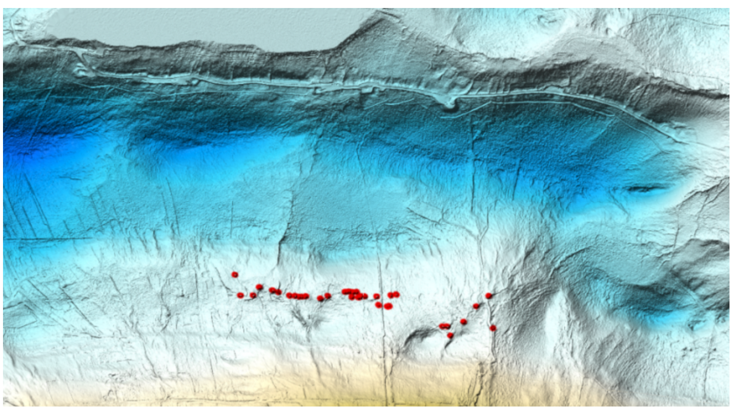

Fig. 1. The GRID of 0.5m size with the presentation of swallow holes (red); mosaics made using "Surfer"

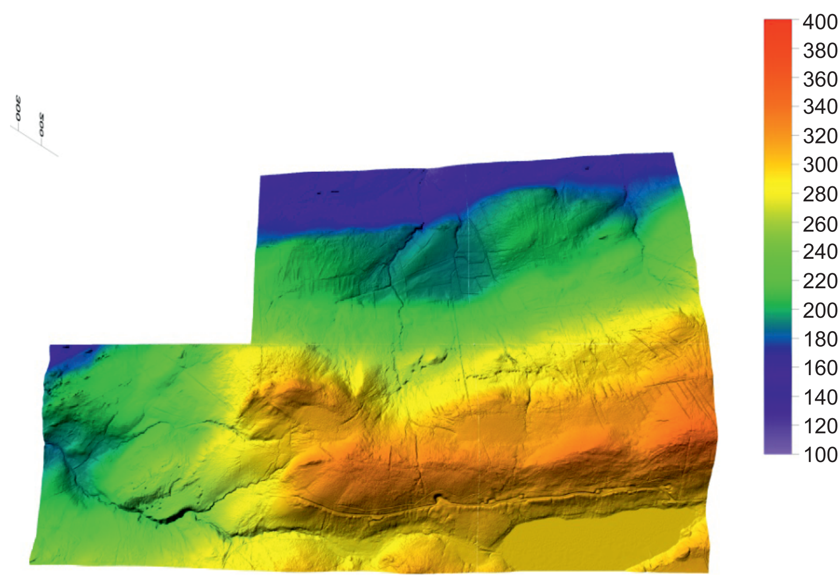

Fig. 2. The range of colors for the height of the tested terrain (in meters)

Visible to the naked eye, regular depressions in the ground can foretell the location of underground space, created or by the flow of water, or due to geological structures characterizing the ground as inconsistent. The confirmation of the assumptions can be supported by geophysical investigation of land using three methods:

– Electrical Resistivity Tomography – ERT,
– GPR method,
– Seismic method.

Based on data obtained from laser scanning, some methods of land survey were selected to confirm suspicions of the content and carrying capacity of land for road construction. Finding the most appropriate methodology is the basis for all research, primarily to determine exactly what type of investigations should be taken into account for economic reasons, as well as external factors (accuracy, size of objects etc.). After an appropriate analysis, some of the methods can be eliminated in order to provide very accurate results without unexpected time investments.

During determining geotechnical conditions of foundations of linear objects such as roads and railways it is imperative to reach a compromise between the amount of field research and the accuracy of geophysical investigation. GPR technique is used for instance in continuous monitoring of the road surface condition or railway subgrade (Geopartner. http://www.geopartner.pl). An important advantage of geophysical survey is non-invasive cappability of determining structures invisible to the eye, sometimes assisted with geological surveys (i.e. trial pits, borehole drilling) confirming data obtained from field measurements. In case of linear objects related to public transport on-going work do not cause any disruption to traffic.

Data obtained with GPR give the ability to identify sub-surface structures, providing information about the uniformity of the structural layers and geology. Proper identification of the layer types ensures quality of the assessment of objects being under investigation and underlain soils. GPR provides continuous information about the type of surface structure, thicknesses of layers, homogeneous sections and existing changes and anomalies (MASER, SCULLION 1991).

The principle of GPR is based on the generation of electromagnetic wave and sending it into tested ground, rock or material. This is accomplished by transmitting antenna (Tx) that generates a signal at a given frequency (<20 ns). The wave passes through objects, where is refracted and reflected of the surface, but encountering objects, infrastructure or other heterogeneities the wave is being diffused. Some of the energy carried by these waves is transmitted to greater and greater depths, while some of the energy is reflected back towards the surface receiver (Rx) whenever a contrast in dielectric properties is encountered. Both antennas are connected to the central unit, which manages the generation of wave and recording its reflected digital signal. The penetration depth achievable depends on the nature of material (especially its electrical conductivity), the location of the water table and on the frequency of transmitted wave. Researches at Lund University in Sweden by ULRIKSEN (1980, 1982, 1983), BJELM, ULRIKSEN (1980) and BJELM (1980) investigated such factors as the effect of frequency of the transmitted wave, the transmission velocity and the technique used for moving the antenna over the ground on the measured results. This work also showed that, not only the material layer thickness could be estimated accurately but also some information about the material situated beneath can be obtained. The receiver measures the variation in the strength of the reflected signals with time (Figs. 3, 4). The resulting profile is called a "scan" and is a one-dimensional representation of the subsurface beneath the antenna. The example is visible on Figures 5 and 6 (RSK Geophysics Mapping the unscene. http://www.environmental-geophysics.co.uk).

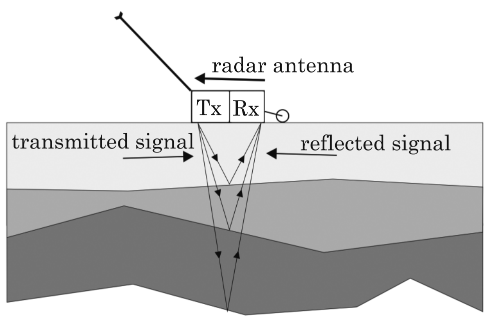

Fig. 3. GPR Principles
Source: RSK Geophysics Mapping the unscene. http://www.environmental-geophysics.co.uk.

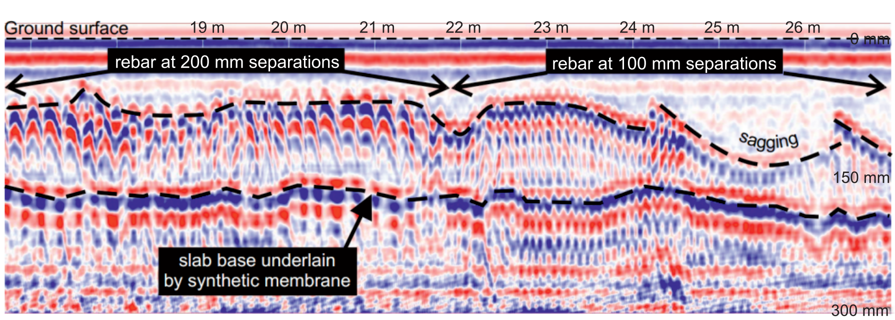

Fig. 4. An example of high frequency (1.5 GHz) radar data collected over a concrete slab
Source: RSK Geophysics Mapping the unscene. http://www.environmental-geophysics.co.uk.

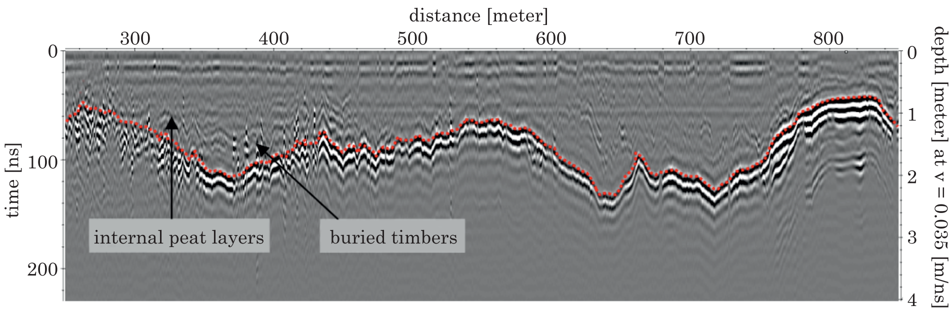

Fig. 5. Example of GPR data: processed section
Source: Near Surface 2009 – 15th European Meeting of Environmental and Engineering Geophysics.

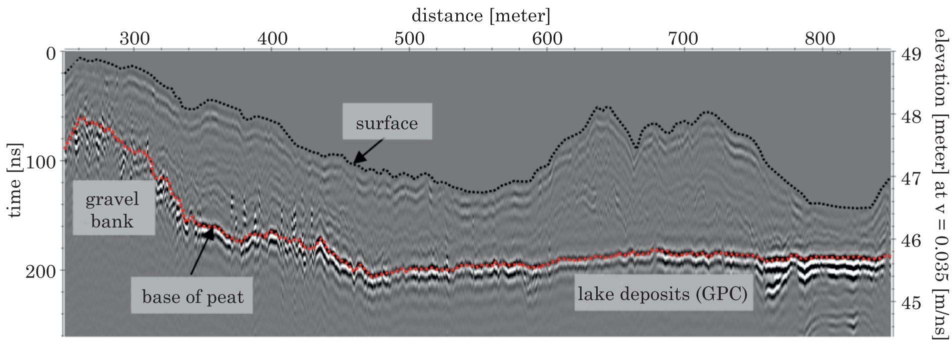

Fig. 6. Example of GPR data: topographically corrected section
Source: Near Surface 2009 – 15th European Meeting of Environmental and Engineering Geophysics.

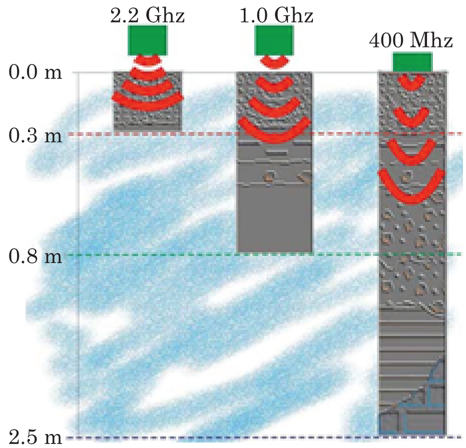

Fig. 7. The range of terrain penetration depending on the frequency of the antenna
Source: SUDYKA (2006).

The accuracy and range of a GPR method depends primarily on the frequency of the emitted electromagnetic signal that ranges from 10 MHz to several GHz. This frequency range causes that the GPR method is provided from a few centimeters to tens of meters (Fig. 7). While the resolution, which means the expected vertical accuracy tests varies from a few millimeters to a few meters. Resolution and coverage dependency is inversely proportional, which means that the higher the frequency of the generated wave is the better resolution is expected, but the range is decreasing (GeoSpectrum. Nowoczesne techniki badawcze. http://www.geospectrum.pl/).

Tests

As part of the research the chosen section of road with a length of 3600 m, running along the geologically diverse area, located on the borders of Northern Ireland was analyzed (Fig. 8).

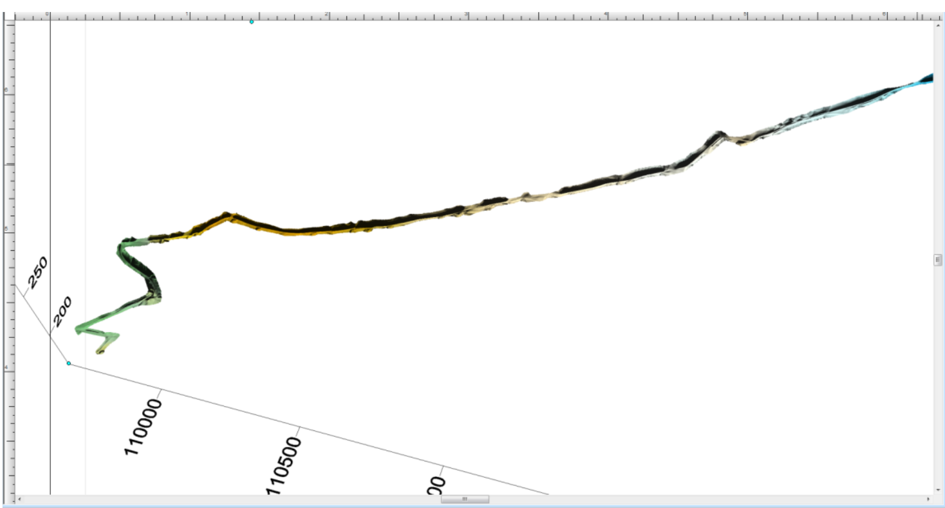

Fig. 8. Analyzed section of the road, cut out from a point cloud using Surfer application

Driving and utility parameters of described road section have significantly degraded. Clearly visible are the structural damages in the form of sinks and surface subsidence, as well as the linear and transverse cracking. In the presented case the proposal provides analysis of the road subsurface intended for modernization, as well as areas in its surroundings, where variety of structures could be built in the future. An investigation has been undertaken to explain the current situation, with the assumption that responsible for the road surface damage are geological structures running under the road, as well as inadequate technical parameters of the road layers, including their layout and thickness. The study was based on data obtained from laser scanning, supplemented by a GPR survey of the investigated road section.

As the first stage of work LIDAR data was used in order to create three-dimensional terrain model, which allowed the insight into the shape of the surface of the considered section. At a later stage LIDAR data was processed using the "Surfer" software. LIDAR data was used to assign an altitude for each one of thousands of the analyzed with GPR method points. Prior to survey appropriate density of readings should be chosen as well as the interval between signals sent by the antenna into analyzed area. It was agreed that for analyzed section the required resolution should be equal to 10 mm, what meant that study of the considered area in a straight line would be investigated at that given density. Antenna was placed under the vehicle (Toyota HiLux 4×4) and set up for simultaneous transmission and collection of reflected signal. The vehicle has been appropriately modified so that at a speed of (not exceeding) 30 km/h the analysis could be carried out smoothly, without requirement for stopping on the road and blocking any of ongoing traffic. Each of the antennas used for the survey was part of Swedish MAL3 X3M™ SYSTEM, which connected with the rear wheel of the vehicle, after proper calibration, allowed to run a survey with a given density (Figs. 9, 10). The X3M is an integrated radar control unit, fitted directly on a shielded antenna and powered externally. No antenna cable was required since the control unit was

Fig. 9. 400 MHz MAL3 X3M™ SYSTEM antenna used during the measurement

Fig. 10. Custom modified vehicle allowing GPR measurements without stopping road traffic at analyzed road sections

mounted directly on top of the MAL3 shielded antenna (in our research up to 1.5 GHz). It communicated directly with the XV11 GPR Monitor that was running GroundVision2 acquisitioning software (Fig. 11). MAL3 allows to gather information from a range of depths (base and sub-base thicknesses) for the entire road construction, for example pavement, supportive layers and base layers, including also evaluations of the asphalt thickness (MAL3. World Leading Ground Radar Solutions. http://www.malagpr.com.au).

Fig. 11. XV11 GPR Monitor with results of the measurement

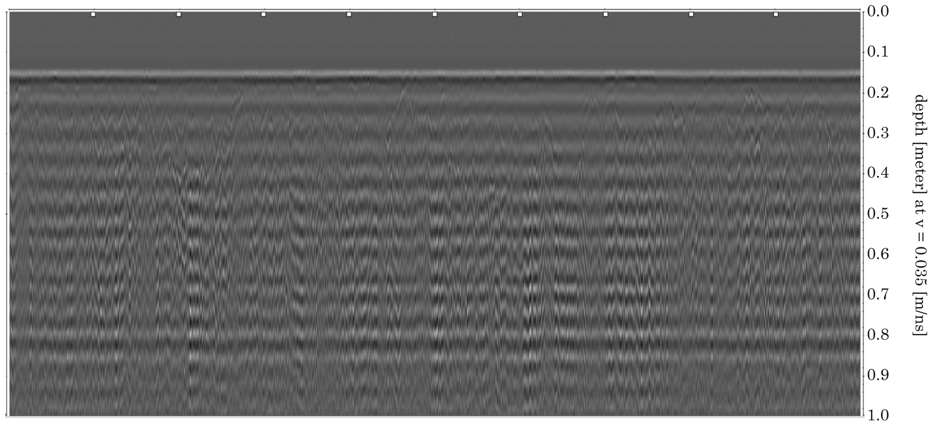

Fig. 12. Raw data in *.DAT format from 400MHz antenna, without implemented filters which allow proper interpretation

For the section of 3,600 m 360,000 signals were sent, each one of them during processing received *X* and *Y* coordinates, together with the elevation. Each analyzed depth – i.e. layer of bitumen or thickness of certain surface had exactly associated *XYZ* value. GPR work is now usually linked to an accurate GPS system which allows spatial relocation to GPS co-ordinates as well as providing topographic information. For the purpose of determining the exact location and correlation between LIDAR data and carried out measurements, on the investigated sections, GPS base stations at distances of 200 m have been placed, measured using GPS Trimble Geo7x with the accuracy of 1 cm. Thanks to laser scanning precision in determining road surface changes or specific characteristics of the analyzed area, allows very accurate indication of road defects that are not visible to the eye ball. Antennas which have been used for the measurement of the section have different frequencies, ranging from 100 MHz up to 1.5 GHz. The lower frequency values allow the analysis of deeper layers of road surface, however resolution decreases with depth, and the possibilities of interpretation are dependent on environmental conditions as well as the characteristics of the terrain. The antenna with a frequency of 1.5 GHz enables very thorough and accurate investigation of shallow surface layers, thus reducing the frequency decreases the resolution of the analyzed object. The research was carried out by analyzing the same road section with each antenna separately, stopping only at the base stations, for which coordinates have been measured earlier. We handled and interpreted all data using MALÅ ObjectMapper software. MALÅ ObjectMapper includes the visualization of several radar profiles simultaneously, robust filtering, capabilities including time gain, band pass, background removal and a report editor to mark and visualize objects on a map. Several different types of markers can be defined to illustrate the position of pipes, single objects etc. Built in data collection management in the MALÅ XV11 GPR Monitor that was used in the experiment allowed to select the base stations, which were presented in the form of white squares on the upper part of Figure 7, that represented the raw data from survey with 400 MHz antenna. Afterwards (in ObjectMapper software) it was automatically adjusted to the baseline and thus aligned for profile to profile target picking.

Results

Before undertaking the process of interpretation the appropriate filters should be applied, which affect the "readability" of data obtained from the field of measurements (IBDiM 2010). A significant factor is the experience of person responsible for work with the data, lack of knowledge of the rules related to reflecting and refraction of waves could have a negative impact on the interpretation results. It is worth remembering that the value of the analyzed data becomes increasingly important in places where the location due to construction defects, or a complicated order of geological layers is an extremely important factor in determining the further decision-making processes. The interpretation process was extremely time-consuming, any breakdown in the image of such high detailed data is linked with the existing situation in the field. The interpretation process is unfortunately not automated – all kinds of changes in the road surface are "outlined" by the interpreter using the mouse. Of course, each of the layers is peeled and marked individually, colors are assigned for easier interpretation of the results, thanks to the perfect matching filters the image becomes clear (Fig. 13).

Interpreted data have been converted to graphs created in spreadsheets using written macros, appropriately modified in a way that fully illustrates the developed interpretation. The determining factor in this case was the appropriate collection and tabulation alignment of measurement figures, so that the result of study is clear, and the interpreter has the ability to see requested data (Fig. 14). It has become apparent that a great deal of information on the sub-peat soils can be determined from the GPR data. It is possible to determine the type of sub-peat deposit and depositional history of an area from the assessment of the GPR response. Different reflection characteristics from within the peat layers can also provide information on the origin and composition of the peat layers.

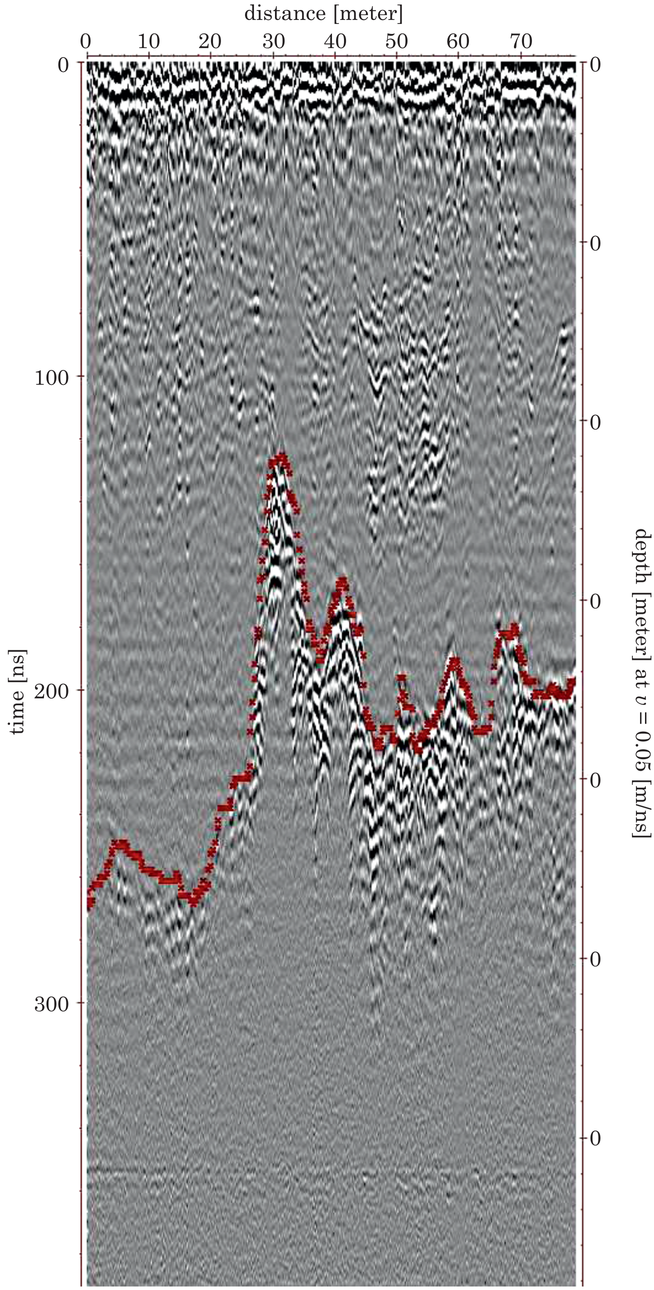

Fig. 13. Data from 400 MHz antenna presenting a 80 m section of road, after applying filters and processes of relocation, with sketched interpretation of Peat Thickness

Sample pavement construction summary table

Chainager	Coordinates			Bituminous material			Subbase material			Peat subgrade			Section
Start (m)	end (m)	easting	northing	min. depth [m]	max depth [m]	avg. depth [m]	min. depth [m]	max depth [m]	avg. depth [m]	min. thickness [m]	max thickness [m]	avg. thickness [m]	
0	125	123456	370810	0.107	0.224	0.167	0.398	0.998	0.689	0.16	2.06	1.27	Section A
125	217.5	123457	370811	0.111	0.226	0.198	0.313	0.521	0.401	–	–	–	Section B
217.5	281	123458	370812	0.084	0.171	0.133	0.313	0.474	0.395				Section B
281	467	123459	370813	0.056	0.137	0.095	0.276	0.499	0.387				Section B
467	600	123460	370814	0.058	0.165	0.084	0.272	0.554	0.346				Section B
600	644.5	123461	370815	0.061	0.277	0.177	0.363	1.718	0.594	0	0.74	0.4	Section C
644.5	875	123462	370816	0.039	0.184	0.096	0.328	0.633	0.505				Section C
875	1024.5	123463	370817	0.108	9.197	0.141	0.425	0.722	0.569	0.13	0.83	0.42	Section D
1024.5	1100	123464	370818	0.098	0.192	0.131	0.522	0.831	0.677	0.31	1.72	1.02	Section E

Fig. 14. Spreadsheet view with evolving data

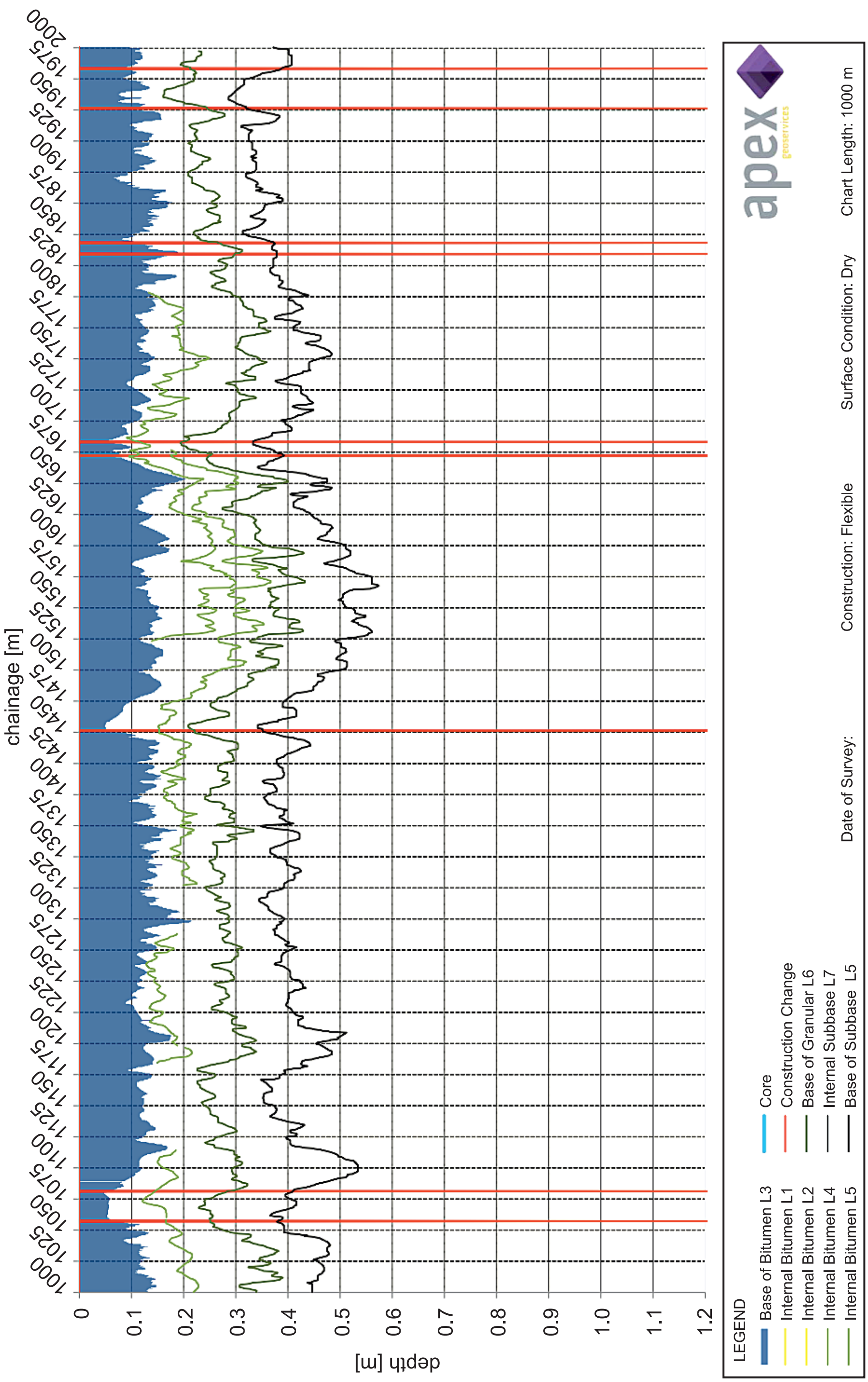

Fig. 15. Graph created with excel macros based on data obtained from the measurement and interpretation process for considered section

Above listed part of final report of surveyed section presenting part of road with selected layers of bitumen (Fig. 15) is also enclosed the aerial view of road where investigated was peat thickness with cross-section for the same area (Figs. 16, 17) – elevation data taken form LIDAR.

Fig. 16. Aerial imagery with overlaid layer of Peat Thickness created in "Surfer" based on GPR Investigation data

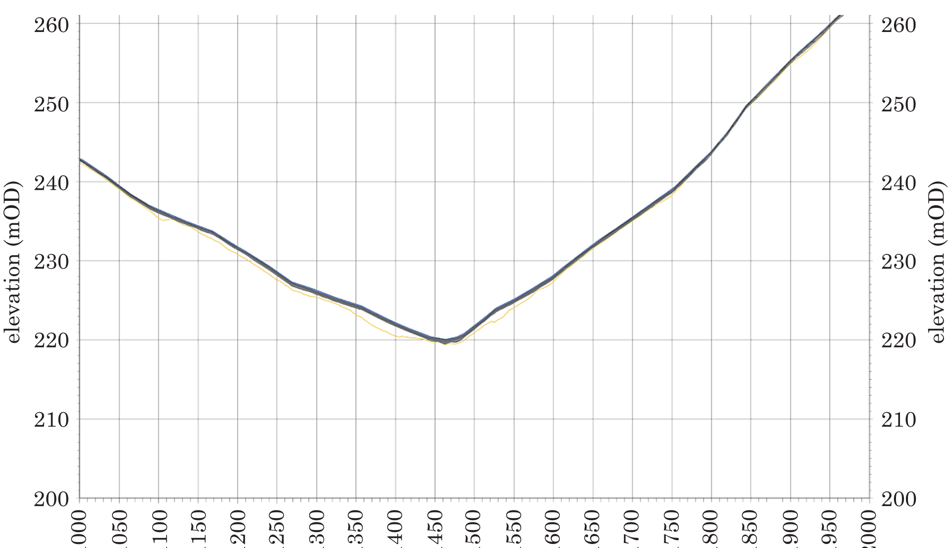

Fig. 17. Cross-section of considered area

Conclusion

Radar technology presented and demonstrated in this article, mainly because of its effectiveness and quality of obtained data, makes it one of the main methods of assessing the structural condition of road surfaces now and in time of near future – especially as currently the determinant of use of specific technologies is the cost factor. Thus, searching for cost-effective and efficient technologies for renovation of the existing road surface by GPR methods seems to be indispensable. The results of research and analysis are based on achievable results, enabling a thorough and honest assessment not only of structural, but also geological layers. GPR measurements should be widely used not only as a complementary element of developed projects, but most of all from the point of i.e. confirmation of structure of newly made roads prior to their release to public. An important advantage of radar systems is their effectiveness, performance and relatively low cost of the research. No interference with the road surface and speed of the measurements cause that radar techniques to be used in a number of so-called measuring circuits, allowing accurate identification of the surface structure also in cross-sections. In addition to the standard information about layer thicknesses it is also possible to assess other parameters of construction such as i.e. layers connection status and their homogeneity. Main factor influencing negatively in the considered solution is the fact that despite of the advanced technology and high quality of the data, problem of automatic processing and interpretation of received data is not yet fully solved. Still, the vast majority of processing and interpretation of the data must be controlled by an experienced engineer. Nevertheless, it is hoped that this new technology will gain a proper place in the area of engineering applications.

References

BJELM L. 1980. *Geological interpretation with subsurface interface radar in peat lands*. 6th International Congress, Duluth, Minnesota.

BJELM L., ULRIKSEN P. 1980. *System for peatland survey by radar. Final Stage*. Faculty of Engineering, Engineering Geology, p. 104

Council Directive 92/43/EEC on the conservation of natural habitats and of wild fauna and flora, 21 May 1992.

DANIELS D.J. 2004. *Ground-Penetrating Radar*. The Institute of Electrical Engineers London.

EN 1997-1: 2004. *European standard "Eurocode 7 – Geotechnical design"*.

Gambit Centrum Oprogramowania i Szkoleń Sp. z o.o. http://www. gambit.net.pl.

Geopartner. http://www.geopartner.pl/.

GeoSpectrum. Nowoczesne techniki badawcze. http://www.geospectrum.pl/.

HOWARD B., PARKER CH. 2009. *LiDAR – So Much More Than A Pretty Picture. An Introduction to the Analytical Capabilities of Topographic and Hydrographic LiDAR Survey Data*. Sarasota.

JERMOŁOWICZ P. 2013. *Wykonywanie robót ziemnych na gruntach słabych i wysadzinowych*. Materiały szkoleniowe. Pokrzywna.

MALÅ. World Leading Ground Radar Solutions. http://www.malagpr.com.au/.

MASER K., SCULLION T. 1991. *Automated detection of pavement layer thicknesses and subsurface moisture using ground penetrating radar*. Transport Research Board.

Ocena geotechniczna podłoża gruntowego techniką radarową ze szczególnym uwzględnieniem stanu hydrologicznego podłoża gruntowego. 2010. Instytut Badawczy Dróg i Mostów, Zakład Diagnostyki Nawierzchni, Warszawa.

Optic.org. The business of photonics. http://optics.org/news/3/6/16.

PN-EN 1997-1:2008. *Building ground – Direct foundation structures – Static calculations and design*.

PNS-02205: 1998. *Road car – Earthworks – Requirements and test methods*.

Regulation of the Minister of Transport and Maritime Economy on the determination of the geotechnical conditions of foundation of buildings, 25 April 2012, Journal of Laws 2012.463.

RockWare. Earth Science and GIS Software. http://www.rockware.com.

RSK Geophysics Mapping the unscene. http://www.environmental-geophysics.co.uk/.

SANDERS J.A., WILKERSON T.D., SCHWEMMER G.K., MILLER D.O., GUERRA D., MOODY S.E. 2000. *Comparison of Two Lidar Methods of Wind Measurement by Cloud Tracking*. http://digitalcommons.usu.edu/cgi/viewcontent.cgi?article=1277&context=spacegrant.

SEREN S., HINTERLEITNER A., LÖCKER K., MELICHAR P., NEUBAUER W. 2009. *High Definition GPR Surveys at the Roman Town Flavia Solva*. European Association of Geoscientists and Engineers, Near Surface 2009 – 15th European Meeting of Environmental and Engineering Geophysics. Dublin, Ireland.

SISKOM. Stowarzyszenie Integracji Stołecznej Komunikacji. http://www.siskom.waw.pl/

Spaceimaging.com. Directiv Authorized Dealer. http://www.spaceimaging.com/

SUDYKA J. 2006. *Technika radarowa w drogownictwie – nowa jakość w ocenie konstrukcji nawierzchni*. Polski Kongres Drogowy.

ULRIKSEN P 1980. *Investigation of peat thickness with Radar*. 6th International Peat Congress, Professional Paper of the Lund Institute of Technology, Department of Engineering Geology, Lund, Sweden.

ULRIKSEN P. 1982. *Application of impulse radar to civil engineering*. PhD Thesis, Lund University of Technology.

ULRIKSEN P. 1983. *Some applications of impulse radar*. Geoexploration, 21: 289–289.

Technical Sciences, 2017, 20(2), 131–147

Quarterly peer-reviewed scientific journal
ISSN 1505-4675
e-ISSN 2083-4527
TECHNICAL SCIENCES
Homepage: www.uwm.edu.pl/techsci/

COMPARING SAT-BASED BOUNDED MODEL CHECKING RTECTL AND ECTL PROPERTIES

Agnieszka M. Zbrzezny

Institute of Mathematics and Computer Science
Jan Długosz University in Częstochowa

Received 24 October 2016, accepted 2 March 2017, available online 21 March 2017

Key words: SAT-based bounded model checking, ECTL, RTECTL, translation.

Abstract

We compare two SAT-based bounded model checking algorithms for the properties expressed in the existential fragment of a soft real-time computation tree logic (RTECTL) and in the existential fragment of computation tree logic (ECTL). To this end, we use the generic pipeline paradigm (GPP) and the train controller system (TC), the classic concurrency problems, which we formalise by means of a finite transition system. We consider several properties of the problems that can be expressed in both RTECTL and ECTL, and we present the performance evaluation of the mentioned bounded model checking methods by means of the running time and the memory used.

Introduction

The problem of model checking (CLARKE et al. 1999) is to check automatically whether a structure M defines a model for a modal (temporal, epistemic, etc.) formula α. The practical applicability of model checking is strongly limited by the state explosion problem, which means that the number of model states grows exponentially in the size of the system representation. To avoid this problem a number of state reduction techniques and symbolic model checking approaches have been developed, among others (BRYANT 1986, CLARKE et al. 1986, LOMUSCIO et al. 2010, MCMILLAN 1993). The SAT-based bounded model

Correspondence: Agnieszka Zbrzezny, Instytut Matematyki i Informatyki, Wydział Matematyczno-Przyrodniczy, Akademia im. Jana Długosza, 42-200 Częstochowa, al. Armii Krajowej 13/15, phone: 34 361 49 18, e-mail: aga.zbrzezny@gmail.com

checking (SAT-BMC) is one of the symbolic model checking technique designed for finding witnesses for existential properties or counterexamples for universal properties. The first BMC method was proposed in (BIERE et al. 1999), and it was designed for linear time properties. Next, in (PENCZEK et al. 2002) the method has been extended to handle branching time properties. Further extensions of the SAT-based BMC method for real-time systems and multi-agent systems can be found, among others, in PENCZEK and LOMUSCIO (2003), WOŹNA and ZBRZEZNY (2004).

The existential fragment of the computation tree logic (ECTL) (PENCZEK et al. 2002) is a formalism that allow for specification of properties such as: "there is a computation such that α will eventually request", or "there is a computation such that α will never be true", but it is impossible to directly express bounded properties like for example "there is a computation such that α will be true in less than 15 unit time", or "there is a computation such that α will never be averted after 15 unit time", or "there is a computation such that α will always be averted between 10 and 20 unit time". Note however that this bounded properties can be formalised in ECTL by using nested applications of the next state operators, but the resulting ECTL formulae can be very complicated and problematic to work with. The existential fragment of the soft real-time CTL (RTECTL) (EMERSON et al. 1992) defeats this restriction by introducing time-bounded temporal operators, and it supplies a much more compact and convenient way of expressing time-bounded properties. The purpose of this paper is to compare the SAT-based BMC of RTECTL (WOŹNA-SZCZEŚNIAK et al. 2011) properties and the SAT-based BMC of equivalent ECTL (ZBRZEZNY 2008) properties and to present a correct and complete translation from RTECTL to ECTL.

We have expected that the BMC for RTECTL would give better performance than the BMC for the ECTL formulae that result from the translation of RTECTL formulae. This is because the size of these ECTL formulae is exponential in the size of the original RTECTL formulae. However, our experiments have shown that for certain RTECTL formulae BMC can be less effective than BMC for their translation into ECTL formulae. These are the formulae for which the interval at the operator **EG** is finite: then after the translation to ECTL, **EG** operator disappears, and there are more paths, but they are much shorter.

Preliminaries

In this section we first define a Transition System (TS), then we recall syntax and semantics of two logics ECTL and RTECTL.

Transition system. The transition system (BAIER, KATOEN 2008) (also called a model) is a tuple $M = (S, Act, \rightarrow, s^0, AP, L)$ where: S is a set of states, Act is a set of actions, $\rightarrow \subseteq S \times Act \times S$ is a transition relation, $s^0 \subseteq S$ is the initial state, AP is a set of atomic propositions, and L: $S \rightarrow 2^{AP}$ is a labelling function. The transition system is called finite if S, Act and AP are finite. For convenience, we write $s \xrightarrow{\sigma} s'$ instead of $(s, \sigma, s') \in \rightarrow$. Moreover, we write $s \rightarrow s'$ if $s \xrightarrow{\sigma} s'$, or some $\sigma \in Act$.

From now on we assume that a considered model has no terminal states, i.e. for every $s \in S$ there exist $s' \in S$ such that $s \rightarrow s'$. The set of all natural numbers is denoted by N, and the set of all positive natural numbers by N_+. A path in M is an infinite sequence $\pi = (s_0, s_1, ...)$ of states such that $s_i \rightarrow s_{i+1}$ for each $i \in N$. For a path $\pi = (s_0, s_1, ...)$ and $i \in N$, the i-th state of π is defined as $\pi(i)$. The i-th prefix of π is defined as $\pi[...i] = (s_0, s_1, ..., s_i)$, and the i-th suffix of π, denoted by π^i, is defined as $\pi^i = (s_i, s_{i+1}, ...)$. Note that if π is a path in M then the suffix π^i is also a path in M. By $\Pi(s)$ we denote the set of all the paths starting at $s \in S$, and by $\Pi(M)$ we denote the set of all the paths in M.

Syntax of ECTL. The syntax of ECTL formulae over the set AP of atomic propositions is defined by the following grammar:

$$\varphi := true \mid false \mid p \mid \neg p \mid \varphi \wedge \varphi \mid \varphi \vee \varphi \mid \boldsymbol{EX}\varphi \mid \boldsymbol{E}(\varphi \boldsymbol{U} \varphi) \mid \boldsymbol{EG}\varphi,$$

where $p \in AP$ and φ is a formula. The symbols $\boldsymbol{X}$, $\boldsymbol{U}$ and $\boldsymbol{G}$ are the modal operators for "next time", "Until" and "Globally", respectively. The symbol $\boldsymbol{E}$ is the existential path quantifier. The derived basic modalities are defined as follows:

$$\boldsymbol{EF}\alpha \stackrel{\text{def}}{=} \boldsymbol{E}(true\boldsymbol{U}\alpha),\ \boldsymbol{E}(\alpha\boldsymbol{R}\beta) \stackrel{\text{def}}{=} \boldsymbol{E}(\beta\boldsymbol{U}(\alpha\wedge\beta))\vee\boldsymbol{EG}\beta.$$

Semantics of ECTL. Let M be a model, and φ an ECTL formula. An ECTL formula φ is true in the model M (in symbols $M \models \varphi$) iff $M, s^0 \models \varphi$ (i.e., φ is true at the initial state of the model M), where:

– $M, s \models true$,		$M, s, \not\models false$,
– $M, s \models p$	iff	$p \in L(s)$,
– $M, s \models \neg p$	iff	$p \notin L(s)$,
– $M, s \models \alpha \wedge \beta$	iff	$M, s \models \alpha$ and $M, s \models \beta$,
– $M, s \models \alpha \vee \beta$	iff	$M, s \models \alpha$ or $M, s \models \beta$,
– $M, s \models \boldsymbol{EX}\alpha$	iff	$(\exists \pi \in \Pi(s))(M, \pi(1) \models \alpha)$,
– $M, s \models \boldsymbol{E}(\alpha \boldsymbol{U} \beta)$	iff	$(\exists \pi \in \Pi(s))(\exists\, m \geq 0)(M, \pi(m) \models \beta)$ and $(\forall\, j < m)(M, \pi(j) \models \alpha)$,
– $M, s \models \boldsymbol{EG}\alpha$	iff	$(\exists \pi \in \Pi(s))(\forall\, m \geq 0)(M, \pi(m) \models \alpha)$.

Syntax of RTECTL. Let $p \in AP$ and I be an interval in $N = \{1, 2, ...\}$ of the form: $[a, b)$ and $[a, \infty)$, for $a, b \in N$. Note that the remaining forms of intervals can be defined by means of $[a, b)$ and $[a, \infty)$. The language RTECTL is defined by the following grammar:

$$\varphi := true \mid false \mid p \mid \neg p \mid \varphi \wedge \varphi \mid \varphi \vee \varphi \mid \boldsymbol{EX}\varphi \mid \boldsymbol{E}(\varphi \boldsymbol{U_I} \varphi) \mid \boldsymbol{EG_I}\varphi$$

The derived basic modalities are defined as follows:

$$\boldsymbol{EF_I}\alpha = \boldsymbol{E}(true\boldsymbol{U_I}\alpha),\ \boldsymbol{E}(\alpha\boldsymbol{R_I}\beta) = \boldsymbol{E}(\beta\boldsymbol{U_I}(\alpha\wedge\beta)) \vee \boldsymbol{EG_I}\beta.$$

Semantics of RTECTL. Let M be a model, and φ an RTECTL formula. An RTECTL formula φ is true in the model M (in symbols $M \models_{rt} \varphi$) iff $M, s^0 \models_{rt} \varphi$ (i.e., φ is true at the initial state of the model M), where:

- $M, s \models_{rt} true,$ $\quad M, s, \not\models_{rt} false,$
- $M, s \models_{rt} p$ iff $p \in L(s)$,
- $M, s \models_{rt} \neg p$ iff $p \notin L(s)$,
- $M, s \models_{rt} \alpha \wedge \beta$ iff $M, s \models_{rt} \alpha$ and $M, s \models_{rt} \beta$,
- $M, s \models_{rt} \alpha \vee \beta$ iff $M, s \models_{rt} \alpha$ or $M, s \models_{rt} \beta$,
- $M, s \models_{rt} \boldsymbol{EX}\alpha$ iff $(\exists \pi \in \Pi(s))(M, \pi(1) \models_{rt} \alpha)$,
- $M, s \models_{rt} \boldsymbol{E}(\alpha\boldsymbol{U_I}\beta)$ iff $(\exists \pi \in \Pi(s))(\exists\, m \in I)(M, \pi(m) \models_{rt} \beta)$ and $(\forall\, i< m)(M, \pi(i) \models_{rt} \alpha)$,
- $M, s \models_{rt} \boldsymbol{EG_I}\alpha$ iff $(\exists \pi \in \Pi(s))(\forall\, m \in I)(M, \pi(m) \models_{rt} \alpha)$.

Translation from RTECTL into ECTL

In this section we present a translation from the RTECTL language to the ECTL language that is based on the intuitive description of such a translation presented in (CAMPOS 1996, EMERSON et al. 1992). We focused on the existential part of RTCTL only, because we use the BMC method. Moreover, we would like to stress that our semantics of the operator $\boldsymbol{G_I}$ is different than the one presented in (CAMPOS 1996, EMERSON et al. 1992), which was not correctly defined. Further, unlike in (CAMPOS 1996, EMERSON et al. 1992), we present the translation for all types of intervals that can appear together with the temporal operators $\boldsymbol{U_I}$ and $\boldsymbol{G_I}$.

Let $p \in AP$, α and β be formulae of RTECTL, $a \in N$, $b \in N \cup \{\infty\}$ and $a < b$. We define the translation from RTECTL into ECTL as a function $tr: RTECTL \to ECTL$ in the following way:

- $tr(p) = p$, $tr(\neg p) = \neg p$, $tr(\alpha\wedge\beta) = tr(\alpha)\wedge tr(\beta)$, $tr(\alpha\vee\beta) = tr(\alpha)\vee tr(\beta)$,
- $tr(\boldsymbol{EX}\alpha) = \boldsymbol{EX}tr(\alpha)$,

– $tr(\boldsymbol{E}\alpha\boldsymbol{U}_{[a,b)}\beta)$ $\begin{cases} tr(\alpha)\wedge\boldsymbol{EX}(tr(\boldsymbol{E}(\alpha\boldsymbol{U}_{[a-1,\,b-1)}\beta))) \text{ if } a>0 \text{ and } 1<b<\infty \\ tr(\beta)\vee tr(\alpha)\wedge\boldsymbol{EX}(tr(\boldsymbol{E}(\alpha\boldsymbol{U}_{[0,b-1)}\beta))) \text{ if } a>0 \text{ and } 1<b<\infty \\ tr(\alpha)\wedge\boldsymbol{EX}(tr(\boldsymbol{E}(\alpha\boldsymbol{U}_{[a-1,\infty)}\beta))) \text{ if } a>0 \text{ and } b=\infty \\ \boldsymbol{E}(tr\,(\alpha)\boldsymbol{U}tr(\beta)) \text{ if } a>0 \text{ and } b=\infty \\ tr(\beta)) \text{ if } a>0 \text{ and } b=1 \end{cases}$

– $tr(\boldsymbol{EG}_{[a,b)}\alpha)$ $\begin{cases} \boldsymbol{EX}(tr(\boldsymbol{EG}_{[a-1,\,b-1)}\alpha)) \text{ if } a>0 \text{ and } 1<b<\infty \\ tr(\alpha)\wedge\boldsymbol{EX}(tr(\boldsymbol{EG}_{[a-1,\,b-1)}\alpha)) \text{ if } a=0 \text{ and } 1<b<\infty \\ \boldsymbol{EX}(tr(\boldsymbol{EG}_{[a-1,\infty)}\alpha)) \text{ if } a>0 \text{ and } b=\infty \\ \boldsymbol{EG}tr(\alpha) \text{ if } a=0 \text{ and } b=\infty \\ tr(\alpha) \text{ if } a=0 \text{ and } b=1 \end{cases}$

Because $\boldsymbol{EF_I}\alpha \overset{\text{def}}{=} \boldsymbol{E}(true\boldsymbol{U_I}\alpha)$ the translation for $\boldsymbol{EF}_{[\mathrm{a,b})}$ can be defined using the translation for $\boldsymbol{E}(\alpha\boldsymbol{U}_{[\mathrm{a,b})}\beta)$.

The following theorem, which can be proven by induction on the length of an RTECTL formula, states correctness of the above translation.

Theorem 1. [Correctness of the translation] Let M be a model, and φ an RTECTL formula. Then $M \models_{rt} \varphi$ if, and only if $M \models tr(\varphi)$.

Proposition 1. Let α be an RTECTL formula, and $a \in N$. Then, $tr(\boldsymbol{EG}_{[\mathrm{a},\infty)}\alpha) = \underbrace{\boldsymbol{EX}\ \ldots\ \boldsymbol{EX}}_{a}(\boldsymbol{EG}tr(\alpha))$.

Example 1. $tr(\boldsymbol{EG}_{[3,\infty)}\alpha) = \boldsymbol{EXEXEX}(\boldsymbol{EG}tr(\alpha))$.

Proposition 2. Let α be an RTECTL formula, and $a, b \in N$. If $a < b < \infty$, then $tr(\boldsymbol{EG}_{[\mathrm{a,b})}\alpha) = \underbrace{\boldsymbol{EX}\ \ldots\ \boldsymbol{EX}}_{a}\ (tr(\alpha)\ \wedge\ \underbrace{\boldsymbol{EX}(tr(\alpha)\ \wedge\ \boldsymbol{EX}(tr(\alpha)\ \ldots\ )))}_{b-a-1}$.

Example 2. $tr(\boldsymbol{EG}_{[3,6)}\alpha) = \boldsymbol{EXEXEX}\ (tr(\alpha)\ \wedge\ \boldsymbol{EX}(tr(\alpha)\ \wedge\ \boldsymbol{EX}(tr(\alpha))))$.

Proposition 3. Let α and β be RTECTL formulae, and $a \in N$. If $a > 0$, then $tr(\boldsymbol{E}(\alpha\boldsymbol{U}_{[\mathrm{a},\infty)}\beta)) = tr(\underbrace{\alpha)\ \wedge\ \boldsymbol{EX}(tr(\alpha)\ \wedge\ \boldsymbol{EX}(tr(\alpha}_{a-1})\ \ldots\ \wedge\ \boldsymbol{E}(tr(\alpha)\ \boldsymbol{U}(tr(\beta)))))$.

Example 3. $tr(\boldsymbol{E}(\alpha\boldsymbol{U}_{[3,\infty)}\beta)) = tr(\alpha)\ \wedge\ \boldsymbol{EX}(tr(\alpha)\ \wedge\ \boldsymbol{EX}(tr(\alpha)\ \wedge\ \boldsymbol{E}(tr(\alpha)\boldsymbol{U}(tr(\beta))))$.

Proposition 4. Let α and β be RTECTL formulae and $a, b \in N$. If $a < b < \infty$, then $tr(\boldsymbol{E}(\alpha\boldsymbol{U}_{[\mathrm{a,b})}\beta))$
$= tr(\alpha)\wedge\underbrace{\boldsymbol{EX}(tr(\alpha)\wedge\boldsymbol{EX}(tr(\alpha)\wedge\ldots}_{a}\wedge\underbrace{\boldsymbol{EX}(tr(\beta)\vee tr(\alpha)\wedge\boldsymbol{EX}(tr(\beta)\vee tr(\alpha)\ldots}_{b-a-1}\wedge\boldsymbol{EX}(tr(\beta)))))))$.

Example 4. $tr(\boldsymbol{E}(\alpha\boldsymbol{U}_{[a,b)}\beta)) =$
$tr(\alpha)\wedge\boldsymbol{EX}(tr(\alpha)\wedge\boldsymbol{EX}(tr(\alpha)\wedge\boldsymbol{EX}(tr(\alpha)\wedge\boldsymbol{EX}(tr(\beta)\vee tr(\alpha)\wedge\boldsymbol{EX}(tr(\beta)\vee tr(\alpha)\wedge\boldsymbol{EX}(tr(\beta)))))))$.

Lemma 1. Let M be a model, and φ an RTECTL formula. Then

$$(\forall s \in S)(M, s \models_{rt} \varphi \Rightarrow M, s \models tr(\varphi)).$$

Proof 1. [Lemma 1] We proceed by induction on the length of formulae. Let $s \in S$, and assume that $M, s \models_{rt} \varphi$. Now consider the following cases:

1. $\varphi \in AP$. Then, since $tr(\varphi) = \varphi$, we have that $tr\ (\varphi) \in AP$. Therefore, $M, s \models_{rt} \varphi \Leftrightarrow \varphi \in L(s) \Leftrightarrow tr(\varphi) \in L(s) \Leftrightarrow M, s \models tr(\varphi)$.
2. $\varphi = \neg p$, where $p \in AP$. Then, $tr(\varphi) = \varphi$. Therefore, $M, s \models_{rt} \varphi \Leftrightarrow M, s \models_{rt} \neg p \Leftrightarrow p \notin L(s) \Leftrightarrow M, s \models \neg p \Leftrightarrow M,s \models tr(\varphi)$.
3. $\varphi = \alpha \wedge \beta$. By the definition of the satisfiability relation we have that $M, s \models_{rt} \alpha$ and $M, s \models_{rt} \beta$. By the inductive hypothesis, we get $M, s \models$ and $M, s \models tr(\beta)$ Thus, $M, s \models tr(\alpha) \wedge tr(\beta)$, and therefore $M, s \models tr(\alpha \wedge \beta)$.
4. $\varphi = \alpha \vee \beta$. By the definition of the satisfiability relation we have that $M, s \models_{rt} \alpha$ or $M, s \models_{rt} \beta$. By the inductive hypothesis, we get $M, s \models tr(\alpha)$ or $M, s \models tr(\beta)$. Thus, $M, s \models tr(\alpha) \vee tr(\beta)$, and therefore $M, s \models tr(\alpha \vee \beta)$.
5. $\varphi = \boldsymbol{EX}\alpha$. By the definition of the satisfiability relation we have that there exists $\pi \in \Pi(s)$ such that $M, \pi(1) \models_{rt} \alpha$. By the inductive hypothesis, we conclude that $M, \pi(1) \models tr(\alpha)$. Thus, $M \models \boldsymbol{EX}tr(\alpha)$, since $\pi(0) = s$. Therefore $M \models tr(\boldsymbol{EX}\alpha)$, since $tr(\boldsymbol{EX}\alpha) = \boldsymbol{EX}tr(\alpha)$.
6. $\varphi = \boldsymbol{EG_I}\alpha$. By the definition of the satisfiability relation we have that there exists $\pi \in \Pi(s)$ such that $(\forall m \in I)(M, \pi(m) \models_{rt} \alpha)$. By the inductive hypothesis, we conclude that there exists $\pi \in \Pi(s)$ such that
   $$(\forall m \in I)(M, \pi(m) \models tr(\alpha)). \qquad (1)$$
   Now consider the following cases:
   a. $I = [a, \infty)$. From (1) we conclude that $M, s \models \underbrace{\boldsymbol{EX} \ldots \boldsymbol{EX}}_{a} (\boldsymbol{EG}tr(\alpha))$. From this, by the Proposition 1, it follows that $M, s \models tr(\boldsymbol{EG}_{[a,\infty)}\alpha)$.
   b. $I = [a, b)$, where $a < b < \infty$. From (1) we conclude that $M, s \models \underbrace{\boldsymbol{EX} \ldots \boldsymbol{EX}}_{a}(tr(\alpha) \wedge \boldsymbol{EX}(tr(\alpha) \wedge \ldots \wedge \underbrace{\boldsymbol{EX} \ldots \boldsymbol{EX}}_{b-a}(tr(\alpha)))$. From this, by the Proposition 2, we get $M, s \models tr(\boldsymbol{EG}_{[a,b)}\alpha)$.
7. $\varphi = \boldsymbol{E}(\alpha \boldsymbol{U_I} \beta)$. By the definition of the satisfiability relation we have that there exists $\pi \in \Pi(s)$ such that $(\exists m \in I)(M, \pi(m) \models_{rt} \beta)$ and $(\forall i < m)(M, \pi(i) \models_{rt} \alpha)$. By the inductive hypothesis, we conclude that
   $$(\exists m \in I)(M, \pi(m) \models_{rt} \beta) \text{ and } (\forall i < m)(M, \pi(i) \models_{rt} \alpha). \qquad (2)$$
   Now consider the following cases:
   a. $I = [a, \infty)$. From (2) we conclude that $M, s \models tr(\alpha) \wedge \underbrace{\boldsymbol{EX}(tr(\alpha) \wedge \boldsymbol{EX}(tr(\alpha) \ldots}_{a-1} \wedge \boldsymbol{E}(tr(\alpha)\boldsymbol{U}(tr(\beta))))$. From this, by Proposition 3, it follows that $M, s \models tr(\boldsymbol{E}(\alpha \boldsymbol{U}_{[a,\infty)}\beta))$.

b. $I = [a, b)$, where $a < b < \infty$. From (2) we conclude that

$$M, s \models tr(\alpha) \wedge \underbrace{\boldsymbol{EX}(tr(\alpha) \wedge \boldsymbol{EX}(tr(\alpha) \wedge \ldots}_{a}$$

$$\wedge \underbrace{\boldsymbol{EX}(tr(\beta) \vee tr(\alpha) \wedge \boldsymbol{EX}(tr(\beta) \vee tr(\alpha) \ldots}_{b-a-1} \wedge \boldsymbol{EX}(tr(\beta))))))).$$

From this, by Proposition 4, it follows that $M, s \models tr(\boldsymbol{E}(\alpha \boldsymbol{U}_{[a,b)}\beta))$.

Lemma 2. Let M be a model, and φ an RTECTL formula. Then

$$(\forall s \in S)(M, s \models tr(\varphi) \Rightarrow M, s \models_{rt} \varphi).$$

Proof 2. [Lemma 2] We proceed by induction on the length of formulae. Let $s \in S$, and assume that $M, s \models tr(\varphi)$. Now consider the following cases:

1. $\varphi \in AP$. Then, since $\varphi = tr(\varphi)$, we have that $tr(\varphi) \in AP$. Therefore, $M, s \models tr(\varphi) \Leftrightarrow \varphi \in L(s) \Leftrightarrow tr(\varphi) \in L(s) \Leftrightarrow M, s \models_{rt} \varphi$.
2. $\varphi = \neg p$, where $p \in AP$. Then, $tr(\varphi) = \varphi$. Therefore, $M, s \models tr(\varphi) \Leftrightarrow M, s \models tr(\neg p) \Leftrightarrow p \notin L(s) \Leftrightarrow M, s \models_{rt} \neg p \Leftrightarrow M,s \models_{rt} \varphi$.
3. $\varphi = \alpha \wedge \beta$. Then, $tr(\varphi) = tr(\alpha \wedge \beta) = tr(\alpha) \wedge tr(\beta)$. By the definition of the satisfiability relation for ECTL we have that $M, s \models tr(\alpha)$ and $M, s \models tr(\beta)$. By the inductive hypothesis, we get $M, s \models_{rt} \alpha$ and $M, s \models_{rt} \beta$ and therefore $M, s \models_{rt} tr(\alpha \wedge \beta)$.
4. $\varphi = \alpha \vee \beta$. Then, $tr(\varphi) = tr(\alpha \vee \beta) = tr(\alpha) \vee tr(\beta)$. By the definition of the satisfiability relation for ECTL we have that $M, s \models tr(\alpha)$ or $M, s \models tr(\beta)$. By the inductive hypothesis, we get $M, s \models_{rt} \alpha$ or $M, s \models_{rt} \beta$ and therefore $M, s \models_{rt} tr(\alpha \vee \beta)$.
5. $\varphi = \boldsymbol{EX}\alpha$. Then, $tr(\varphi) = tr(\boldsymbol{EX}\alpha) = \boldsymbol{EX}tr(\alpha)$. By the definition of the satisfiability relation we have that there exists $\pi \in \Pi(s)$ such that $M, \pi(1) \models tr(\alpha)$. By the inductive hypothesis, we conclude that $M, \pi(1) \models_{rt} \alpha$. Thus, $M, s \models_{rt} \boldsymbol{EX}\alpha$, since $\pi(0) = s$.
6. $\varphi = \boldsymbol{EG_I}\alpha$. Consider the following cases:

   a. $I = [a, \infty)$. From (1) we conclude that $M, s \models \underbrace{\boldsymbol{EX} \ldots \boldsymbol{EX}}_{a} (\boldsymbol{EG}tr(\alpha))$. From this it follows that there exists $\pi \in \Pi(s)$ such that $(\forall m \geq a)(M, \pi(m) \models tr(\alpha))$. By the inductive hypothesis, we conclude that $(\forall m \geq a)(M, \pi(m) \models_{rt} \alpha)$, and therefore $M, s \models_{rt} \boldsymbol{EG_I}\alpha$.

   b. $I = [a, b)$, where $a < b < \infty$. From (2) we get that $M, s \models \underbrace{\boldsymbol{EX} \ldots \boldsymbol{EX}}_{a}(tr(\alpha) \wedge \boldsymbol{EX}(tr(\alpha)) \wedge \ldots \wedge \underbrace{\boldsymbol{EX} \ldots \boldsymbol{EX}}_{b-a}(tr(\alpha)))$. From this, it follows that there exists $\pi \in \Pi(s)$ such that $(\forall m \in [a, b))(M, \pi(m) \models tr(\alpha))$. By the inductive hypothesis, we conclude that $(\forall m \in [a, b))(M, \pi(m) \models_{rt} \alpha)$, Therefore $M \models_{rt} \boldsymbol{EG_I}\alpha$.

7. $\varphi = \boldsymbol{E}(\alpha \boldsymbol{U_I} \beta)$. Consider the following cases:
   a. $I = [a, \infty)$. From the Proposition 3, we get that $M, s \models tr(\boldsymbol{E}(\alpha \boldsymbol{U}_{[a,\infty)}\beta)) = tr(\alpha) \wedge \underbrace{\boldsymbol{EX}(tr(\alpha) \wedge \boldsymbol{EX}(tr(\alpha) \ldots}_{a-1} \wedge \boldsymbol{E}(tr(\alpha)\boldsymbol{U}(tr(\beta))))$. From this it follows that there exists $\pi \in \Pi(s)$ such that $(\forall m < a)(M, \pi(m) \models tr(\alpha))$ and $(\exists m \geq a)$ $(M, \pi(m) \models \boldsymbol{E}(tr(\alpha)\boldsymbol{U}tr(\beta))$. By the inductive hypothesis, we conclude that $(\forall m < a)(M, \pi(m) \models_{rt} \alpha)$ and $(\exists m \geq a)(M, \pi(m) \models_{rt} \boldsymbol{E}(\alpha \boldsymbol{U} \beta)$, and therefore $M, s \models \boldsymbol{E}(\alpha \boldsymbol{U_I} \beta)$.
   b. $I = [a, b)$, where $a < b < \infty$. From Proposition 4 we get that

$$tr(\boldsymbol{E}(\alpha \boldsymbol{U}_{[a,b)}\beta) = tr(\alpha) \wedge \underbrace{\boldsymbol{EX}(tr(\alpha) \wedge \boldsymbol{EX}(tr(\alpha) \wedge \ldots}_{a}$$
$$\wedge \underbrace{\boldsymbol{EX}(tr(\beta) \vee tr(\alpha) \wedge \boldsymbol{EX}(tr(\beta) \vee tr(\alpha) \ldots}_{b-a-1} \wedge \boldsymbol{EX}(tr(\beta)))))).$$

From this it follows that there exists $\pi \in \Pi(s)$ such that $(\forall m < a)(M, \pi(m) \models tr(\alpha))$ and $(\exists b - a - 1 > m)(M, \pi(m) \models tr(\alpha) \vee tr(\beta))$ and $(\forall m < b)(M, \pi(m) \models tr(\beta))$. By the inductive hypothesis, we conclude that $(\forall m < a)(M, \pi(m) \models_{rt} (\alpha))$ and $(\exists b - a - 1 > m)(M, \pi(m) \models_{rt} \alpha \vee \beta)$ and $(\forall m < b)(M, \pi(m) \models_{rt} \beta)$, and therefore $M, s \models \boldsymbol{E}(\alpha \boldsymbol{U_I} \beta)$.

Proof 3. [Theorem 1] This follows from Lemma 1 and Lemma 2.

Bounded model checking

The SAT-based Bounded Model Checking (BMC) is a popular model checking technique for the verification of concurrent systems. Given a model M, an existential modal formula φ, and a non-negative bound k, the SAT-based BMC consists in searching for a non-empty set of paths of the length k that constitute a witness for the checked property φ. In particular, the bounded model checking algorithms generate a propositional formula which is satisfiable if and only if the mentioned set of paths exist. The propositional formula is usually obtained as a combination of a propositional encoding of the unfolding of the transition relation of the given model, and a propositional encoding of the property in question. If the generated propositional formula is not satisfiable, then k is incremented until either the problem becomes intractable due to the complexity of solving the corresponding SAT instance, or k reaches the upper bound of the bounded model checking problem for the language under consideration.

All the SAT-based BMC, so the one for ECTL and RTECTL as well, are based on so called bounded semantics, which are the base of translations of specifications to the SAT-problem. In definitions of the bounded semantics one needs to represent cycles in models in a special way. To this aim k-paths, i.e., finite paths of the length k, and loops are defined. These definitions have evolved over the last decade, and they have had a major impact on the effectiveness of the BMC encodings.

The SAT-based BMC method for ECTL was introduced in (PENCZEK et al. 2002), and then it was improved in (ZBRZEZNY 2008). In this paper we use the definition and implementation of the SAT-based BMC for ECTL that was presented in (ZBRZEZNY 2008). The SAT-based BMC method for RTECTL was introduced in (WOŹNA-SZCZEŚNIAK 2009), and then it was improved in (WOŹNA--SZCZEŚNIAK et al. 2011). In this paper we use the definition and implementation of the SAT-based BMC for RTECTL that was presented in (WOŹNA-SZCZEŚNIAK et al. 2011).

Experimental results

A Train Controller System

In this section we present a comparison of a performance evaluation of two SAT-based BMC algorithms: for RTECTL, and for ECTL. In order to evaluate the behaviour of the algorithms, we have tested it on several RTECTL properties and equivalent ECTL properties. An evaluation of both BMC algorithms, which have been implemented in C++ is given by means of the running time, the memory used, and the number of generated variables and clauses.

To evaluate the BMC technique for RTECTL and ECTL, we analyse a scalable concurrent system, which is a train controller system (TC). The system consists of a controller, and n trains (for $n \geq 2$), and it is assumed that each train uses its own circular track for travelling in one direction. All trains have to pass through a tunnel, but because there is only one track in the tunnel, arriving trains cannot use it simultaneously. There are signal lights on both sides of the tunnel, which can be either red or green. All trains notify the controller when they request entry to the tunnel or when they leave the tunnel. The controller controls the colour of the signal lights. The controller does not ensure the mutual exclusion property: two trains never occupy the tunnel at the same time.

An automata model of the TC system is shown in the Figure 1.

The specifications for it are given in the existential form, i.e., they are expressed in the RTECTL language:

- $\varphi_1 = \boldsymbol{EF}_{[0,\infty)}\ (InTunnel_1 \wedge \boldsymbol{EG}_{[1,n+2)}(\bigwedge_{n=1}^{n} \neg\ InTunnel_i))$ – states that there exists the case that Train_1 is in the tunnel and either it and other train will not be in the tunnel during the next $n+1$ time units, where n is the number of trains.
- $\varphi_2 = \boldsymbol{EF}_{[0,\infty)}\ (InTunnel_1 \wedge \boldsymbol{EG}_{[1,n+2)}(\bigwedge_{n=1}^{n} \neg\ InTunnel_i))$ – expresses that there exists the case that Train_1 is in the tunnel or either it or other train will not

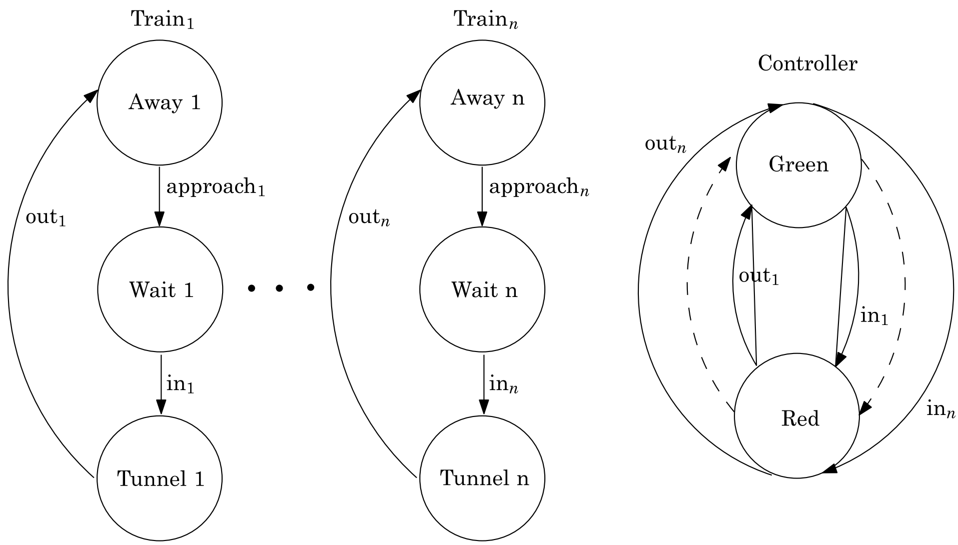

Fig. 1. A network of automata for a train controller system

be in the tunnel during the next $n+1$ time units, where n is the number of trains.

The equivalent ECTL formulae for $n=2$ are:

– $tr(\varphi_1) = \boldsymbol{EF}(InTunnel_1 \wedge \boldsymbol{EX}((\neg\, InTunnel_1 \wedge \neg InTunnel_2) \wedge \boldsymbol{EX}((\neg InTunnel_1 \wedge \neg InTunnel_2) \wedge \boldsymbol{EX}(\neg InTunnel_1 \wedge \neg InTunnel_2)))$,

– $tr(\varphi_2) = \boldsymbol{EF}(InTunnel_1 \vee \boldsymbol{EX}((\neg\, InTunnel_1 \vee \neg InTunnel_2) \wedge \boldsymbol{EX}((\neg InTunnel_1 \vee \neg InTunnel_2) \wedge \boldsymbol{EX}(\neg InTunnel_1 \vee \neg InTunnel_2)))$.

In the Figure 2 we present a comparison of total time usage and total memory usage for the formula φ_1. An analysis of the experimental results for the formula φ_1 leads to the conclusion that BMC for ECTL uses less time and memory comparing to BMC for RTECTL. The reason is that although BMC needs much more paths for the verification in case of ECTL, but these paths are significantly shorter.

In the Figure 3 we present a comparison of total time usage and total memory usage for the formula φ_2. An observation of the experimental results for the formula φ_2 leads to the conclusion that the BMC for RTECTL uses less time and memory comparing to the BMC for ECTL. The reason is that the BMC needs much more paths for verification in case of ECTL.

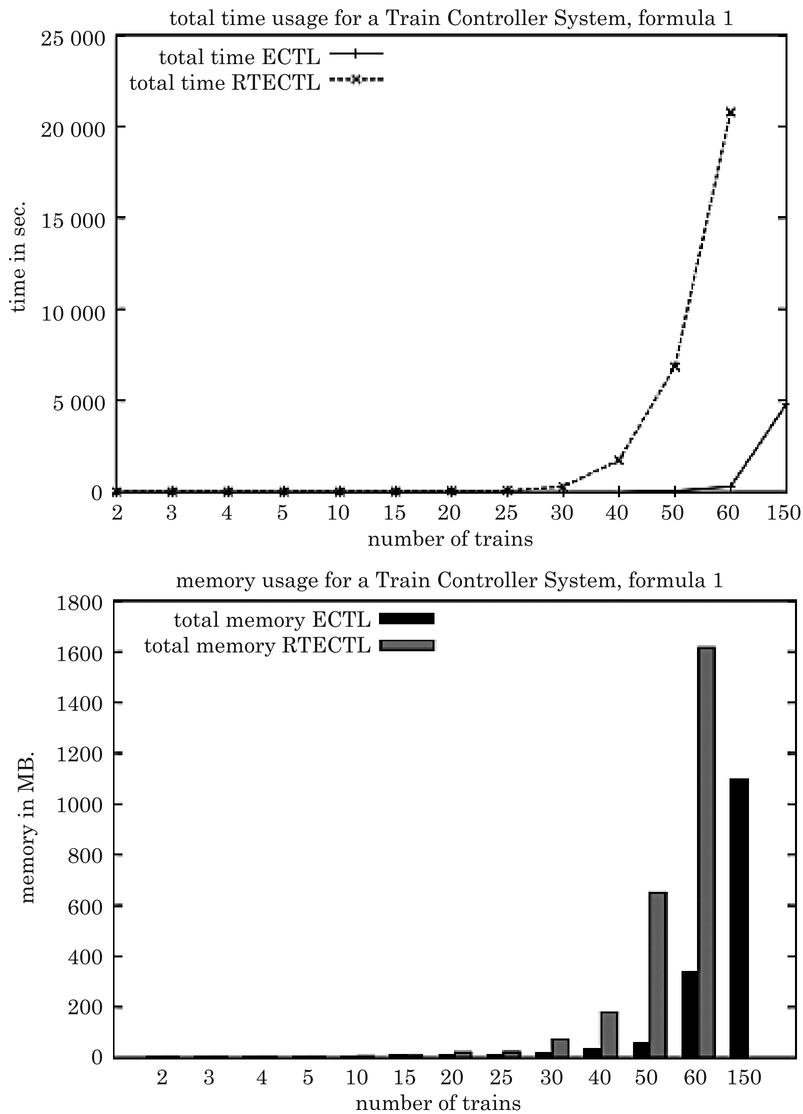

Fig. 2. A comparison of total time usage and total memory usage for the formula φ_1

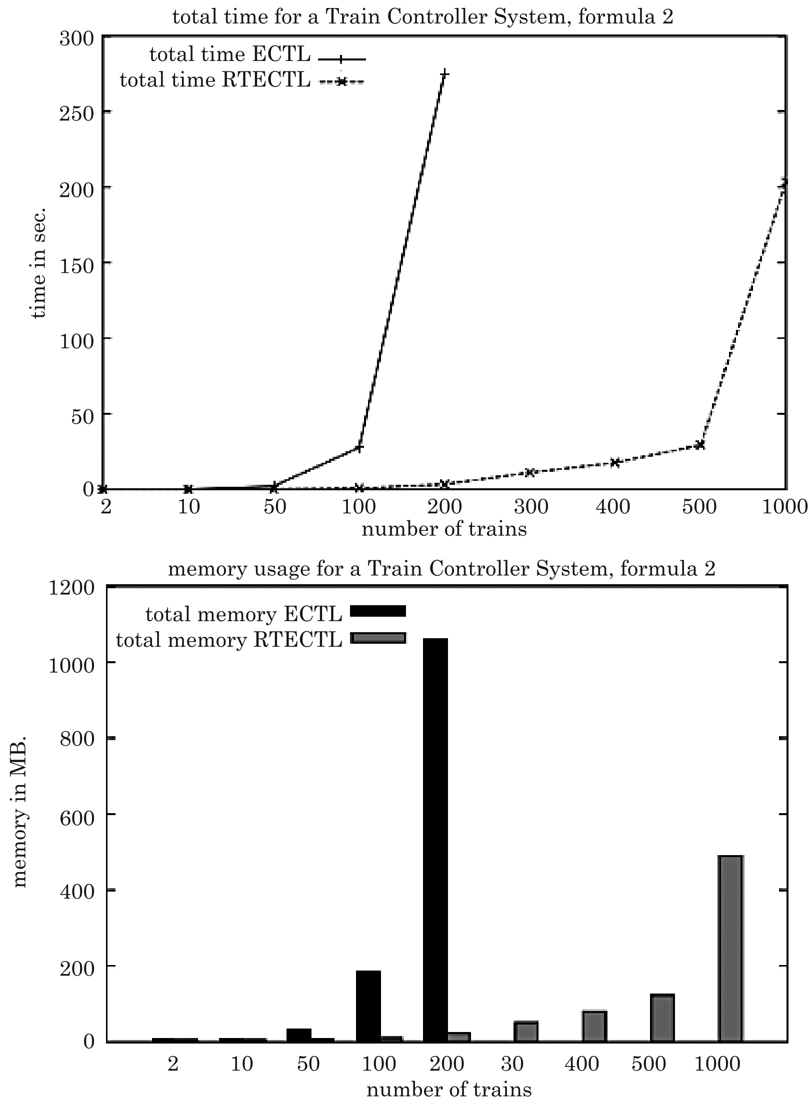

Fig. 3. A comparison of total time usage and total memory usage for the formula φ_2

Generic Pipeline Paradigm

The benchmark we consider is the generic pipeline paradigm (GPP) (PELED 1993), which consists of three parts: Producer producing data, Consumer receiving data, and a chain of n intermediate Nodes that transmit data produced by Producer to Consumer. The local states for each component (Producer, Consumer, and intermediate Nodes), and their protocols are shown in the Figure 4.

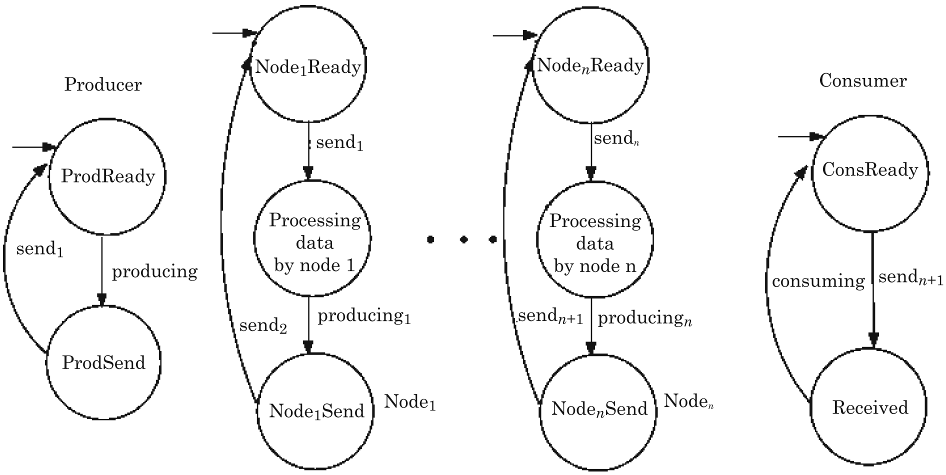

Fig. 4. The GPP system

The comparison of both BMC algorithms for RTECTL and ECTL with respect to the GPP system has been done by means of the following RTECTL specification:

– $\varphi_3 = \boldsymbol{EG}_{[0,\infty)}((\neg ProdSend \vee \boldsymbol{EF}_{[2n+1,2n+2)}(Received))$,

– $\varphi_4 = \boldsymbol{EG}_{[0,n^2+2n+1)}(Received)$, where n is the number of nodes.

The equivalent ECTL formulae for $n=2$ are:

– $tr(\varphi_3) = \boldsymbol{EG}(\neg ProdSend \vee \boldsymbol{EX}(\boldsymbol{EX}(\boldsymbol{EX}(\boldsymbol{EX}(\boldsymbol{EX}(Received))))))$,

– $tr(\varphi_4) = \boldsymbol{EX}(Received \wedge \boldsymbol{EX}(Received \wedge \boldsymbol{EX}(Received \wedge \boldsymbol{EX}(Received \wedge \boldsymbol{EX}(Received \wedge \boldsymbol{EX}(Received \wedge \boldsymbol{EX}(Received \wedge \boldsymbol{EX}(Received \wedge \boldsymbol{EX}(Received \wedge Received)))))))))$.

In the Figure 5 we present a comparison of total time usage and total memory usage for the formula φ_3. An observation of the experimental results for the formula φ_3 leads to the conclusion that the BMC for RTECTL uses less time and memory comparing to the BMC for ECTL. The reason is that although BMC needs much more paths for verification in case of ECTL.

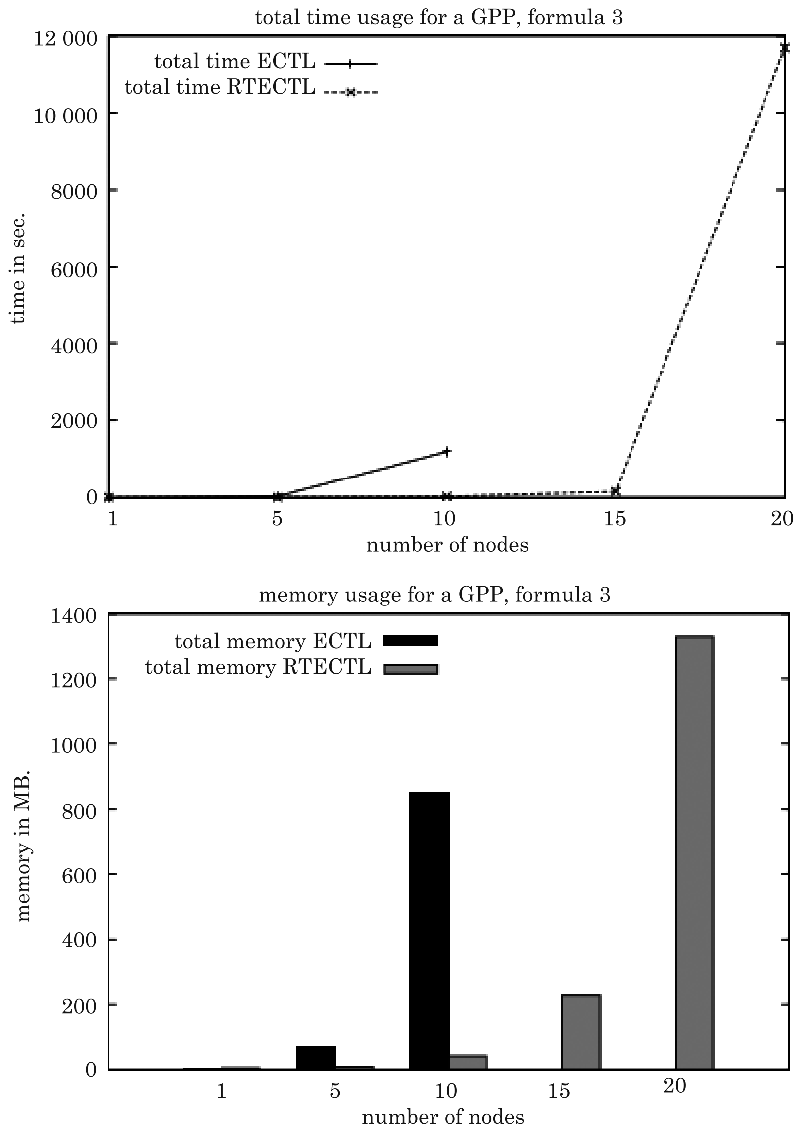

Fig. 5. A comparison of total time usage and total memory usage for the formula φ_3

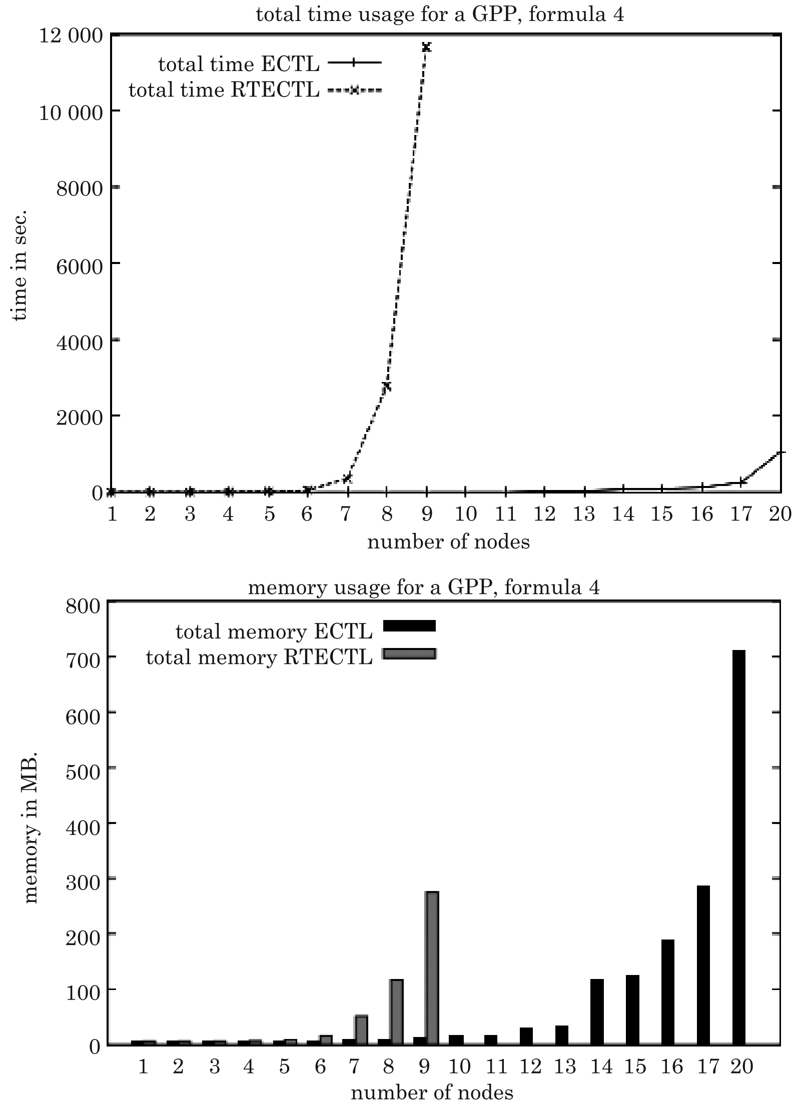

Fig. 6. A comparison of total time usage and total memory usage for the formula φ_4

In the Figure 6 we present a comparison of total time usage and total memory usage for the formula φ_4. An analysis of experimental results for the formula φ_4 leads to the conclusion that the BMC for ECTL uses less time and memory comparing to the BMC for RTECTL. The reason is that although BMC needs much more paths for verification in case of ECTL, but these paths are significantly shorter.

For the tests we have used a computer equipped with AMD Phenom™ 9550 Quad-Core 2200 MHz processor and 8 GB of RAM, running Ubuntu Linux with kernel version 3.5.0-17-generic. We have used the state of the art SAT-solver MiniSat 2 (EÉN, SÖRENSSON 2005, *MiniSat* 2006), which is one of the best SAT-solver.

Conclusions

In this paper we have presented a comparison between the BMC method for ECTL and the BMC method for RTECTL. Moreover, we have presented a correct translation for operator $\boldsymbol{EG_I}$, which was not defined in (CAMPOS 1996, EMERSON et al. 1992).

Further, we have tested and compared with each other on to standard benchmarks the BMC translations for RTECTL and ECTL incremented in (WOŹNA-SZCZEŚNIAK et al. 2011, ZBRZEZNY 2008). We have observed that for the RTECTL formulae for which the interval at the operator ***EG*** is finite, the BMC can be less effective than BMC for their translation into ECTL formulae.

Acknowledgements

The author wishes to thank Bożena Woźna-Szcześniak and Andrzej Zbrzezny for valuable comments and numerous suggestions which helped to improve this paper.

Partly supported by National Science Centre under the grant No. 2014/15/N/ST6/05079.

References

BAIER C., KATOEN J.-P. 2008. *Principles of model checking*. MIT Press.

BIERE A., CIMATTI A., CLARKE E., ZHU Y. 1999. *Symbolic Model Checking without BDDs*. Proceedings of the 5th Int. Conf. on Tools and Algorithms for the Construction and Analysis of Systems (TACAS;99), LNCS. Springer-Verlag, p. 193–207.

BRYANT R., 1986. *Graph-Based Algorithms for Boolean Function Manipulation*. IEEE Trans. Comput, 35(8): 677–691.

CAMPOS S.V.A. 1996. *A quantitative approach to the formal verification of real-time systems*. School of Computer Science, Carnegie Mellon University, Pittsburgh, PA, USA.

CLARKE E., EMERSON E.A., SISTLA A.P. 1986. *Automatic Verification of Finite State Concurrent Systems Using Temporal Logic Specifications: A Practical Approach*. ACM Trans. Program. Lang. Syst., 8(2): 244–263.

CLARKE E., GRUMBERG O., PELED D. 1999. *Model Checking*. MIT Press.

EMERSON E.A., MOK A.K., SISTLA A.P., SRINIVASAN J. 1992. *Quantitative Temporal Reasoning*. Real-Time Syst., 4: 331–352.

LOMUSCIO A., PENCZEK W., QU H. 2010. *Partial order reduction for model checking interleaved multi-agent systems*. Proceedings of the 9th International Conference on Autonomous Agents and Multi-Agent Systems (AAMAS;2010). IFAAMAS Press, p. 659–666.

MCMILLAN K.L. 1993. *Symbolic Model Checking*. Kluwer Academic Publishers.

PENCZEK W., LOMUSCIO A. 2003. *Verifying Epistemic Properties of Multi-Agent Systems via Bounded Model Checking*. Fundam. Informaticae, 55: 167–185.

PENCZEK W., WOŹNA B., ZBRZEZNY A. 2002. *Bounded Model Checking for the Universal Fragment of CTL*. Fundam. Informaticae, 51(1–2): 135–156.

WOŹNA B., ZBRZEZNY A. 2004. *Checking ACTL* Properties of Discrete Timed Automata via Bounded Model Checking*. Proceedings of the 1st Int. Workshop on Formal Analysis and Modeling of Timed Systems (FORMATS'03), LNCS. Springer-Verlag, p. 18–33.

WOŹNA-SZCZEŚNIAK B., ZBRZEZNY A.M., ZBRZEZNY A. 2011. *The BMC method for the existential part of RTCTLK and interleaved interpreted systems*. Proceedings of the 15th Portuguese Conference on Artificial Intelligence (EPIA;2011), LNAI. Springer-Verlag, p. 551–565.

ZBRZEZNY A. 2008. *Improving the Translation from ECTL to SAT*. Fundam. Informaticae 85(1–4): 513–531.

Technical Sciences, 2017, 20(2), 149–160

UNIWERSYTET WARMIŃSKO-MAZURSKI W OLSZTYNIE

Quarterly peer-reviewed scientific journal

ISSN 1505-4675
e-ISSN 2083-4527

TECHNICAL SCIENCES

Homepage: www.uwm.edu.pl/techsci/

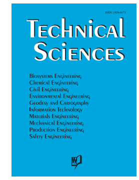

MODELLING OF OPTIMUM CASCADE OF IDEAL MIXING REACTORS

German Efremov, Julia Geller

Moscow Technological Institute, Russia

Received 11 November 2016, accepted 12 March 2017, available online 27 March 2017

Key words: optimization, cascade reactors, dynamic programming, polymerization.

Abstract

It is discussed the using of dynamic programming method to optimize the parameters of the cascade of ideal mixing reactors, which is held isothermal first order reaction. It is found, that the minimum volume of the cascade of reactors corresponds to the minimum residence time of substance in this cascade. The optimum value of residence time for all reactors are equal and all ratio of input and output concentrations are equal, hence, and all volumes of reactors are also equal. A total volume of the cascade of reactors is less than the amount single. Application of the method of dynamic programming is illustrated with an example of the calculation of the polymerization in a cascade of four reactors according to the literature experimental data.

Nomenclature

G – mass, mole
i – index of component
k – reaction rate constant, h^{-1} l $mole^{-1}$
N – number of reactors
r – reaction rate, h^{-1}
u – control action
V – volume, l
v – volumetric flow, h^{-1}
x – concentration, mole l^{-1}
τ – residence time, h

Correspondence: German Efremov, Moscow Technological Institute, Lenin avenue 38A, 199334 Moscow, RUSSIA; e-mail: efremov_german@mail.ru

Introduction

Mixing of single and multiphase fluids in stirred tanks is a common operation in chemical process industries. Proper knowledge of fluid flow is essential for scale-up, equipment design, process control, and economic factors. The cascade of mixing reactors is used in various chemical industries (BOYARINOV, KAFAROV 1975, EFREMOV 2001, 2016, LEVENSPIEL 1965, *Handbook of Industrial Mixing: Science and Practice* 2004, BRAYNES 1976, ARIS 1976, KRAMERS, WESTERTERP 1963, HARRIOTT 2003, COKER 2001, KOROBOV, OCHKOV 2011). In such devices, due to the intense mixing, there is no temperature and concentration gradients (HARRIOTT 2003). It is shown (COKER 2001) that the reactors of continuous mixing action are preferable to the batch reactors and the total volume of the cascade of reactors is less than the amount single. If the reaction can result in only one product, the mixing and mass transfer can influence only the reaction rate. If more than one product is possible, contacting can influence the product distribution as well. For the solution of tasks of modeling and optimization of multi-stage processes have been developed and successfully applied the method of dynamic programming (KRAMERS, WESTERTERP 1963, EFREMOV 2016).

At the modeling as a stage of processes the one of elements is accepted, on which it is possible to divide the process parameters, as in time, and as in space. Stage in this case represent a sequence of the same type of equipment (reactors, agitators), in which the flow of raw materials undergoes sequential processing.

The status of the individual stages of the process is described by a set of input and output parameters *h*i. The output of each stage serves as input to the subsequent stage.

In addition to the input and output variables at each stage it is necessary to select a group of control actions *ui* (Fig. 1).

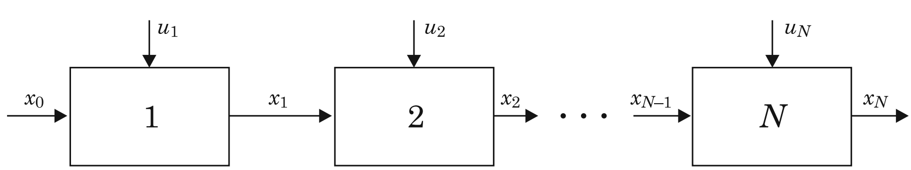

Fig. 1. Diagram of the multistage process

The principle of optimality in dynamic programming allows optimization starting from the last stage, through the selection of control parameters for this stage. Then consider the last two stages, the last three stages etc., reaching the first one. It should be noted that dynamic programming allows to replace a complicated task by the more simple for the next individual stages.

In this paper it is considered the application of dynamic programming method to optimize the parameters of the cascade of reactors of ideal mixing, which is held isothermal first order reaction. The purpose of the calculation is to find the minimum total volume of the reactor system at a given initial concentration and to obtain the given final concentration of the original substance.

Theoretical analysis

The purpose of the calculation is to find the minimum residence time of the reaction mixture in the system of reactors of ideal mixing for the given initial concentration of x_0 to obtain the desired final concentration of the initial substance.

Considering the model of ideal mixing of volume V, introducing the value of the volumetric flow $v = V/\Delta\tau$ to mass of substance $G_i = Vx_i$ at the input is equal

$$\frac{G_i^0}{\Delta\tau} = \frac{Vx_i^0}{\Delta\tau} = vx_i^0 \tag{1}$$

Accordingly, the mass flow at the output is equal to

$$\frac{G_i}{\Delta\tau} = \frac{Vx_i}{\Delta\tau} = vx_i \tag{2}$$

Given (1) and (2) a change of mass flow in the apparatus is

$$\frac{\mathrm{d}(Vx_i)}{\mathrm{d}\tau} = v(x_i^0 - x_i) \tag{3}$$

Considering isothermal chemical reactions (rate of reaction r_i), at stationary regime the equation (3) is

$$v(x_i^0 - x_i) + Vr_i = 0 \tag{4}$$

Below it is considered the cascade of three reactors for a given initial concentration $x_0 = 1\%$ and at a given final concentration of the initial substance x_3, equal to 10%. The rate constant of the chemical reaction is $k = 1\ h^{-1}(mol/l)^{-1}$.

Using for the cascade the concentration of the initial substance on the entrance to each unit and on the exit from it as x_{i-1} and x_i, given the rate of reaction of the first order

$$r_i = kx_i \tag{5}$$

denoting the residence time of the substance $\tau_i = V_i/v$, taking into account equations (4) and (5), it may be obtained, respectively, for each of the three reactors (BOYARINOV, KAFAROV 1975, EFREMOV 2001, 2016, LEVENSPIEL 1965, *Handbook of Industrial Mixing: Science and Practice* 2004, BRAYNES 1976, ARIS 1976, KRAMERS, WESTERTERP 1963):

$$\frac{x_1}{x_0} = \frac{1}{1 + k\tau_1}; \quad \frac{x_2}{x_1} = \frac{1}{1 + k\tau_2}; \quad \frac{x_3}{x_2} = \frac{1}{1 + k\tau_3}; \tag{6}$$

The start of the optimization is from the last reactor. Thus, taking into account the initial data of (6), the process time is

$$\tau_3 = \frac{1}{k}\left(\frac{x_2}{x_3} - 1\right) \tag{7}$$

The dependence of τ_3 on x_2, according to (7), is a straight line. Thus, to minimize τ_3 is necessary to select the concentration of x_2.

Similarly, the process time for the second reactor is

$$\tau_2 = \frac{1}{k}\left(\frac{x_1}{x_2} - 1\right) \tag{8}$$

The formula (8) is built in MathCAD in the coordinates of τ_2, x_2 for different values of x_1 (0.1, 0.3, 0.5, 0.7, 0.9) and shown in Figure 2.

For the last two reactors, the total residence time $\tau_2 + \tau_3$ is a function of the concentration of the substance entering to the second reactor x_1

$$\tau_2 + \tau_3 = \frac{1}{k}\left(\frac{x_1}{x_2} + \frac{x_2}{x_3} - 2\right) \tag{9}$$

$$i = 1...5$$

$$\frac{1}{k}\cdot\left(\frac{x_1^i}{x_2}-1\right)$$

$$x_1^i = \begin{pmatrix} 0.1 \\ 0.3 \\ 0.5 \\ 0.7 \\ 0.9 \end{pmatrix}$$

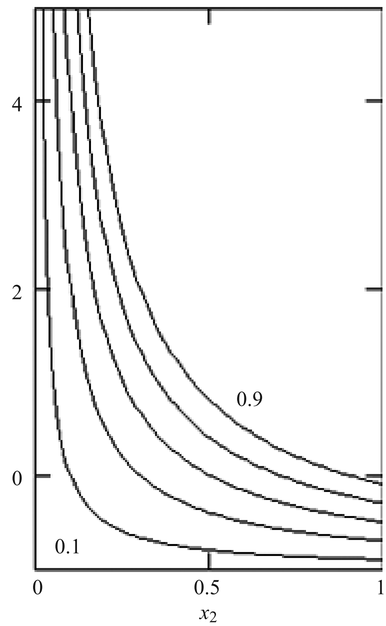

Fig. 2. Dependence of the residence time in the 1st reactor vs. the concentration in the 2nd reactor

The dependence (9) can be also presented in the system MathCAD as function ($\tau_2 + \tau_3$) vs. x_2 for different values of x_1 (Fig. 3).

$$i = 1...5$$

$$\frac{1}{k}\cdot\frac{x_1^i}{x_2}+\frac{x_2}{x_3}-2$$

$$x_1^i = \begin{pmatrix} 0.1 \\ 0.3 \\ 0.5 \\ 0.7 \\ 0.9 \end{pmatrix}$$

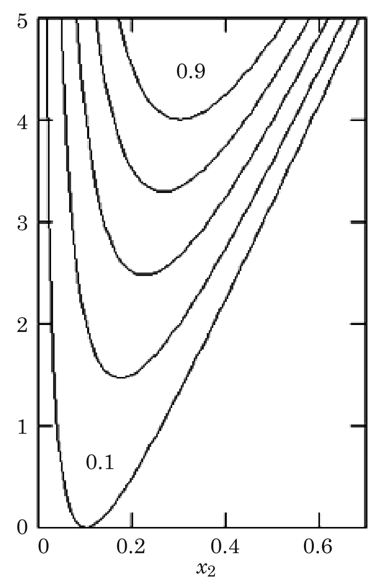

Fig. 3. Dependence of the total residence time in the 2-nd and 3-rd reactors vs. concentration in the 2-nd reactor

For the optimization it is necessary to find the minimum value of $(\tau_2 + \tau_3)$ and the optimal value of x_{2opt} for the adopted above values of x_1. To do this, it is necessary to find the derivative of the function (9) by x_2 and to equate it to zero. As the result, the next dependence appears

$$x_{2opt} = \sqrt{x_1 \, x_3} \tag{10}$$

Substituting the values of x_{2opt} from the equation (10), the minimum value of the sum $(\tau_2 + \tau_3)_{min}$ as a function of x_1 can be calculated

$$(\tau_2 + \tau_3)_{min} = \frac{1}{k}\left(2\sqrt{\frac{x_1}{x_3}} - 2\right) \tag{11}$$

The equation (11), as a function of x_1 is a power-law dependence in the form

$$(\tau_2 + \tau_3)_{min} = A \cdot \left(\frac{x_1}{x_3}\right)^n - B \tag{12}$$

From equations (11) and (12) it follows that the minimum of $(\tau_2 + \tau_3)$ is dependent on the concentration in the first reactor x_1.

With the found values of the coefficients A, B and n the graph, according to the equation (11) in the coordinates $(\tau_2 + \tau_3)_{min}$ vs. x_1 is shown on Figure 4. In this graph, marked also adopted higher values of x_1. As can be seen from Figure 4 good agreement with the calculation by equation (11) is obtained.

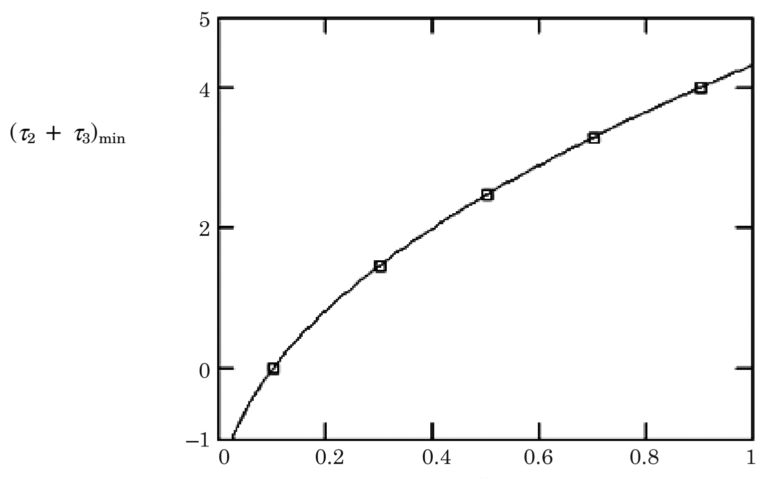

Fig. 4. Dependence of total time in 2-nd and 3-rd reactors vs. concentration in 1-st reactor

Next, the addition of the process time dependence for the first reactor

$$\tau_1 = \frac{1}{k}\left(\frac{x_0}{x_1} - 1\right) \tag{13}$$

in the equation (11) gives by result

$$\tau_1 + \tau_2 + \tau_3 = \frac{1}{k}\left(2\sqrt{\frac{x_1}{x_3}} + \frac{x_0}{x_1} - 3\right) \tag{14}$$

The diagram of dependence $(\tau_2 + \tau_3 + \tau_1)$ vs. x_1 is submitted in a Figure 5.

For finding of a minimum of function $(\tau_2 + \tau_3 + \tau_1)_{\min}$ it is necessary to equate to zero the derivative of function (14) on x_1. This value at the accepted above parameters makes 0.4642. This value $x_{1\text{opt}}$ is shown by a dotted line on the diagram (Fig. 5). Substituting the found value in the equation (13), the appropriate value of time $\tau_1 = 1.1542/k$ may be finding.

Further at optimum value of $x_{1\text{opt}}$ from the equation (14) the value $(\tau_1 + \tau_2 + \tau_3)_{\min} = 3.4633/k$ and from the equation (11) the value $(\tau_1 + \tau_2)_{\min} = 2.3087/k$ may be calculated. From equation (10) the optimum value of $x_{2\text{opt}} = 0.2155$.

Knowing the optimum values of all concentration, the ratio of entrance and outlet concentrations for all reactors is.

$$\frac{x_0}{x_1} = \frac{x_1}{x_2} = \frac{x_2}{x_3} = 2.1542$$

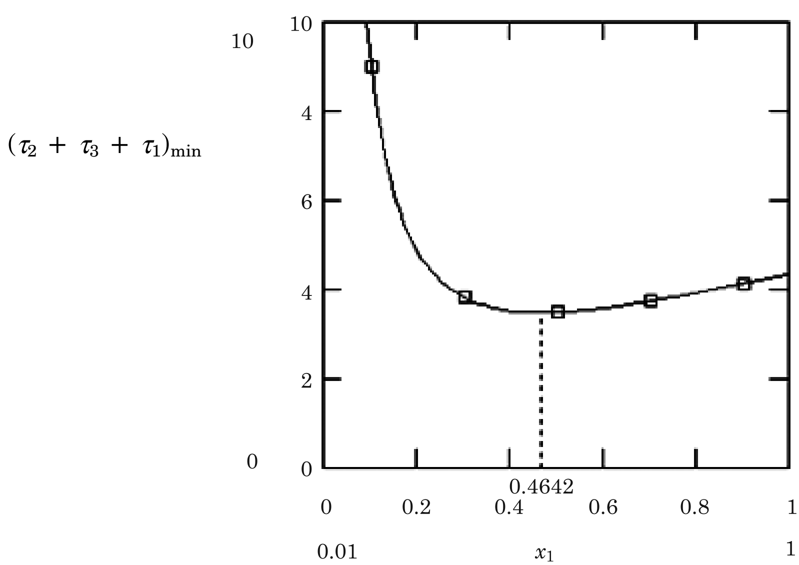

Fig. 5. Dependence of total time in 3 reactors vs. concentration in the 1-st reactor

It is obtained the same ratio of the input and output concentrations for all reactors and, according to equations (7), (8) and (13) the residence times are

$$\tau_1 = \tau_2 = \tau_3 = 1.1542/k.$$

All calculations and graphics are realized in MathCAD.

For optimization, in the general case, N series of the cascade of isothermal ideal mixing reactors it is necessary to find the minimum of the sum of the residence time in all reactors

$$\Sigma\tau = \frac{1}{k}\sum_{i=0}^{N}\left(\frac{x_i}{x_{i+1}} - 1\right) \tag{15}$$

under the condition of positivity of the values of all concentrations. Since the residence time in the reactor is equal to τ_i, the ratio of the output and input concentrations of the cascade of N reactors with (6) can be calculated as

$$\frac{x_N}{x_0} = \frac{1}{(1 + k\tau_i)^N} \tag{16}$$

Minimizing of the residence time in the cascade of isothermal ideal mixing reactors can be realized in MathCAD or Excel (add-in "solver"). Such calculations for given initial concentrations were performed for cascades of 2 to 7 reactors. The results are shown in the Table 1.

Table 1

The parameters of the cascades of isothermal ideal mixing reactors

Number of reactors, N	$k\ \Sigma\tau_{\min}$	x_i/x_{i+1}	$\tau_i\ k$
2	4.3246	3.163	2.163
3	3.4633	2.154	1.154
4	3.1131	1.778	0.778
5	2.9264	1.585	0.585
6	2.8106	1.468	0.468
7	2.7943	1.399	0.399

The results of calculations show that the optimal values of residence time of the reactors within each of the cascades are equal, the ratio of input and output concentrations are equal also, therefore, all the volumes of the reactors are equal for each cascade.

In literature (EFREMOV 2001) it is observed that the concentrations in the cascade of reactors of ideal mixing can be represented graphically. Each reactor of the cascade is one-step concentration change as the concentration changes abruptly. The line connecting the top of each step of the reactor cascade corresponds to the same curve of the ideal isothermal plug flow reactor. The graphic for the cascade of five reactors (Table 1) is shown in Figure 6 in the coordinates of the concentration – residence time. The curve connecting the top of the steps of the reactors of the cascade, is built on the equation of isothermal ideal plug flow reactor (KRAMERS, WESTERTERP 1963, EFREMOV 2016).

$$x/x_0 = \exp(-k \ \tau) \tag{17}$$

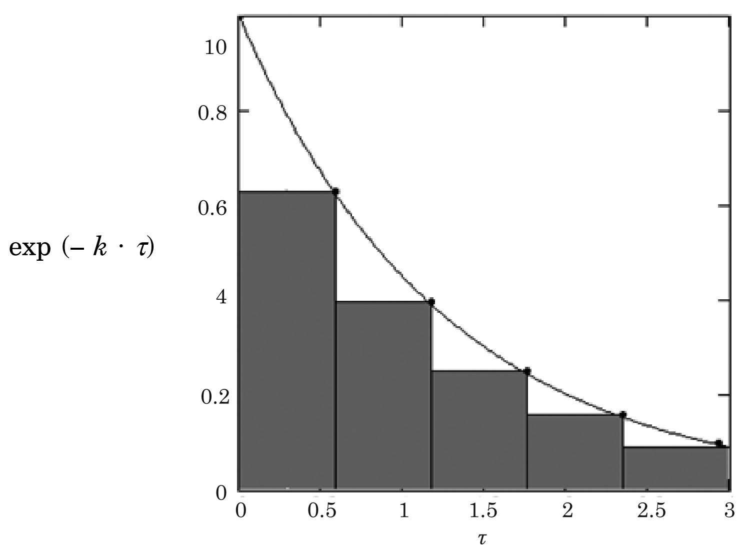

Fig. 6. Dependence of the concentration x from the residence time p for the cascade of five reactors

Experimental part

As an example of the using of the dynamic programming PC method, the design optimization of a polymerization process in the four ideal mixing reactors cascade is considered. The experimental data are used from (HARRIOTT 2003). The reaction of polymerization is the first order. The degree of conversion is 95%, i.e. the concentration at the outlet of the last reactor $x_4 = 0.05$. Calculation of reaction rate constants is made according to the experiment in a single reactor, where the residence time to reach a given degree of conversion amounted to $\tau = 6$ h. The constant for the rate of the first order chemical reaction was calculated according to the equation

$$k = \frac{1}{\tau} \ln \left(\frac{1}{x_4} \right) \tag{18}$$

In Figure 7 the calculation in MathCAD the optimal parameters of the polymerization process (HARRIOTT 2003) in the cascade of four ideal mixing reactors is shown. Calculation of reaction rate constant according to equation (18) yields the value $k = 0.499$ $h^{-1}(mole/l)^{-1}$.

The residence time in the each reactor (Fig. 7) is written similarly to equations (7), (8), (13).

Optimization function $f(x_1, x_2, x_3)$ is the total residence time in all reactors. Unknown values are the concentrations at the outlet of the first three reactors: x_1, x_2, x_3. When calculating the specified initial approximation for these positive values of concentrations, then by the code word "Given" a program to find the minimum value of the total residence time in the cascade of reactors starts:

$$P = \text{minimize}\ (f, x_1, x_2, x_3).$$

The calculation results are obtained in the concentration of $x_1 = 0.4728$ h^{-1} l $mole^{-1}$, $x_2 = 0.2236$ h^{-1} l $mole^{-1}$ and $x_3 = 0.1057$ h^{-1} l $mole^{-1}$. The minimum value of the total residence time is 8.928 h, and the residence time in each reactor is 2.235 h. The value of the ratio of output and input concentrations in each reactor is 0.473.

Conclusion

The modeling and optimization of multi-stage processes in cascade of consecutive ideal mixing isothermal reactors by the method of dynamic programming are considered. It is found, that the minimum volume of the cascade of reactors for isothermal reaction of the first order corresponds to the minimum residence time of substance in this cascade. In this case, the optimum meanings of residence time for all reactors are equal and all ratio of input and output concentration are equal. Hence, and all volumes of reactors are also equal.

The modeling and optimization of N consistently connected isothermal reactors can be similarly executed, that also gives result in equality of volumes of reactors and equality of residence time of the reactive mixture in each reactor.

Initial data: $x_4 = 0.05$ outlet concentration for 4-th reactor, mole/l
$\tau = 6$ residence time for single reactor, h
$x_0 = 1$ inlet concentration for first reactor, mole/l

Chemical rate constant: $k = \dfrac{\ln\left(\dfrac{1}{x_4}\right)}{\tau}$ $k = 0.499$ $\mathrm{h^{-1}}$

Residence time for 4-th reactor: $\tau_4 = \dfrac{1}{k}\left(\dfrac{x_3}{x_4} - 1\right)$

Residence time for 3-rd reactor: $\tau_3 = \dfrac{1}{k}\left(\dfrac{x_2}{x_3} - 1\right)$

Residence time for 2-nd reactor: $\tau_2 = \dfrac{1}{k}\left(\dfrac{x_1}{x_2} - 1\right)$

Residence time for 1-st reactor: $\tau_1 = \dfrac{1}{k}\left(\dfrac{x_0}{x_1} - 1\right)$

Find concentrations x_1, x_2 and x_3

Residence time for 4 reactors: $\tau_1 + \tau_2 + \tau_3 + \tau_4 = \dfrac{1}{k}\left(\dfrac{x_0}{x_1} + \dfrac{x_1}{x_2} + \dfrac{x_2}{x_3} + \dfrac{x_3}{x_4} - 4\right)$

Calculation of x_1, x_2 and x_3

Optimization function: $f(x_1 + x_2 + x_3) = \dfrac{1}{k}\left(\dfrac{x_0}{x_1} + \dfrac{x_2}{x_3} + \dfrac{x_1}{x_2} + \dfrac{x_3}{x_4} - 4\right)$

$x_1 = 1$ $x_2 = 1$ $x_3 = 1$ Given $x_1 \geq 0 x_2 \geq 0$ $x_3 \geq 0$

$P = \text{Minimize}\ (f, x_1, x_2, x_3)$ $P = \begin{pmatrix} 0.4728 \\ 0.2236 \\ 0.1057 \end{pmatrix}$ $f(P_0, P_1, P_2) = 8.9306$

$(\tau_1 + \tau_2 + \tau_3 + \tau_4)_{\min} = 8.9358$ $x_1 = 0.4728$ $x_2 = 0.2236$ and $x_3 = 0.1057$

Residence time for each reactor: | Ratio of output and input concentrations:

$\tau_1 = \dfrac{1}{k}\left(\dfrac{x_0}{x_1} - 1\right)$ $\tau_1 = 2.233$ $\dfrac{x_1}{x_0} = 0.473$ $\dfrac{x_0}{x_1} = 2.115$

$\tau_2 = \dfrac{1}{k}\left(\dfrac{x_1}{x_2} - 1\right)$ $\tau_2 = 2.232$ $\dfrac{x_2}{x_1} = 0.473$ $\dfrac{x_1}{x_2} = 2.114$

$\tau_3 = \dfrac{1}{k}\left(\dfrac{x_2}{x_3} - 1\right)$ $\tau_3 = 2.234$ $\dfrac{x_3}{x_2} = 0.473$ $\dfrac{x_2}{x_3} = 2.115$

$\tau_4 = \dfrac{1}{k}\left(\dfrac{x_3}{x_4} - 1\right)$ $\tau_4 = 2.231$ $\dfrac{x_4}{x_3} = 0.473$ $\dfrac{x_3}{x_4} = 2.114$

Total residence time for cascad of 4 reactors: 42.232 = 8.928 h

Fig. 7. Calculation in MathCAD of optimal parameters for polymerization process (HARRIOTT 2003) in the cascade of four ideal mixing reactors

Permission

The authors of the article have the permission from Moscow Technological Institute to publish this paper.

References

ARIS R. 1976. *Introduction to the Analysis of Chemical Reactors*. Chemistry, Leningrad.
BOYARINOV A.I., KAFAROV V.V. 1975. *Methods of optimization in chemical technology*. In: *Chemistry*. Ed. 2, Moscow.
BRAYNES J.M. 1976. *Introduction in theory and calculations of chemical and petrochemical reactors*. Chemistry, Moscow.
COKER A.K. 2001. *Modeling of Chemical Kinetics and Reactor Design*. Gulf Publishing Company, Houston, Texas.
EFREMOV G.I. 2001. *Macrokinetics of transfer processes*. MSTU, Moscow.
EFREMOV G.I. 2016. *Modeling of chemical technological processes*. INFRA-M, Moscow.
Handbook of Industrial Mixing: Science and Practice. 2004. Eds. E.L. Paul, V.A. Atiemo-Obeng, S.M. Kresta. John Wiley & Sons, Inc. New York.
HARRIOTT P. 2003. *Chemical Reactor Design*. Marcel Dekker Inc., New York.
KOROBOV V.I., OCHKOV V.F. 2011. *Chemical Kinetics with Mathcad and Maple*. Springer-Verlag, Wien.
KRAMERS H., WESTERTERP K. 1963. *Elements of Chemical Reactor Design and Operation*. Netherlands University Press.
LEVENSPIEL O. 1965. *Chemical Reaction Engineering*. John Willey and Sons, Inc. New York.

Technical Sciences, 2017, 20(2), 161–169

UNIWERSYTET WARMIŃSKO-MAZURSKI W OLSZTYNIE

Quarterly peer-reviewed scientific journal
ISSN 1505-4675
e-ISSN 2083-4527
TECHNICAL SCIENCES
Homepage: www.uwm.edu.pl/techsci/

THE IMPACT OF PRETREATMENT SEMI-PRODUCTS ON THE TEXTURE OF FRIED POTATOES

***Zygmunt Sobol*[1], *Tomasz Hebda*[2], *Bogusława Łapczyńska-Kordon*[2]**

[1] Institute of Machinery Management Ergonomics and Production Processes
University of Agriculture of Krakow
[2] Department of Mechanical Engineering and Agrophysics
University of Agriculture of Krakow

Received 25 March 2016, accepted 21 March 2017, available online 27 March 2017

Key words: potato tuber, fried products, texture.

Abstract

The aim of the study was to determine the effects of time and temperature during the pre-treatment in hot water semi-products obtained from potatoes. This treatment results in leaching of reducing sugars and influences on the texture of fried potato products. Studies were carried out on samples of potatoes in the form of slices (having a diameter of 57 mm and a thickness of 4 mm) and sticks having a cross section of 10×10 mm and a length of 100 mm.The semi-products formed had a comparable weight of ca. 10 g. Prepared semi-product were immersed in demineralised water at temperature 20^{o}C, 30^{o}C, 40^{o}C. The immersion time was 5 min, 10 min, 15 min, 20 min.

Ater 10 minutes from frying ended, the products were subjected to loads in which unit cutting resistance values were measured (N:mm-1), which served as the texture indicators. The product shape, temperature of water for washing sugars and treatment time are statistically significant for product texture. Lower texture values are found in the slices. The sample tested significantly differs, in unit cutting resistance values, from other samples subjected to washing ope1ration.

Correspondence: Bogusława Łapczyńska-Kordon, Katedra Inżynierii Mechanicznej i Agrofizyki, Wydział Inżynierii Produkcji i Energetyki, Uniwersytet Rolniczy im. Hugona Kołłątaja, ul. Balicka 120, 30-149 Kraków, phone: 12 662 46 42, e-mail: Boguslawa.Lapczynska-Kordon@ur.krakow.pl

Introduction

The basic technological processes of production of French fries are classified as: blanching, drying up, stir-frying and frying (ABGLOR, SCANLON 1998). Blanching is one of the most important stages of the manufacturing process chips. In industrial practice used to blanch french fries in water at different temperatures and for different lengths of time (JASWAL 1970, LISIŃSKA, LESZCZYŃSKI 1989) All these processes cause a change in the texture of the finished product.

Texture is one of the most important quality features thermally processed potatoes. It is a feature of a qualitative multidimensional, defined as a general structural characteristics and rheological properties of the product (SURMACKA-SZCZEŚNIAK 2002). Texture is described by a number of parameters, such as hardness, consistency, viscosity, elasticity, adhesiveness, gumminess and chewiness. These parameters are measured instrumentally using a texture analyzer, which enable the various tests consisting in the cutting, crushing, penetration and tensile samples (CIVILLE, SURMACKA-SZCZEŚNIAK 1973). Apparatus for measuring texture are related to sensory evaluation since they are important components which affect the evaluation of the texture of food. Therefore, the correlation between the measurements instrumental and sensory analysis is related, as it enables a more complete interpretation of the results of the sensory properties of the products. This method has been widely used to assess the impact properties of potatoes, pretreatment and process parameters on the texture of the product subjected to thermal processing. The measurement consisted in determining the strength characteristics of the product (eg. French fries) (PEDRESCHI et al. 2004, STONEHAM et al. 2000). Changes in texture properties depend mainly on the chemical composition of the raw material. On the basis of presented in the literature, it can be concluded that the effect on changes in texture potatoes are: dry matter content, and compounds such as starch, polysaccharides, and in particular the compounds of pectin (pectin total protopectin, pectin soluble) that are present in the spaces intercellular, as a binder not woody plant cell wall (TAJNER-CZOPEK et al. 2003, GOŁUBOWSKA, LISIŃSKA 2005). It has been found that potato bulb with a higher dry matter content reflect less water during frying, which leads to increased productivity and, moreover, are more crunchiness and brighter color (LISIŃSKA 2006, LISIŃSKA, LESZCZYŃSKI 1989, JASWAL 1991). The literature shows that chips made from potato bulb with a higher starch content are crisp, tender, low in fat, and their texture is not greasy (LESZCZYNSKI, LISIŃSKA 1985). Potato tubers for french fries should contain 14 to 18% starch, because too much of this ingredient causes unfavorable color changes and the formation of a spongy fried structure during frying. While too little starch content causes the tubers absorb more fat during frying (TAJNER-CZOPEK et al. 2008). Important from the point of view of the structural characteristics of French fries has a fiber content in potato tubers – the higher, the better the quality of the fries (JARVIS, DUNCAN 1992, ANDERSSON et al. 1994). Research has shown that the heat treatment of potato tubers, among other things, soaking in warm water, a change in the chemical composition of potatoes, and the same texture. It was found that during peeling, blanching and deep-frying content increases protopectin in pectin and potato dry matter (GOŁUBOWSKA, LISIŃSKA 2005).

Soaking in water entails a reduction in the density of semi-finished products for chips (SOBOL 2007a, b, 2009, 2010). On the dynamics of changes in the density of semi-finished products is affected by water temperature and duration of the process (elution time) and physiological age tubers (SOBOL 2007a, b, 2009, 2010). Also, the shape and size of semi-finished products is influenced on the process of soaking in water. The dimension determines the kinetics of diffusion processes, among other sugars and the solid, thus causing lowering of density values. Research has shown that even a 5 minute soaking in water semi reduces the density of technologically significant value (SOBOL 2007b, LISIŃSKA 2006). Lowering of density may result in changes in the conditions of frying, and it affects the consistency of the finished products. It has been found that the structure of the potato change during processing due to water loss and tissue damage. This in turn influences the change of non-starch polysaccharides and lignin. The greatest changes in the tissue of potato result from thermal processes: blanching, drying and pre-frying (GOŁUBOWSKA, LISIŃSKA 2006). The observed amendments are affecting a texture of the product.

Hence the aim of the research was to determine the influence of time and temperature while the pre-treatment in hot water semi- products of the potato on a consistency of fries.

Materials and Methods

Sticks and slices made of Arielle potato specie were used for the tests. Arielle potato is a very early edible B type (general purpose) specie with oval tubers and light yellow pulp. It contains ca. 12.5% starch. The sticks were cut from tubers along the axis connecting the top and bottom part, and slices were cut transversely to that line. The semi-products formed had a comparable weight of ca. 10 g. The strips were square in cross section with 10 mm long sides, with the length 100 mm. The slices were 57 mm in diameter and 4 mm thick. Following the forming, all samples were shortly washed with running water and wiped with a paper towel. The formed semi-products were immersed in demineralised water at the temperature of 20, 30, 40°C. The immersion time was 5, 10, 15 and 20 minutes. The tested sample contained semi-products without pre-treatment. Samples with the weight of ca. 120 g (12 pieces) were fried in refined rapeseed oil (3 litres) in a deep fryer. Frying temperature was equal for the sticks and slices and it was 170°C. Frying time was selected experimentally in preliminary tests, and it was 7.5 min. for the sticks and 7 min. for slices. After frying, the strips and slices were drained of the excess oil on the fryer basket and paper towels and, 10 min after frying, subjected to load, to measure the unit cutting resistance ($N \cdot mm^{-1}$). The strips were cut laterally (in the middle) and the slices laterally, along the diameter. Unit cutting resistance values were determined by referencing the maximum cutting force to the active blade length. For cutting resistance measurements, a 0.6 mm thick steel knife, sharpened at the angle 14°, was used. The tests were performed with Insight 2 (Insight Testing System) MTS (made in USA) strength testing machine controlled by a PC with the TestWorks 4 control and recording software. The application allows broad use of the machine for testing material strength. The objects tested were fixed horizontally to a stationary table and cut with a knife mounted in the measuring head clamp, moving at constant speed ($10 \ mm \cdot min^{-1}$). The measurement was continued until complete splitting of a strip or slice. After prior implementation of the procedure for unit cutting resistance calculations in the Test Works 4 software, it continually analysed the results obtained, proposing location of specific points on the plot, including the one corresponding to the maximum force applied in the test. On completion of tests, the program automatically stored the results (HEBDA, FRANCIK 2008, HEBDA et al. 2012).

Test results were statistically processed with STATISTICA 10 software, using variance analysis for factor-based systems, and homogeneous groups in the post-hock tests, were determined with Duncan's multiple range test.

Results and Discussion

On the basis of analysis of variance in the classification triple was found that all adopted experimental factors – a shape of a semi-product, the water temperature, time soaking in water – have had the statistically significant effect on a cutting resistance the tested products. Also, the interaction between the factors – the shape of the semi-products and the time of pre-treatment samples in hot water – was the statistically significant (Tab. 1).

Table 1

Results of one-dimensional significance test, semi-product shape, temperature of water and the pre-treatment time effects on the variations of unit cutting resistance values of the fried products (α = 0.05 significance level assumed)

Quality predictor	Sum of squares	Degrees of freedom	Average square	F	p
Absolute term	16.99019	1	16.99019	7404.700	0.000000
{1}Product shape	2.99588	1	2.99588	1305.669	0.000000
{2} Temperature	0.02291	2	0.01145	4.992	0.007312
{3}Water sorption time	0.03653	4	0.00913	3.980	0.003613
1·2	0.00602	2	0.00301	1.313	0.270533
1·3	0.02496	4	0.00624	2.720	0.029689
2·3	0.01495	8	0.00187	0.814	0.590471
1·2·3	0.01962	8	0.00245	1.069	0.384455
Error	0.75719	330	0.00229	–	–

The analysis of the obtained results show that the individual resistance of cutting slices (0.13 N · mm^{-1}) are smaller than strips (0.31 N · mm^{-1}) (Fig. 1). The difference in unit values cutting resistances between products of accepted forms is high – resistance to fries are ca. 2.4 times higher than for slices (Fig. 1). Such a large difference may be due to simultaneous interaction of several factors. First of all, a different rate of diffusion of the nutrients contained in the cell juice and leaching solid. Samples in the form of slices are thinner than fries and probably, the process of diffusion and leaching proceeded faster. It could be the case of loss of a weight and a structure of the material, and thus a density and a consistency (SOBOL 2007b).

The differences in consistency of the tested object with different shape can also be sought in different loading orientation of the samples tested and share of tissue in the loading zone. The strips were subjected to transverse load to the centreline (axis between the top and bottom part), with the predominant share of core pulp and internal core cells. The slices were loaded along the longitudinal axis and, at the cutting zone (at the active blade length), cells of cortex pulp, fibro vascular bundles, core pulp and internal core. In the tests carried out by the authors, high consistency was achieved as compared to the results presented by KOWALCZYK and GUSTAW (2009). In this experiment involving coating the semi-products for French fries (with cross sectional dimension 10 × 10 mm) with hydrocolloidal solutions, while cutting the sample strips, the resistance of 3.22 N was noted. Strips coated with the solutions tested were characterised by much denser texture, from 3.85 to 6.06 N (KOWALCZYK, GUSTAW 2009).

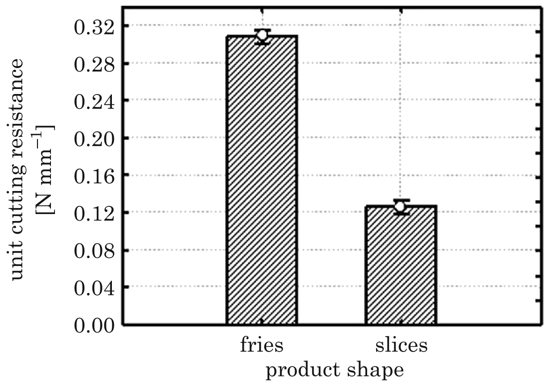

Fig. 1. Effects of product shape on the unit cutting resistance values

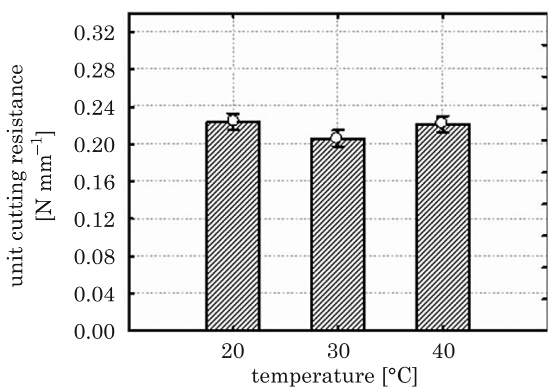

Fig. 2. Effect of the temperature of water on the unit cutting resistance

Analysis of the results of measurement for various temperatures during pre-treatment samples in hot water showed that the use of water baths at different temperatures helped to change the consistency (Fig. 2, 3). Statistically significant changes (on the basis of the test Duncan) were found between the texture of products in the bath at 30°C (0.21 N · mm^{-1}) and those from the other experimental combinations (0.22 N · mm^{-1}) (Fig. 2).

The time pre-treatment semi-products in hot water affected considerably the texture of tested products (Fig. 4, 5, 6). According to the Duncan test, consistency of the test sample (0.23 N · mm^{-1}) differs considerably from other samples texture (0.20–0.22 N · mm^{-1}) (Fig. 4).

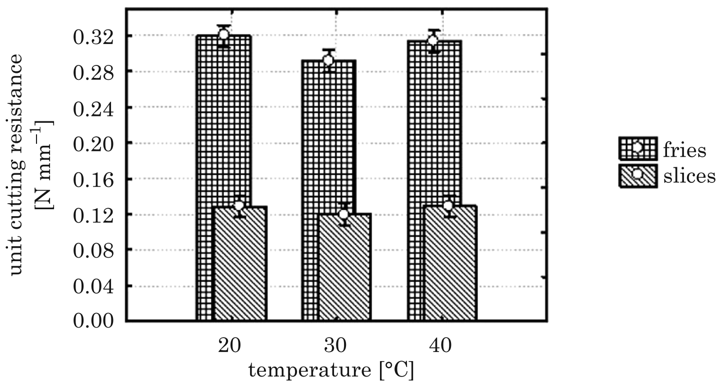

Fig. 3. Effects of the temperature of water on the unit cutting resistance of strips and slices

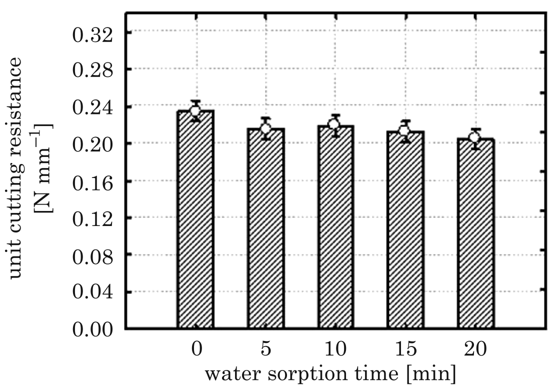

Fig. 4. Effects of the time pre-treatment in hot water on the unit cutting resistance

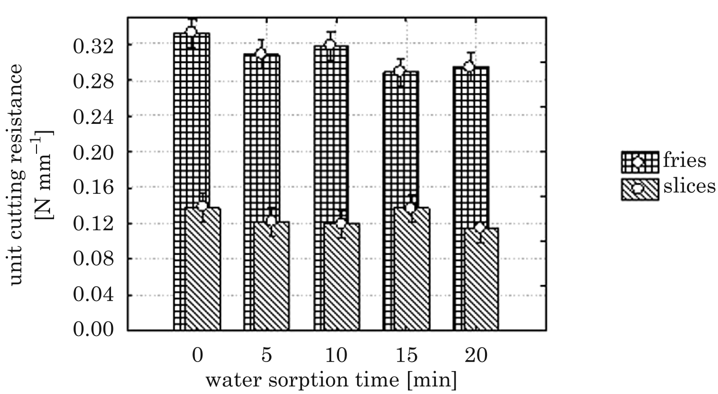

Fig. 5. Effects of the time pre-treatment semi-products in hot water on the unit cutting resistance of strips and slices

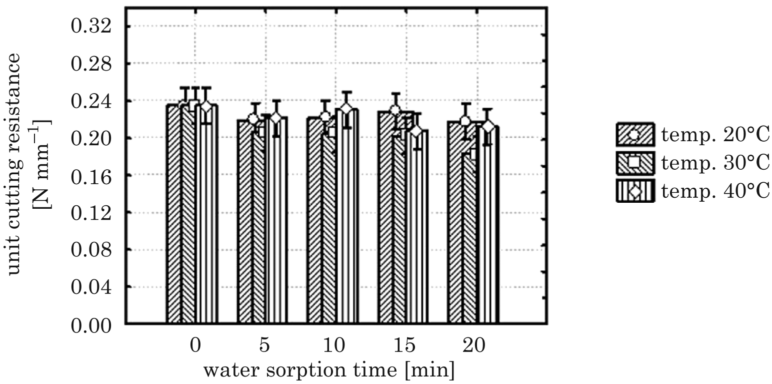

Fig. 6. Effect of the time pre-treatment semi-products in hot water on the unit cutting resistance in the temperature range applied

In the experiment analysed, the value of unit cutting resistance was mostly affected by the product shape (table 1) (Fig. 1, 3, 5), and the effects of other factors were statistically significant, but much weaker (Tab. 1, Fig. 2, 3, 4, 5), and there is no knowledge if this is sensed by the consumer.

Conclusions

1. All the experimental factors assumed, product shape, temperature of water for pre-treatment semi-products of a potate and treatment time are statistically significant for the product texture.

2. Much thinner texture (measured by unit cutting resistance values) have sliced products as compared to the strips.

3. Pre-treatment semi-products in water at temperature 30°C resulted in a decline in unit cutting resistance to the lowest value in the field of research.

4. The time of pre-treatment semi-products in hot water are insignificant for the texture, however, considerable difference occurs as compared to the test sample.

References

ABGLOR A., SCANLON M.G., 2000. *Processing conditions influencing the physical properties of French fries potatoes.* Potato Res., 43: 163–178.

ANDERSSON A., GEKAS V., LIND I., OLIVEIRA F., ÖSTE R., AGUILFRA J.M. 1994. *Effect of preheating on potato texture.* Critical Reviews in Food Science & Nutrition, 34(3): 229–251.

CIVILLE G.V., SZCZESNIAK A. S. 1973. *Guidelines to training a texture profile panel*. Journal of Texture Studies, 4(2): 204–223.

GOŁUBOWSKA G., LISIŃSKA G. 2005. *Changes in the content of pectic substances and in texture of potatoes during the production of French fries*. Food. Science. Technology. Quality, 1 (42): 63–70.

HEBDA T., FRĄCZEK J., ŁAPCZYŃSKA-KORDON B. 2012. *Influance of storing time on some of qualitative properties of celery root*. Engineering Sciences and Technologies. 3(6): 65–78.

HEBDA T., FRANCIK S. 2008. *SSN model of determination of the force destroying the walnut cover.* Agricultural Engineering, 11(109): 83–90.

JARVIS M.C., DUNCAN H.J. 1992. *The textural analysis of cooked potato.* 1. *Physical principles of the separate measurement of softness and dryness*. Potato Research, 35(1), 83–91.

JASWAL A.S. 1970. *Effects of various chemical blanchings on the texture of French fries.* American Journal of Potato Research, 47(1), 13–18.

KOWALCZYK D., GUSTAW W. 2009. *Effect of hydrocolloid coatings on quality parameters of French fries.* Food. Science. Technology. Quality, 6(67): 72–80.

LESZCZYŃSKI W., LISIŃSKA G. 1985. *Effect of herbicides on chemical composition of potato tubers and quality of the subsequent chips and starch.* Starch-Stärke, 37(10): 329–334.

LISIŃSKA G. 2006. *Technological value and quality of polish potatoes.* Advances of Agricultural Sciences Problem, 511(I): 81–94.

LISINSKA G., LESZCZYNSKI W. 1989. *Potato tubers as a raw material for processing and nutrition*. Potato Science and Technology, 11: 113.

PEDRESCHI F., SEGNINI S., DEJMEK P. 2004. *Evaluation of the texture of fried potatoes.* Journal of Texture Studies, 35(3): 277–291.

SOBOL Z. 2007a. *Changes of potato bulb density caused by water transpiration and absorption during storage.* Agricultural Engineering, 6(94): 231–240.

SOBOL Z. 2007b. *Changes in density losses in posts and slices cut out from potato tubers, resulting from water absorption.* Acta Agrophysica, 151: 219–228.

SOBOL Z. 2009. *The impact of blanching and water sorption on the change in density of semi-finished products for chips*. Agricultural Engineering, 9(118): 257–264.

SOBOL Z. 2010. *The impact of temperature of water sorbed by ready-to-cook potato chips semiproducts on change in their density*. Acta Agrophysica, 182: 435–450.

STONEHAM T.R., LUND D.B., TONG C.H. 2000. *The use of fractional conversion technique to investigate the effects of testing parameters on texture degradation kinetics.* Journal of Food Science, 65(6): 968–973.

SURMACKA-SZCZEŚNIAK A. 2002. *Texture is a sensory property*. Food Quality and Preference. 13(4): 215–225.

TAJNER-CZOPEK A. 2003. *Changes of pectic substances concentration in potatoes and French fries and the effect of these substances on the texture of the final product.* Molecular Nutrition & Food Research, 47(4): 228–231.

TAJNER-CZOPEK A., KITA A., LISIŃSKA G. 2008. *The content of acrylamide in French fries depending on the temperature and time of frying*. Zesz. Probl. Post. Nauk Roln., 530: 371–379.

TAJNER-CZOPEK A., KITA A., RYTEL E., GOŁUBOWSKA G. 2003. *The content of non-starch polysaccharides and lignin in potato tubers of differing lengths of the vegetation period.* Zesz. Probl. Post. Nauk Rol., 489: 291–299.

Technical Sciences, 2017, 20(2), 171–179

Quarterly peer-reviewed scientific journal
ISSN 1505-4675
e-ISSN 2083-4527
TECHNICAL SCIENCES
Homepage: www.uwm.edu.pl/techsci/

CHARACTERISTICS OF POROUS BEDS BASED ON FRACTAL PARAMETERS

***Mirosław Bramowicz*[1], *Sławomir Kulesza*[2], *Wojciech Sobieski*[3]**

[1] Department of Materials and Machine Technology
[2] Department of Relativistic Physics
[3] Department of Mechanics and Basics of Machine Construction
University of Warmia and Mazury in Olsztyn

Received 6 October 2016, accepted 25 March 2017, available online 27 March 2017

Key words: granular beds, porosity, fractal analysis, numerical modelling.

Abstract

The paper presents the results of a fractal analysis of the cross-sections of a porous mineral deposit consisting of spherical elements which formed a spatial system with varying porosity (0.4 to 0.95). The virtual deposit was generated using the Discrete Element Method in the YADE code by means of the so-called Radius Expansion Method. The fractal analysis was carried out using the structure function method, determining the fractal dimension (D), the topothesy (L) and the corner frequency (l) (MAINSAH et al. 2001). The conducted simulations have confirmed to a considerable extent the test results available in the literature involving the fractal analysis of mineral deposits with varying porosity. They clearly indicate that the fractal dimension does not change along with the porosity of the deposit, if the autocorrelation function or their transformations (e.g. structure function) methods are used. Moreover, based on the information available in the literature, it can be concluded that the value of the fractal dimension corresponds to mineral deposits with the specified geometric shapes of the elements which form them.

Introduction

The term “fractal” was introduced near the end of the 20th century by Benoit Mandelbrot; in Latin it means “broken, fractional” (MANDELBROT 1982). It is most commonly used to describe self-similar objects, meaning those whose certain small fragment is a scaled copy of the entire object. Therefore,

Correspondence: Katedra Technologii Materiałów i Maszyn, Wydział Nauk Technicznych, Uniwersytet Warmińsko-Mazurski, 10-719 Olsztyn, ul. Oczapowskiego 11, phone: 89 523 38 55, e-mail: miroslaw.bramowicz@uwm.edu.pl

the entire fractal object may be depicted by the subsequent iterations of that small fragment.

Fractal methods are widely used, primarily in computer science, mathematics and in many related fields of science, e.g. materials engineering, geology and even economics. Not only does their use focus on the geometric analysis of physical objects, but it also exceeds beyond it. They are found useful in the description of non-geometric values, e.g. the domain structures of magnetic materials, tendencies in financial markets, etc. (BRAMOWICZ et al. 2014, ANDRONACHE et al. 2016).

Several methods of fractal analyses are in common use, the main ones being: the variance method, box-counting, methods based on the structure function analysis S(l) (SAYLES, THOMAS 1977, MAINSAH et al. 2001) and the spectral density function PSD (KULESZA, BRAMOWICZ 2014, YADAV et al. 2015). As is known from the comparison of the results of a previously conducted experiments and computer simulations, the value of the fractal parameter heavily depends on the used method, which is why in these types of analyses the method should always be specified (KULESZA, BRAMOWICZ 2014).

Fractal methods were also found useful in the description of porous deposits (SUN, KOCH 1998) and turbulent flows (VAN'YAN 1996). The present paper uses the structure function method S(l) for the first time to correlate the characteristics of porous deposits and fractal parameters. When analysing the S(l) dependence plotted on a log-log graph and described by the formula (1), we can determine the above-mentioned fractal parameters: D, Λ, l (Fig. 1).

$$S(l) = \Lambda^{2(D-1)} l^{2(2-D)} \tag{1}$$

where:
l – the distance [m] between two points on the cross-section of the analysed deposit,
D – fractal dimension ($2<D<3$) [–],
Λ – topothesy [–].

The goal of the research described in the paper was to check the dependencies between the porosity of a granular deposit and the fractal parameters, especially in relation to a paper (SUN, KOCH 1998) which stated that for a virtual deposit generated according to the TBM model (Turning Bands Methods) there is no correlation between the fractal dimension and the porosity of the deposit. It should be pointed out that the research conducted in the paper cited herein was related to geological issues, in which the geometric structure of the porous medium was considerably different from the structure of the granular system used in the tests described in this paper.

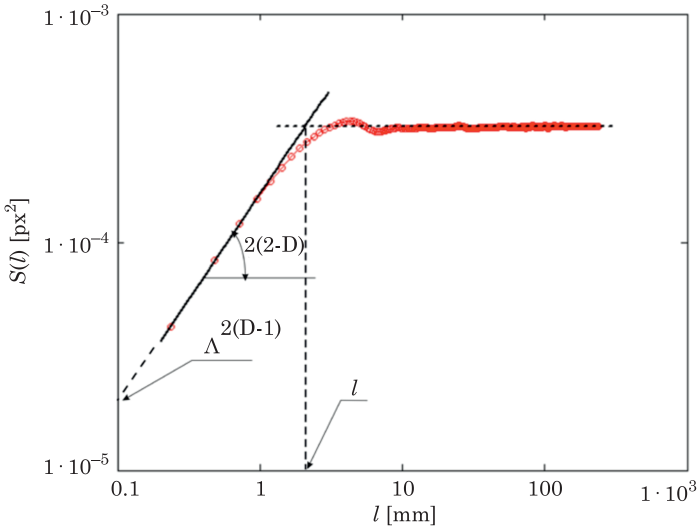

Fig. 1. A sample plot of the structure function

The material present in the article constitutes a fragment of broader research associated, among others, with the methods of the dimensional characterization of the spatial structure of granular deposits (e.g. SOBIESKI, LIPIŃSKI 2016, SOBIESKI et al. 2016). This issue is important not just in the context of the description of the porous material itself, but also in the context of predicting fluid flow resistances in such media. The search for possibilities of introducing fractal parameters into analytical models, such as the Forchheimer equation (SOBIESKI, TRYKOZKO 2011), became the main motivation to commence the research. No attempts to conduct any analyses of similar types had been made in the literature known to the authors.

Virtual deposits

The main parameter that characterizes porous beds is their porosity, that is the ratio of the volume of empty spaces randomly distributed within a solid to its total volume. In order to examine the impact of the degree of porosity of the deposit on the fractal parameters, a set of virtual granular deposits was generated with identical macroscopic dimensions (0.08×0.08×0.16 [m]) and porosities ranging between 0.4 and 0.95 (Fig. 2). The deposits were generated in the Yade numerical code (YADE 2016) using the Discrete Element Method (CUNDALL, STRACK 1979). The number of particles in each deposit was identical and amounted to 5000. The so-called Radius Expansion Method was used in order to obtain various porosities (Yade Documentation 2016, SOBIESKI et al. 2016). This method involves gradually increasing the radius of all particles in the initial cloud (generated randomly), until obtaining the specified porosity. These radii were constant in each particle cloud and depended only on the target porosity (Fig. 3).

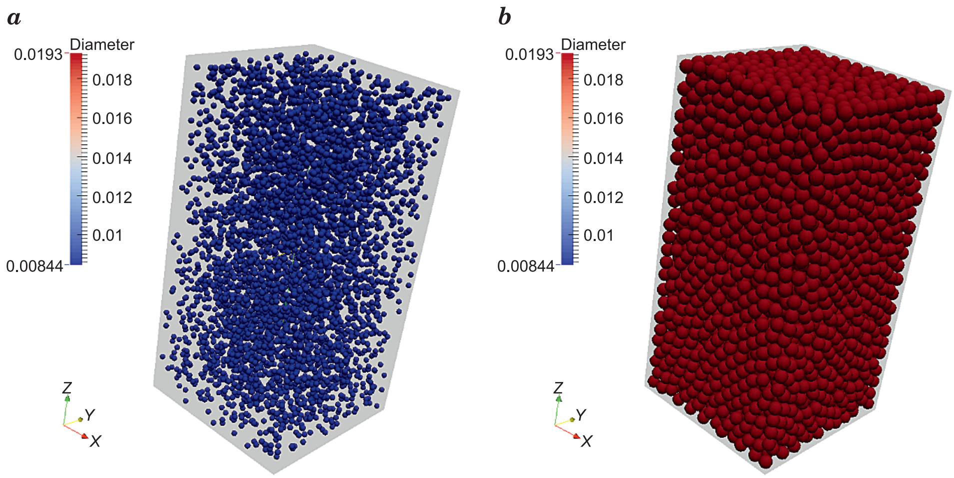

Fig. 2. Visualization of a deposit with porosities of 0.95 (*a*) and 0.4 (*b*)

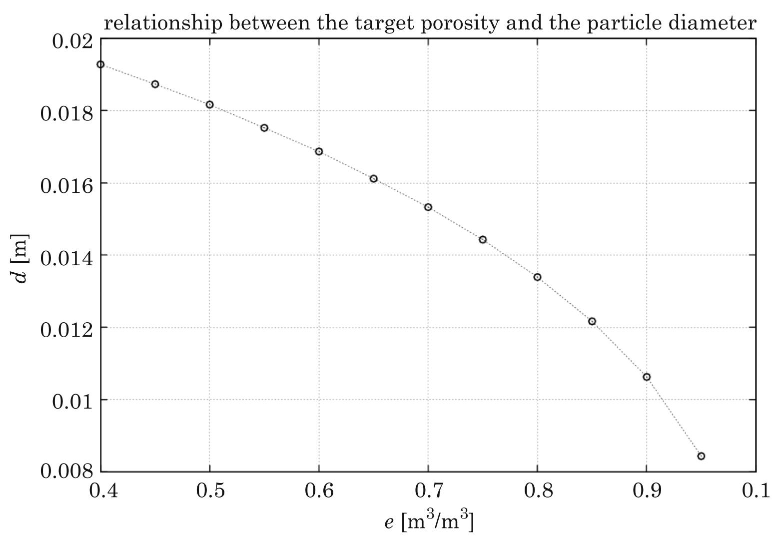

Fig. 3. Plot of particle diameters as a function of porosity

Because fractal analysis is generally performed for shapes in a 2D space, a binarised cross-section in the *YZ* plane was prepared for each virtual deposit for further purposes, passing through the centre of the deposit. Figure 4 presents four selected cross-sections of this type.

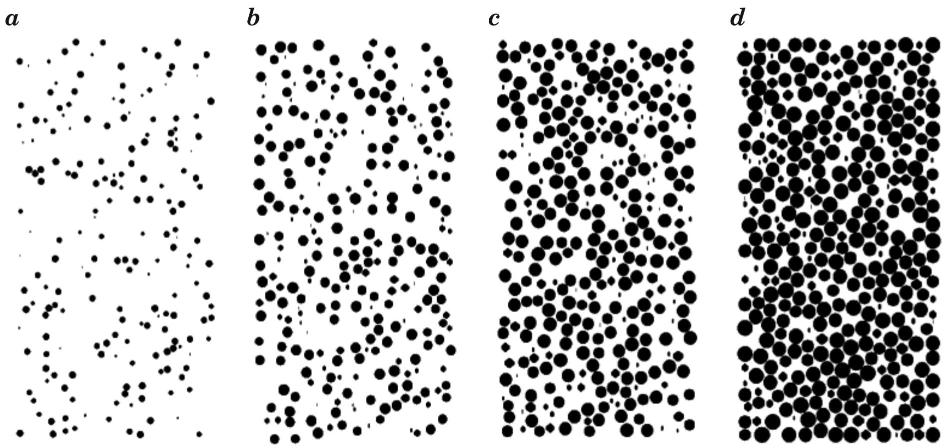

Fig. 4. Visualisation of selected cross-sections of deposits with the following porosities: *a* – 0.95, *b* – 0.8, *c* – 0.6, *d* – 0.4

Fractal analysis of cross-sections of virtual deposits

Subsequently, fractal parameters were determined based on the mean $S(l)$ profiles of the generated deposits, the obtained results being presented in Figure 5.

The conducted simulations indicate that a change in the porosity slightly affects the fractal dimension and other parameters. Observed changes can be fitted numerically with the following function (2–4):

$$D = 0.221P^2 - 0.339P + 2.642 \tag{2}$$

$$l = -16.837P^3 + 28.528P^2 - 14.52P + 4.335 \tag{3}$$

$$\Lambda = \frac{-4.643P + 4.857}{1000} \tag{4}$$

Both fractal dimension and corner frequency depend non-monotonically upon porosity approaching extreme values for P near to 0.8. In contrast, the topothesy is found to decay linearly with the porosity. However, a certain functional dependence is observed with a minimum for $P \approx 0.8$. By determining the average value of the fractal dimension D_{mean} we then get: $D_{mean} = 2.52 \pm 0.01$, while the corner frequency increases to $P \approx 0.8$ and subsequently, after reaching its maximum, it begins to decrease.

The small value of the standard deviation suggests that the fractal dimension can describe granular deposits regardless of their porosity. Similar results, i.e. the lack of a significant impact of the porosity on the fractal dimension, were obtained in a paper (SUN, KOCH 1998). The value of the fractal parameter $D = 2.82 \pm 0.03$ was then obtained for deposits generated using the above-mentioned TBM method. SUN and KOCH (1998) determined the fractal dimension using the autocorrelation function (ACF), which is associated with the structure function according to the formula (5) (MAINSAH et al. 2001):

$$S(l) = 2[ACF(l = 0) - ACF(l)] \tag{5}$$

Therefore, we could say that the results obtained in both experiments are derived using similar method based on the autocorrelation function, which lead to similar conclusions. Detailed analysis of results presented in Figure 4 by SUN and KOCH (1998) exhibits similar trend in the fractal dimension as in our paper providing that the vertical axis is extended.

In the case in question, a decrease in the value of topothesy along with the degree of porosity can also be observed (Fig. 5*b*). In order to examine this trend more precisely, the shape of the autocorrelation function map was analysed (Fig. 6*a*) for the cross-sections of the investigated deposits. Based on the symmetrical shapes of the central peak, it can be unambiguously concluded that in each case under study the deposits are highly isotropic. Using the anisotropy ratio (S_{tr}) of the surface geometrical structure included in the quality standards (PN EN ISO 25178-2:2012, PN EN ISO 25178-3:2012), it can be observed that an increase in porosity is accompanied by a slight increase towards a virtuallỳ ideal' isotropy of the deposits (Fig. 6*b*). Based on the results presented in Figure 4*b* and Figure 5*b*, confirmation of the conclusions presented in papers: THOMAS et al. (1999), BRAMOWICZ (2008) and BRAMOWICZ et al. (2013) was obtained. In these papers it was concluded that slight changes in the anisotropy of the geometric structure are accompanied by changes in topothesy, while the fractal dimension remains unchanged.

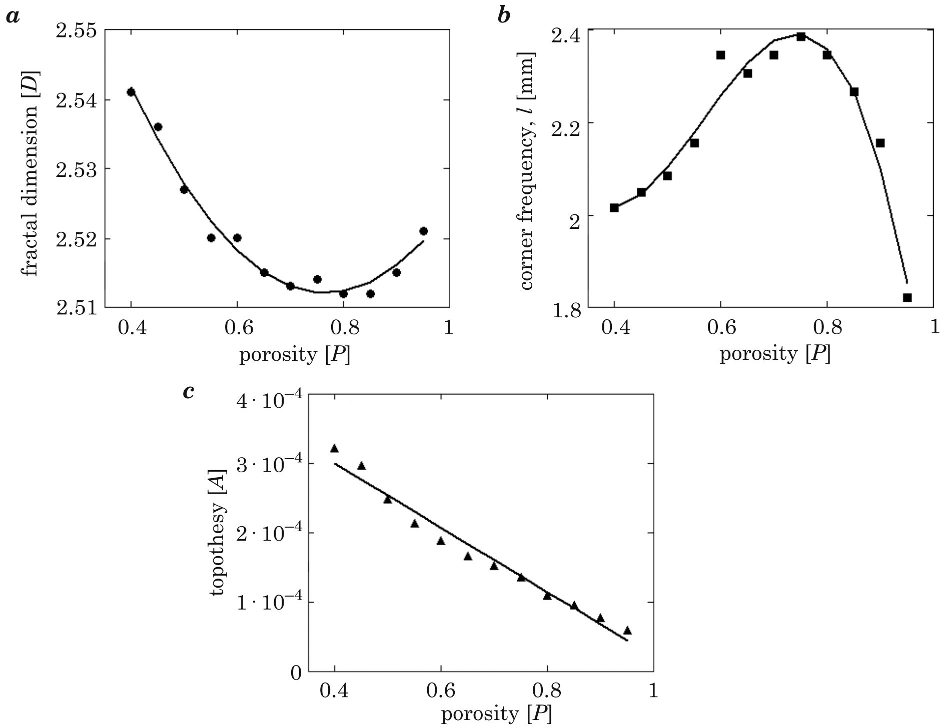

Fig. 5. The influence of the porosity on: *a* – the fractal dimension, *b* – the corner frequency, *c* – the topothesy

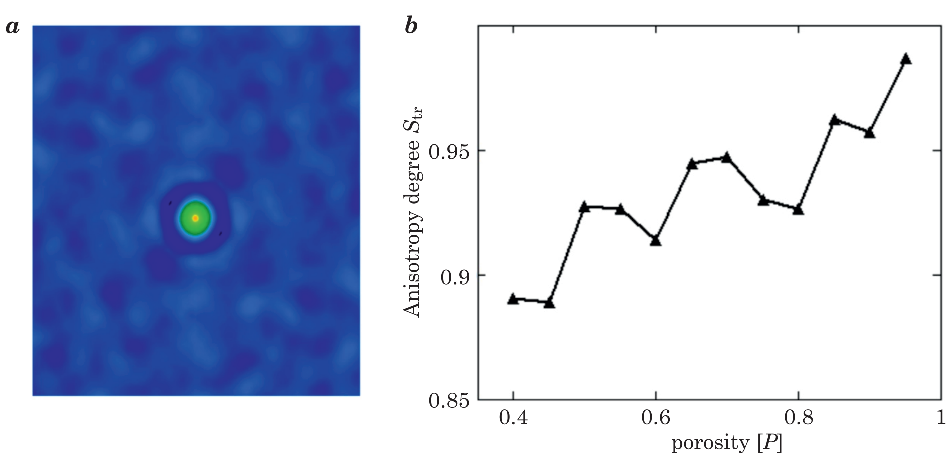

Fig. 6. A sample image of the autocorrelation function of the cross-section of a porous deposit with spherical components (*a*), the plot of porosity vs. anisotropy ratio of the geometric structure of the cross-sections of the analysed deposits (*b*)

Summary

Based on performed simulations the following conclusions can be drawn:

1. Virtual deposits generated by means of the Discrete Element Method may constitute a source of data for fractal analysis.

2. The fractal dimension is most likely dependent on the shape of the deposits' components instead of the degree of their porosity. In this study the components were represented by spherical particles.

3. The fractal dimension determined using the structure function method remains constant at 2.52 ± 0.01.

4. Slight changes in the anisotropy ratio (S_{tr}) for an isotropic cross-sections of deposits composed of spherical particles correspond to changes in the topothesy and the corner frequency.

References

ANDRONACHE I.C., PEPTENATU D., CIOBOTARU A.M., GRUIA A.K., GROPOSILĂ M.N. 2016. *Using fractal analysis in modeling trends in the national economy*. Procedia Environmental Sciences, 32: 344–351.

BRAMOWICZ M., KULESZA S., CZAJA P., MAZIARZ W. 2014. *Application of the autocorrelation function and fractal geometry methods for analysis of MFM images*. Archives of Metallurgy and Materials, 59(2): 441–457.

BRAMOWICZ M. 2008. *Analiza morfologii mikrostruktury martenzytycznej w stopie Ni-Mn-Ga z magnetyczną pamięcią kształtu*. Rozprawa doktorska. UWM Olsztyn.

BRAMOWICZ M., KULESZA S., LIPIŃSKI T., SZABRACKI P., PIATKOWSKI P. 2013. *Fractal Analysis of AFM Data Characterizing Strongly Isotropic and Anisotropic Surface Topography*. Solid State Phenomena, 203–204: 86–89.

CUNDALL P.A., STRACK O.D. 1979. *A Discrete Element Model for granular assemblies.* Géotehnique, 29: 47–65.

KULESZA S., BRAMOWICZ M. 2014. *A comparative study of correlation methods for determination of fractal parameters in surface characterization*. Applied Surface Science, 293: 196–201.

MAINSAH E., GREENWOOD J.A., CHETWYND D.G. 2001. *Metrology and Properties of Engineering Surfaces*. Kluwer Academic Publishers Inc., Norwell, MA.

MANDELBROT B.B. 1982. *The Fractal Geometry of Nature*. W.H. Freeman & Company, New York.

SAYLES R.S., THOMAS T.R. 1977. *Spatial representation of surface roughness by means of structure function – practical alternative to correlation*. Wear, 42: 263–276.

SOBIESKI W., LIPIŃSKI S. 2016. *PathFinder User's Guide*. http://www.uwm.edu.pl/pathfinder (access: 1.05. 2016).

SOBIESKI W., LIPIŃSKI S., DUDDA W., TRYKOZKO A., MAREK M., WIĄCEK J., MATYKA M., GOŁEMBIEWSKI J. 2016. *Grannular porous media*. Department of Mechanics and Machine Design, Olsztyn.

SOBIESKI W., TRYKOZKO A. 2011. *Sensitivity aspects of Forchheimer's approximation*. Transport In Porous Media, 89(2): 155–164.

SUN H., KOCH M. 1998. *Numerical generation of porous structure with fractal properties*. Computational Methods in Water Resources, XII(2): 149–157.

THOMAS T.R., ROSE'N B.G., AMINI N. 1999. *Fractal characterisation of the anisotropy of rough surfaces*. Wear, 232: 41–50.

VAN'YAN P.L. 1996. *Structure function of the velocity field in turbulent flows*. Journal of Experimental and Theoretical Physics, 82(3): 580–586.

YADAV R.P., KUMAR M., MITTAL A.K., PANDEY A.C. 2015. *Fractal and multifractal characteristics of swift heavy ion induced self-affine nanostructured BaF2* thin film surfaces. Chaos, 25: 083115-083115-9.

Yade. https://yade-dem.org/doc/ (access: 1.05. 2016).

Yade Documentation. https://launchpad.net/yade (access: 1.05. 2016).

PN EN ISO 25178-2:2012. *Specyfikacje geometrii wyrobów (GPS) – Struktura geometryczna powierzchni: przestrzenna*. Część 2. *Terminy, definicje i parametry struktury geometrycznej powierzchni.*

PN EN ISO 25178-3:2012. *Specyfikacje geometrii wyrobów (GPS) – Struktura geometryczna powierzchni: przestrzenna*. Część 3. *Specyfikacje operatorów.*

Technical Sciences, 2017, 20(2), 181–198

Quarterly peer-reviewed scientific journal
ISSN 1505-4675
e-ISSN 2083-4527
TECHNICAL SCIENCES
Homepage: www.uwm.edu.pl/techsci/

THE COMPARISON OF EGNOS PERFORMANCE AT THE AIRPORTS LOCATED IN EASTERN POLAND

Adam Ciećko, Grzegorz Grunwald

Geospatial and Civil Engineering
University of Warmia and Mazury in Olsztyn

Received 17 February 2016, accepted 29 March 2017, available online 30 March 2017

Key words: GNSS, EGNOS, Safety of Life service, air navigation.

Abstract

The European Geostationary Navigation Overlay Service (EGNOS) is the first pan-European satellite navigation system. EGNOS makes GPS suitable for safety critical applications such as flying and landing an aircraft. To use EGNOS in aviation the system monitoring and validation in certain localization in needed, as well as official flight procedure design and certification. According to these rules, several GNSS/EGNOS stations located at Polish airfields are currently operational, permanently collecting EGNOS data. The newest monitoring station was established and put into operation at the Polish Air Force Academy in Dęblin in the beginning of 2016.

Dęblin is situated in central-eastern part of Poland (south of Warsaw). Until recently this area was on the edge of official coverage of EGNOS services, especially Safety-of-Life (SoL) service. Latest official documents declare that theoretically the eastern part of Poland is currently fully covered with EGNOS SoL service, however this still needs to be practically confirmed. New station equipped with the newest Javad Delta-3 GNSS receiver will allow to evaluate practical quality of EGNOS in this area.

The article presents preliminary results of EGNOS Safety of Life service performance in Dęblin in comparison to the results obtained in Olsztyn which is situated in north-eastern part of Poland (north of Warsaw). The main parameters characterizing navigational system i.e. accuracy, integrity, continuity and availability were analyzed in detail. The results can be the basis to assess the possibility of implementation of the EGNOS APV approach and landing procedures in Dęblin and Olsztyn.

Correspondence: Adam Ciećko, Katedra Geodezji Satelitarnej i Nawigacji, Wydział Geodezji, Inżynierii Przestrzennej i Budownictwa, Uniwersytet Warmińsko-Mazurski, ul. Heweliusza 5, 10-724 Olsztyn, phone: 89 523 45 24, e-mail: adam.ciecko@uwm.edu.pl

Introduction

Present Global Navigation Satellite Systems (GNSS) undergo significant developments and quality improvements. The number of operational GNSS satellites is growing, allowing for new possibilities in positon determination. Although new multi-constellation techniques (LI et al. 2015a, b), using satellites of GPS, GLONASS, BeiDou and Galileo provide reliable and accurate positioning, this kind of solution cannot be used today for safety of life applications, which require certified augmentation system. EGNOS (European Geostationary Navigation Overlay Service) is a Satellite Based Augmentation System (SBAS) developed by the European Space Agency, the European Commission and EUROCONTROL. Currently it augments the US GPS satellite navigation system and makes it suitable for safety critical applications such as flying aircraft (ALLIEN et al. 2009, GRZEGORZEWSKI et al. 2008, GRUNWALD et al. 2016). EGNOS system has also potential use in other applications not related to aviation such as: navigating ships through narrow channels, road and rail transport, agriculture, surveying, etc. (BAKUŁA et al. 2015, FELSKI et al. 2013). ESA watched over the proper development, validation and practical use of EGNOS since 2009. In contrast, EUROCONTROL was responsible for establishing requirements for the users of the system in civil aviation. The task of the European Union was the development of requirements for the other users of the system.

EGNOS supports GPS since 2005 through the transmission of signals via geostationary satellites, derived on a basis of terrestrial network of permanent stations and control centers which supervise the proper operation of the system (ALLIEN et al. 2009). EGNOS currently supports the GPS system by:

– improvement of the positioning accuracy,
– providing information concerning integrity of positioning,
– synchronizing time in which user's position is calculated with UTC time (Coordinated Universal Time).

EGNOS in aviation

Prior to the implementation of EGNOS in aviation, it is necessary to fulfill a number of requirements and adapt to existing international guidelines required by ICAO (International Civil Aviation Organization). The basic premise of validation of EGNOS is to prove that the system can be used in safety of live applications. This is only possible if the EGNOS signal – SIS (Signal-In-Space) over the area covered by the validation procedure meets the international requirements contained in the ESSC (EGNOS System Safety

Case) (*2014 Federal Radionavigation Plan* 2015, FELSKI et al. 2013). On March 2, 2011 the Safety-of-Life (SoL) Service of EGNOS, devoted mainly to aviation users, was officially announced operational (GSA 2015). The EGNOS SoL service provides timing and positioning information improved from the GPS one, adding integrity data to materialize signal-in-space (SiS) performance compliant with aviation requirements defined in the International Civil Aviation Organization (ICAO) Standard and Recommended Practices (SARPS) for SBAS (ICAO 2006).

Integrity is the measure of the trust that can be placed in the correctness of the information supplied by a navigation system. Integrity includes also the ability of the system to provide timely warnings to users when the system should not be used for the intended operation or phase of flight (*2014 Federal Radionavigation Plan* 2015). The integrity monitoring system assures that, in the absence of an integrity alert, the estimated position is within the volume defined by the HPL (Horizontal Protection Level) and VPL (Vertical Protection Level), which are smaller than HAL (Horizontal Alarm Limit) and VAL (Vertical Alarm Limit) respectively (Fig. 1*a*). When any of the protection levels exceeds the alert limit, the integrity monitoring system should warn the user that an operating parameter of a navigation system is out of tolerance (Fig. 1b). Failure to do so constitutes a hazardous condition, which should not occur more frequently than a strict probability specification.

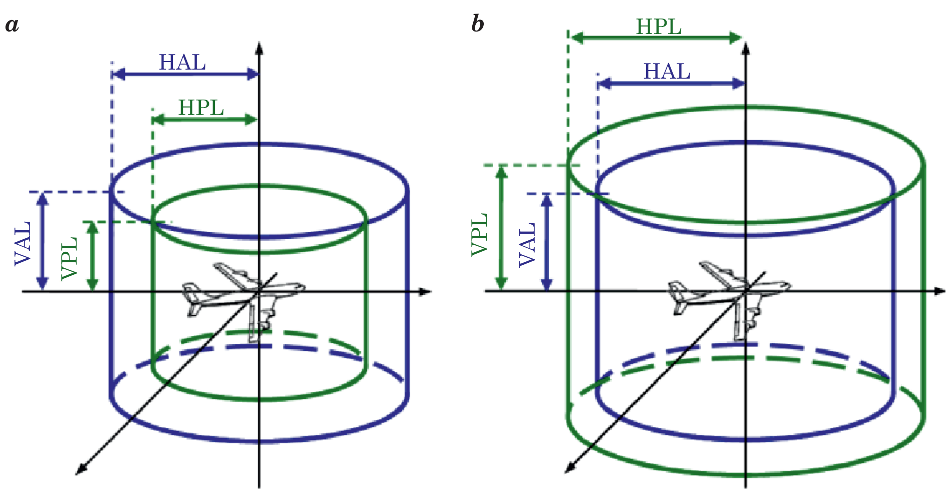

Fig. 1. Relationship between alert and protection levels: *a* – system can be used for the applicable phase of flight, *b* – lost integrity of the navigation system
Source: SALÓS ANDRÉS (2012).

The values of integrity and other fundamental navigation parameters in aviation are highly dependent on the phase of flight. Typical ICAO performance requirements are given in Table 1.

Table 1

Performance requirements for different phases of flight and landing of a civil aircraft

<table>
<tr><th rowspan="3">Aircraft phase of flight</th><th colspan="2">Accuracy</th><th colspan="3">Integrity</th><th colspan="2">Maximum probabilities of failure</th></tr>
<tr><th colspan="2">(2 σ or 95%)</th><th colspan="2">alert limits (4-6σ)</th><th rowspan="2">time to alert</th><th rowspan="2">integrity</th><th rowspan="2">continuity</th></tr>
<tr><th>vertical</th><th>horizontal</th><th>vertical</th><th>horizontal</th></tr>
<tr><td>En-route, Terminal</td><td>N/A</td><td>0.74 – 3.7 km</td><td>N/A</td><td>1.85 – 7.4 km</td><td>5 min – 15 s</td><td>10^{-7}/hr</td><td>10^{-4}/hr</td></tr>
<tr><td>NPA, Initial Approach, Departure</td><td>N/A</td><td>0.22 – 0.74 km</td><td>N/A</td><td>1.85 – 3.7 km</td><td>10–15 s</td><td>10^{-7}/hr</td><td>10^{-4}/hr</td></tr>
<tr><td>LNAV/VNAV</td><td rowspan="3">20 m</td><td>220 m</td><td rowspan="3">50 m</td><td>556 m</td><td rowspan="3">10 s</td><td rowspan="6">1–2 · 10^{-7}/ 150 s</td><td rowspan="6">4–8 · 10^{-6}/ 15 s</td></tr>
<tr><td>LPV</td><td rowspan="5">16 m</td><td rowspan="5">40 m</td></tr>
<tr><td>APV-I</td></tr>
<tr><td>APV-II</td><td>8 m</td><td>20 m</td><td rowspan="3">6 s</td></tr>
<tr><td>LPV 200</td><td rowspan="2">4 m</td><td>35 m</td></tr>
<tr><td>Precision approach CAT I</td><td>10 m</td></tr>
<tr><td>Precision approach CAT II/III</td><td>< 2.9 m</td><td>< 6.9 m</td><td>5.3 m</td><td>< 17 m</td><td>< 2 s</td><td><10^{-9}/ 150 s</td><td><4 · 10^{-6}/ 15 s</td></tr>
</table>

Source: ICAO (2006), Ene (2009).

To use EGNOS in aviation the system validation in certain localization in needed, as well as official flight procedure design and certification. Today over 150 European airports use EGNOS-based flight procedures (LPV) and it is estimated that by 2018 the number will increase to 440. These procedures provide a cost effective alternative equivalent to conventional ILS CAT I instrument landing procedures. LPV procedures offer similar performance without the need for significant on-site infrastructure installation and maintenance. For these reasons, they are becoming a very valuable navigation aid to small and medium-size airports, increasing safety and accessibility to those aerodromes.

EGNOS performance in eastern Poland

As a part of the preliminary research the quality of EGNOS positioning at new location in the Polish Air Force Academy in Dęblin was analyzed, using data recorded on 02–04.04.2016 (CIEĆKO et al. 2016). In the next step the results from Dęblin were compared with calculations made during the same days in Olsztyn. Developed results are characterized by accuracy, integrity, continuity and availability of GPS/EGNOS positioning. The study aims to test the applicability of the system in safety of life applications with the focus to the procedures which are at least compatible with APV-1. The analyzed data were recorded by the permanent GNSS monitoring stations located in eastern Poland (Dęblin and Olsztyn).

The station at the Polish Air Force Academy in Dęblin was installed in January 2016 and is equipped with the latest Javad Delta-3 (S/N: 02345) multi constellation & multi frequency GNSS receiver and multi frequency GNSS antenna – AT 1675 (S/N: 5480), mounted on a mast on the roof of Air Navigation Department – Figure 2.

Fig. 2. Equipment of permanent GNSS monitoring station in Dęblin

Javad Delta-3 GNSS receiver with 864 channels along with three powerful processors and program memory allows for tracking all current and future satellite signals. Delta-3 is a newly introduced (in 2015), powerful and reliable receiver for high-precision navigation systems it can also operate as a receiver for post-processing, as a Continuously Operating Reference Station (CORS) or portable base station for Real-Time Kinematic (RTK) applications, and as a scientific station collecting information for special studies, such as ionosphere monitoring.

Data from Olsztyn were acquired at a permanent EGNOS monitoring station located at the airport Olsztyn-Dajtki EPOD in northeastern Poland. The observations were recorded on the same days 02–04.04.2016 with a Septentrio AsteRx2e_HDC (S/N: 8512000440) receiver connected to a choke-ring NovAtel ANT-C2GA-TW-N (S/N: 224444) antenna mounted on a specially adapted mast – Figure 3. The selected location had been previously tested for the presence of potential interference of the GNSS signal with signals generated by the communications equipment installed at the airport.

Fig. 3. GNSS equipment installed in the building of the Aeroclub of Warmia and Mazury

Recorded data were elaborated using PEGASUS software, which is a set of tools developed in Matlab environment, allowing for detailed analyses of GNSS data collected from a variety of SBAS and GBAS systems, using positioning models defined in the MOPS (Minimum Operational Performance Standards) documents for aviation. This software uses only the algorithms that are consistent with the relevant RTCA guidelines (RTCA 2013). PEGASUS is used as a basic tool in the monitoring of the EDCN network for applications of APV-1 and LPV-200 procedures (Felski et al. 2011, www.eurocontrol 2016). Figure 4 shows the main window of PEGASUS software.

Each of analysed 24-hour sessions is characterized by the same configuration of parameters, compliant with RTCA (RTCA 2013): a minimum topocentric height of satellites at 5 degrees, exclusion from the positioning the ranges to geostationary satellites, data logging interval of 1 second and the use of EGNOS satellite PRN120. The calculation was performed only with the data (valid samples) which were not considered during the registration and processing as invalid. According to the RTCA, the information indicated by the SBAS data analysis software can be described as erroneous because of:

– error log – part of the data has not been registered,
– rejection of the data in the process of filtration,
– due to tuning of the software filters.

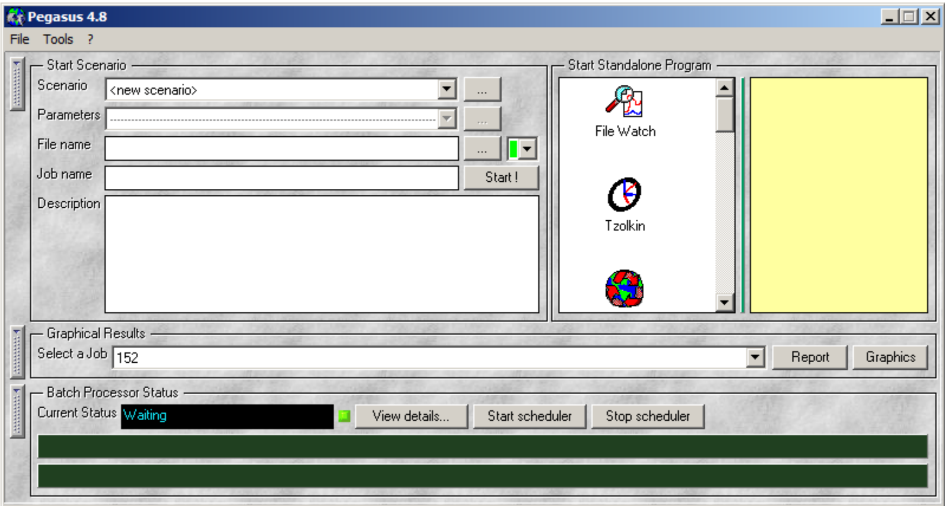

Fig. 4. The main window of PEGASUS software

The GPS/EGNOS positioning accuracy was examined on the basis of the true coordinates of the GNSS station antenna, calculated using data of CORS network belonging to the ASG-EUPOS (part of the European system EUPOS). Figure 5 represents the horizontal deviation from the reference position.

Horizontal positioning error in the three measurement sessions, for both locations shows not large but systematic shift of point clouds to the north. Positioning accuracy in the directions east and west stands at a maximum of about 4 m of the true position in Dęblin and about 2 m in Olsztyn. The maximum northerly error reached approximately 3 m and 2.5 m in Dęblin and Olsztyn respectively, while the south was about 2 m for both locations. From the above analysis, it can be clearly seen that the horizontal positioning accuracy at tested locations meets the requirements for approach APV-1 (HPE<16 m). Almost 100% of analysed epochs (in Olsztyn – 100%) also meet the EGNOS accuracy standard (HPE<3 m) published in GSA 2015. Table 2 contains the numerical values characterizing the accuracy results of the horizontal and vertical error analyses.

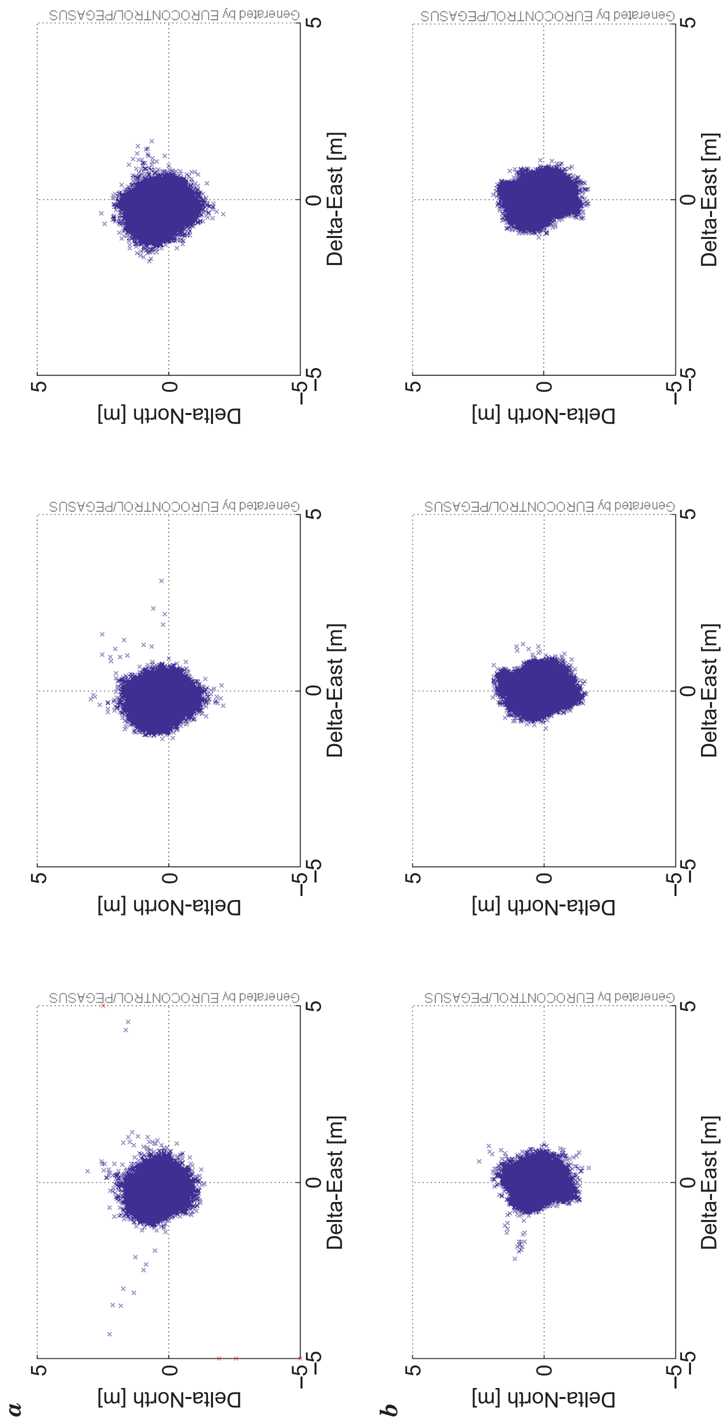

Fig. 5. Horizontal deviation of the GPS/EGNOS positioning for a sessions performed on 02–04.04.2016, *a* – Dęblin, *b* – Olsztyn

Table 2

The accuracy analyses of GPS/EGNOS positioning at Dęblin and Olsztyn airport

Parameter	Day	02.04.2016		03.04.2016		04.04.2016	
		Dęblin	Olsztyn	Dęblin	Olsztyn	Dęblin	Olsztyn
Accuracy	HPE 95% NPA [m]	1.18	0.92	1.12	0.95	1.15	0.98
	HPE 95% APV-1 [m]	1.18	0.92	1.12	0.95	1.15	0.98
	VPE 95% NPA [m]	1.72	1.81	1.89	2.00	1.90	2.06
	VPE 95% APV-1 [m]	1.72	1.81	1.89	2.00	1.90	2.06
	HPE_{max} [m]	23.43	2.52	3.14	2.04	2.57	1.93
	VPE_{max} [m]	48.79	3.25	10.34	4.46	11.46	3.44
	$HPE_{avg.}$ [m]	0.63	0.48	0.56	0.47	0.61	0.50
	$VPE_{avg.}$ [m]	0.73	0.81	0.75	0.87	0.80	0.97
	$HPE_{st.dev.}$ [m]	0.30	0.25	0.30	0.27	0.58	0.27
	$VPE_{st.dev.}$ [m]	0.52	0.54	0.58	0.62	2.34	0.61

In Table 2 the accuracy test results are expressed as HPE 95%, and VPE 95% shown separately for the use in NPA and APV-1. The value of HPE 95% NPA and VPE 95% NPA corresponds to measurement epochs, which satisfy the requirements of the NPA – namely HPL<556 m. HPE 95% APV-1 is to include only the epochs that satisfy HPL<40 m and VPE 95% APV-1 corresponds to epochs for which VPL<50 m – see Table 1. For each of analysed sessions, the positioning accuracy of NPA corresponds to that obtained for an APV-1 approach. The results of horizontal (HPE 95%<1.2 m) and vertical (VPE 95%<2.1 m) accuracy at both airfields meet the requirements for the use of EGNOS in aviation. The interesting fact is that horizontal positioning was slightly better in Olsztyn, while vertical was better in Dęblin.

The integrity of positioning is mainly expressed through the Protection Levels (PL) and their relationship with accuracy (OLIVEIRA et al. 2009, TIBERIUS, ODIJK 2008). Stanford diagrams presented in Figures 6–8 show the results of horizontal and vertical calculation carried out on the basis of three measurement sessions collected on 02–04.04.2016 in Dęblin and Olsztyn.

Test results presented above show that a total of 13 epochs (13 epochs in Dęblin, 0 epochs in Olsztyn) were not available for both the horizontal and vertical approach APV-1 (HPL <40 m, VPL<50 m). The factor SI – safety index (the ratio of XPE/XPL) for the analysed data reaches low values, which indicates proper function of the integrity algorithm at both stations. Generally, the HPL values are at a satisfactory level of less than 30 m and VPL values are less than 40 m.

Table 3 shows the results of the availability analysis based on the same period of observations made on 02–04.04.2016. The analysed values were: the SIS (Signal In Space) availability, NPA operational availability and APV-1 operational availability.

a

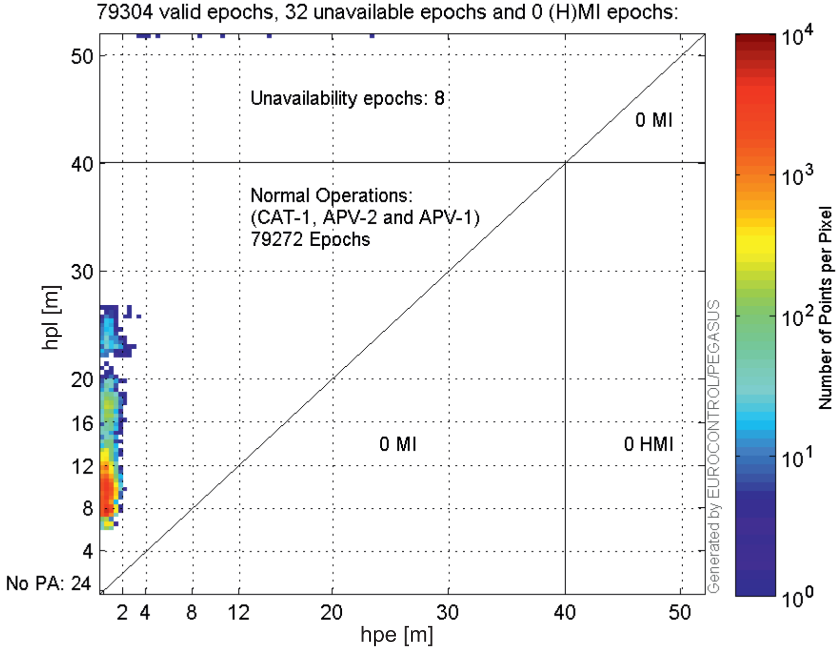

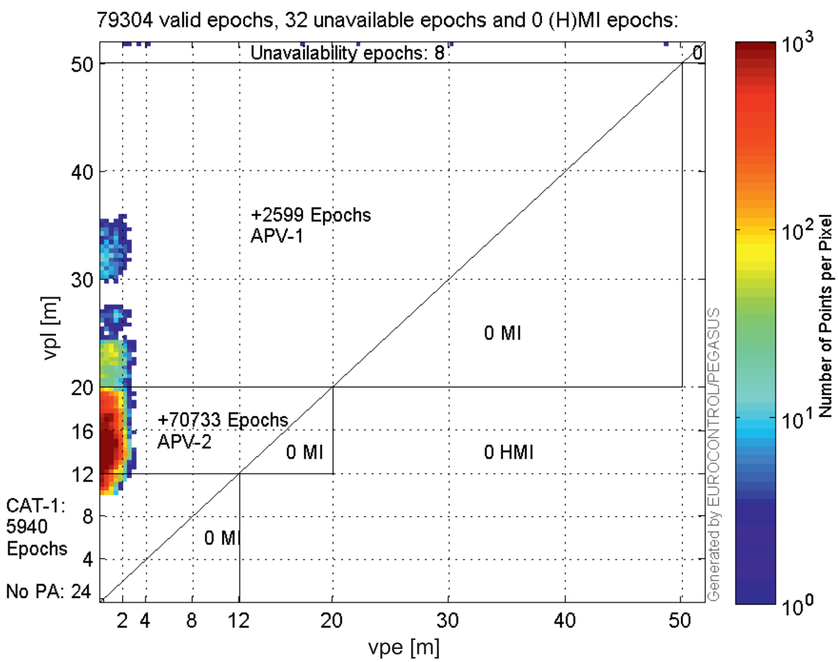

Fig. 6. Stanford diagrams generated for 02.04.2016: *a* – Dęblin, *b* – Olsztyn

b

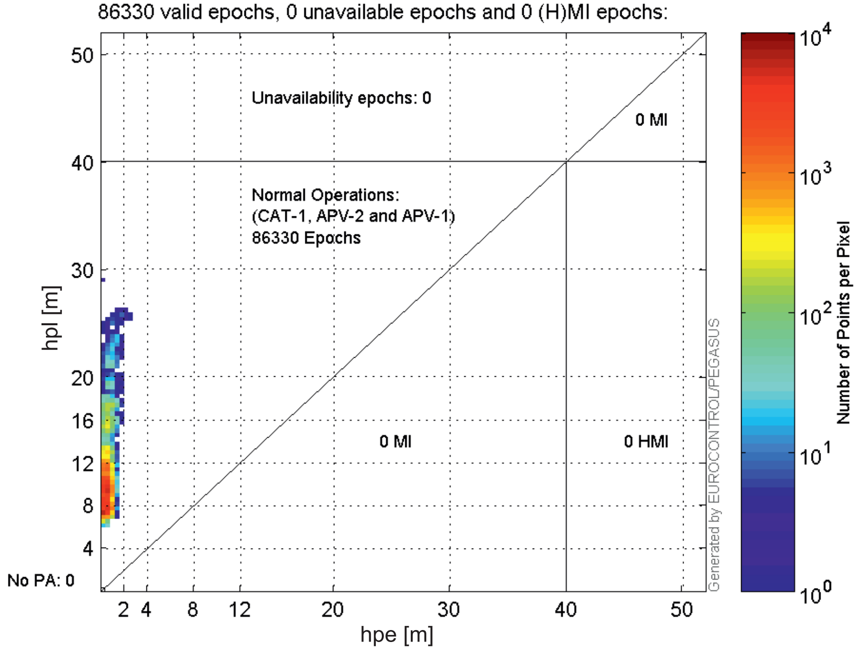
86330 valid epochs, 0 unavailable epochs and 0 (H)MI epochs:
Unavailability epochs: 0
0 MI
Normal Operations:
(CAT-1, APV-2 and APV-1)
86330 Epochs
0 MI
0 HMI
No PA: 0
hpl [m]
hpe [m]
Generated by EUROCONTROL/PEGASUS
Number of Points per Pixel

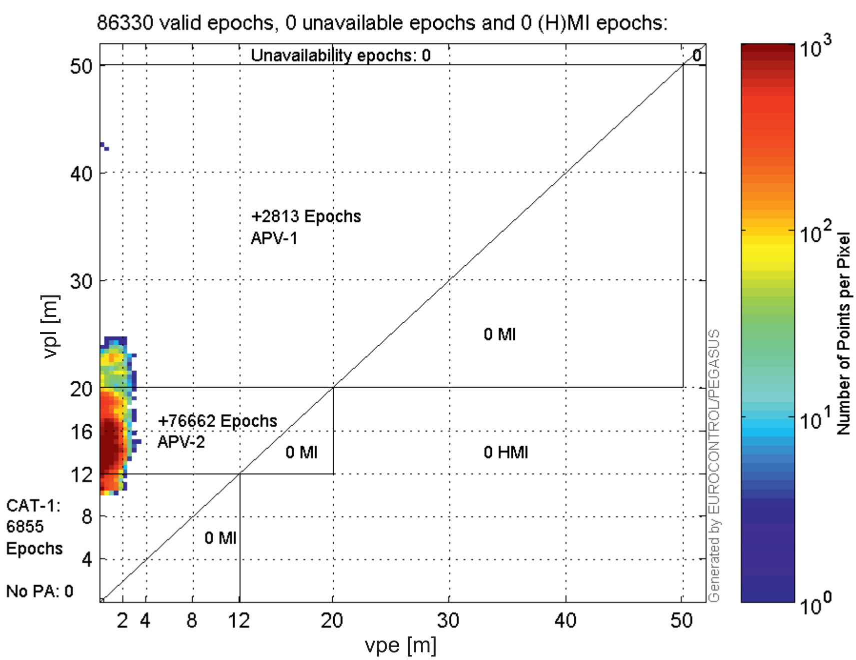
86330 valid epochs, 0 unavailable epochs and 0 (H)MI epochs:
Unavailability epochs: 0
0
+2813 Epochs
APV-1
0 MI
+76662 Epochs
APV-2
0 MI
0 HMI
0 MI
CAT-1:
6855
Epochs
No PA: 0
vpl [m]
vpe [m]
Generated by EUROCONTROL/PEGASUS
Number of Points per Pixel

a

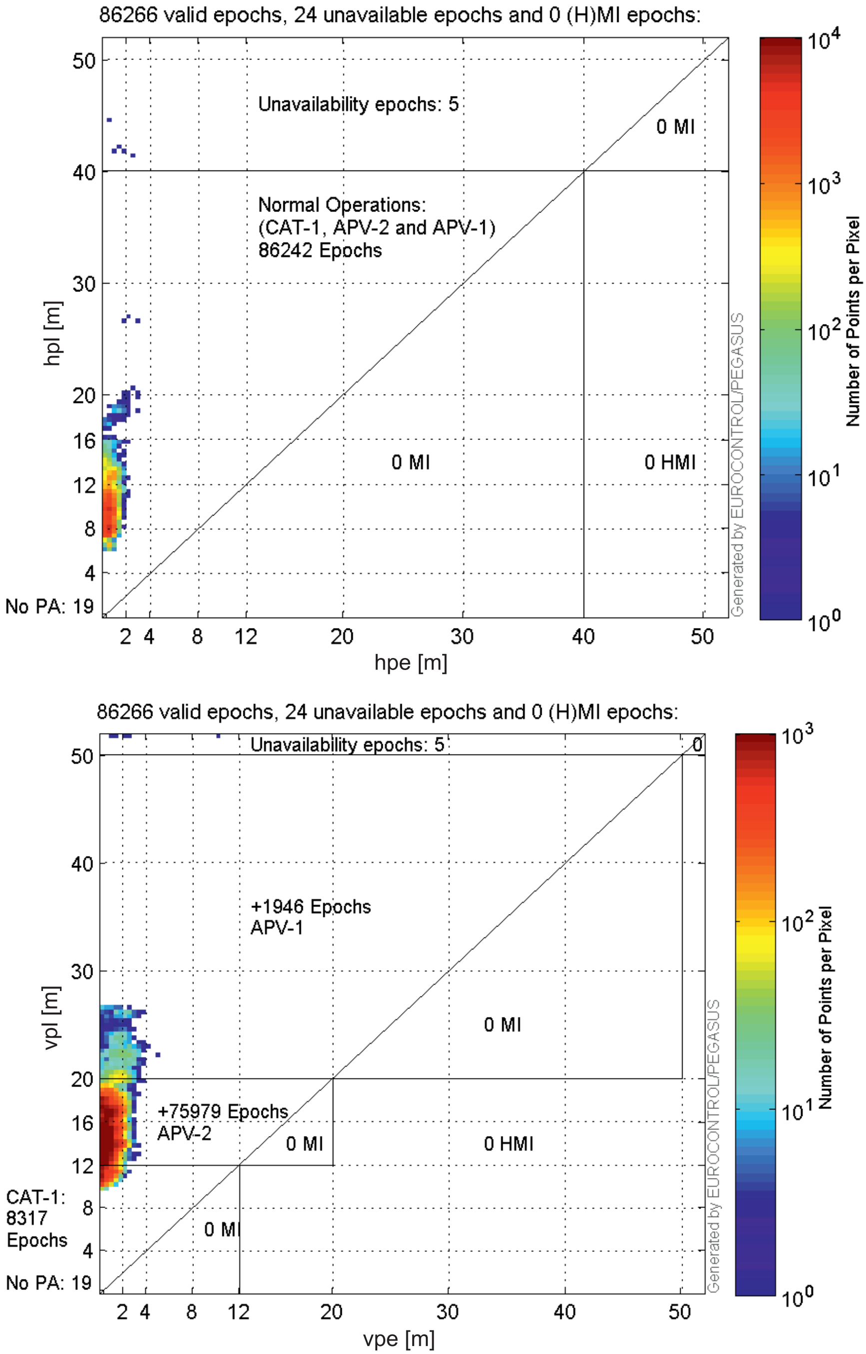

Fig. 7. Stanford diagrams generated for 03.04.2016: *a* – Dęblin, *b* – Olsztyn

b

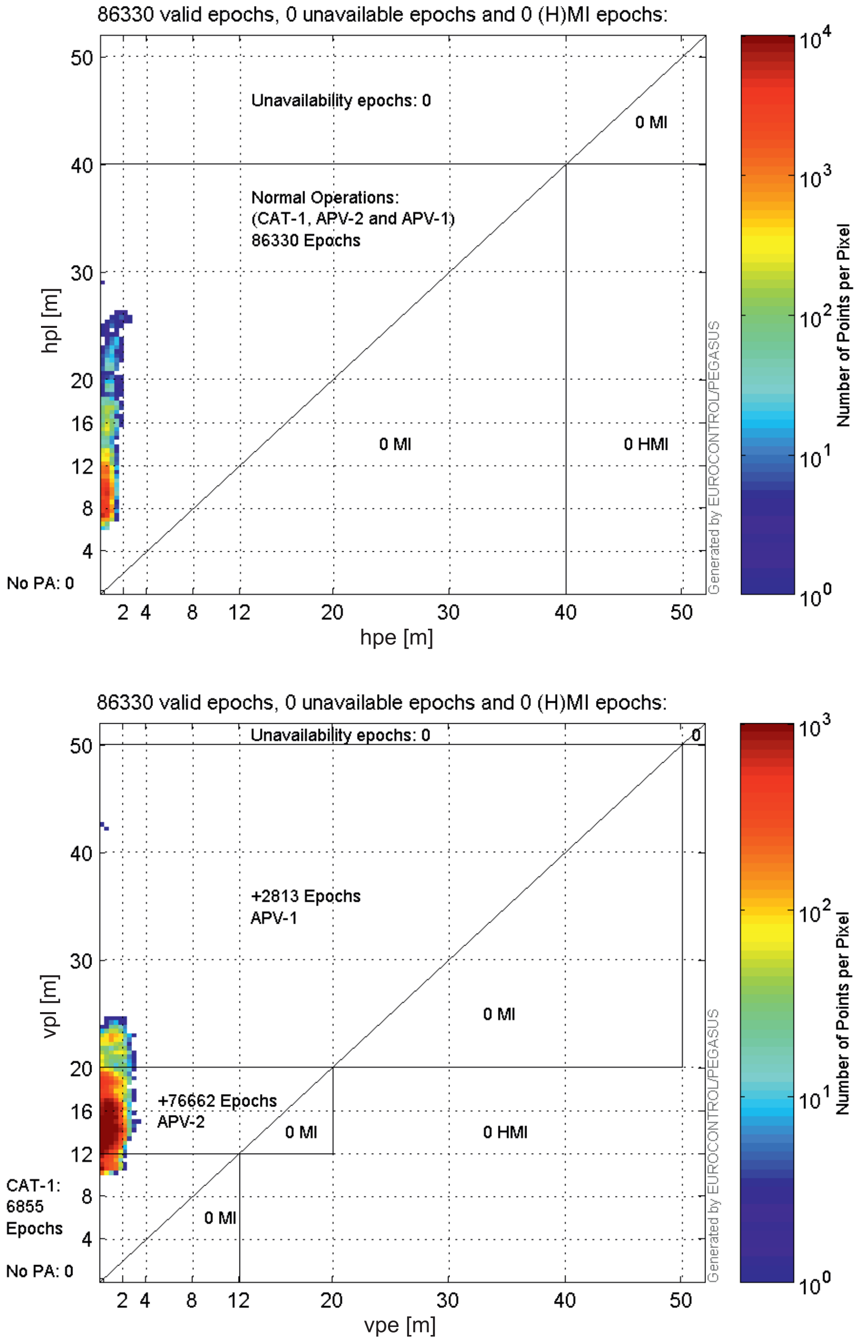
86330 valid epochs, 0 unavailable epochs and 0 (H)MI epochs:
Unavailability epochs: 0
0 MI
Normal Operations:
(CAT-1, APV-2 and APV-1)
86330 Epochs
0 MI
0 HMI
No PA: 0
hpl [m]
hpe [m]
Generated by EUROCONTROL/PEGASUS
Number of Points per Pixel
86330 valid epochs, 0 unavailable epochs and 0 (H)MI epochs:
Unavailability epochs: 0
0
+2813 Epochs
APV-1
0 MI
+76662 Epochs
APV-2
0 MI
0 HMI
0 MI
CAT-1:
6855
Epochs
No PA: 0
vpl [m]
vpe [m]
Generated by EUROCONTROL/PEGASUS
Number of Points per Pixel

a

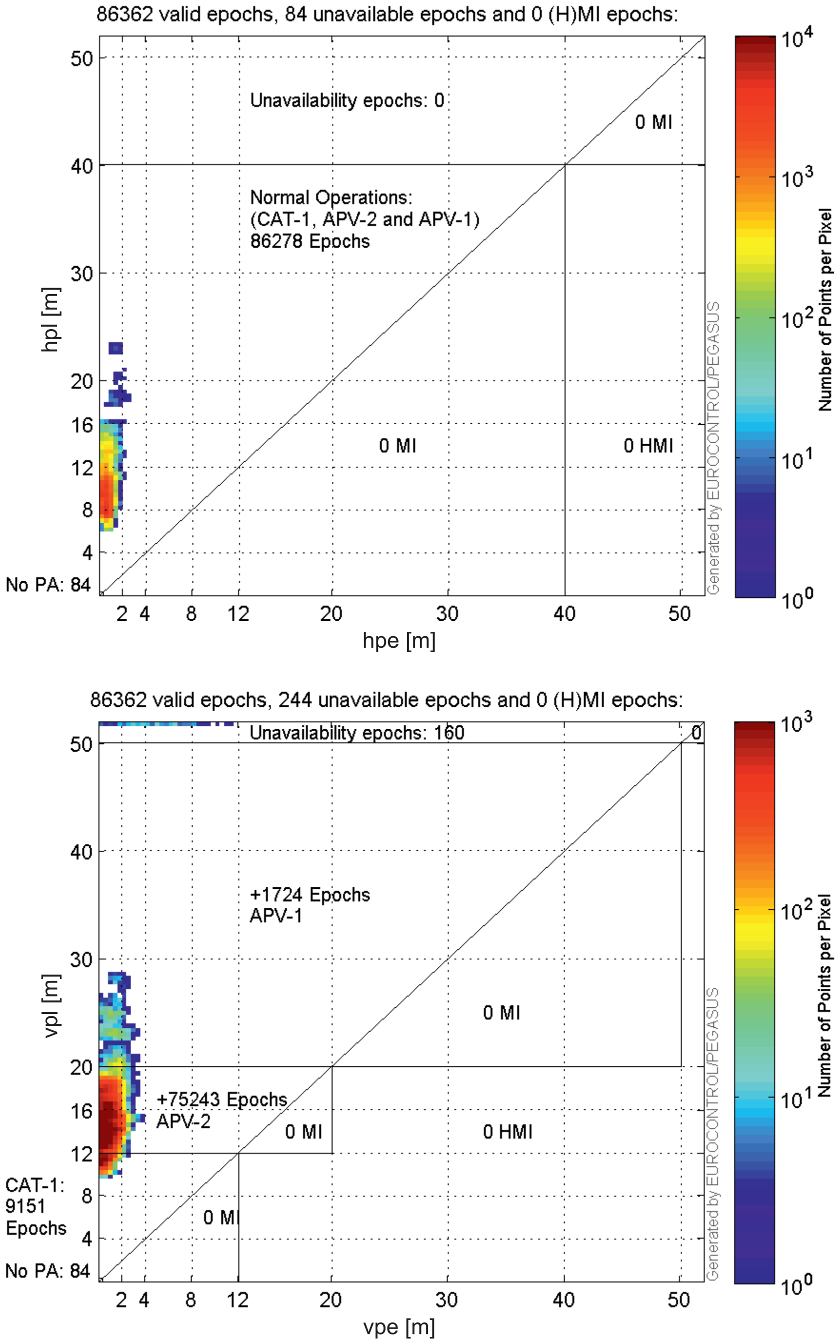

Fig. 8. Stanford diagrams generated for 04.04.2016: *a* – Dęblin, *b* – Olsztyn

b

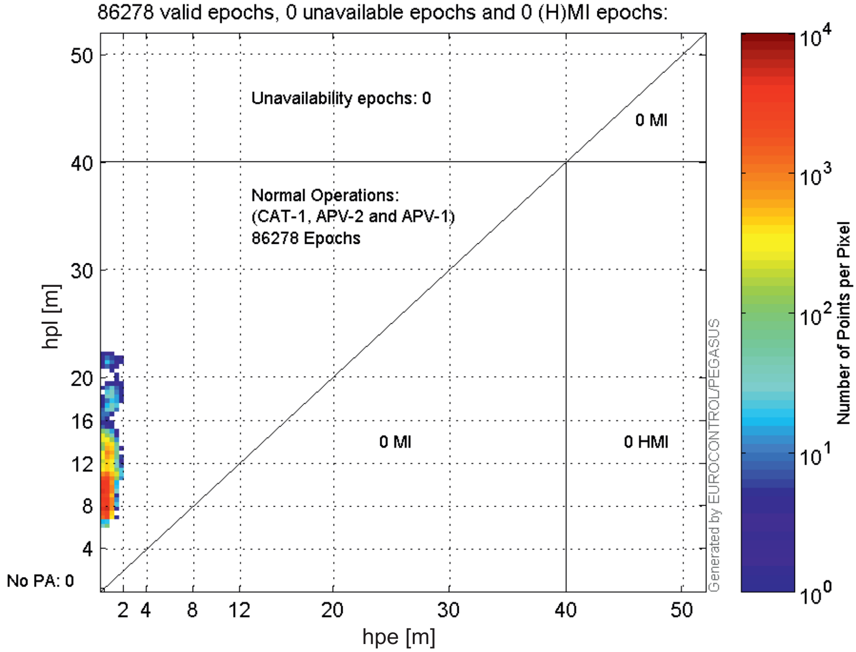

86278 valid epochs, 0 unavailable epochs and 0 (H)MI epochs:
Unavailability epochs: 0
0 MI
Normal Operations:
(CAT-1, APV-2 and APV-1)
86278 Epochs
0 MI
0 HMI
No PA: 0
hpl [m]
hpe [m]
Generated by EUROCONTROL/PEGASUS
Number of Points per Pixel

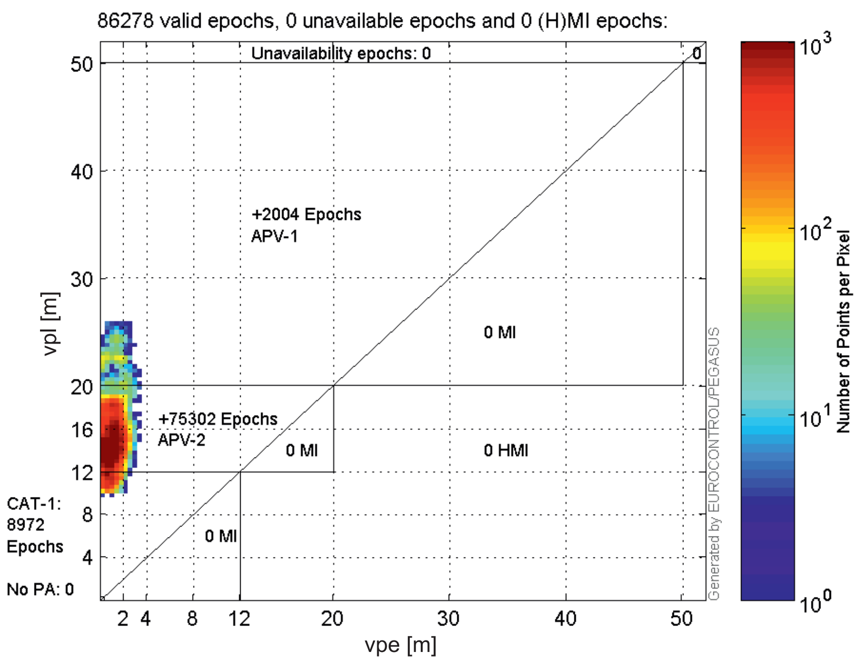

86278 valid epochs, 0 unavailable epochs and 0 (H)MI epochs:
Unavailability epochs: 0
0
+2004 Epochs
APV-1
0 MI
+75302 Epochs
APV-2
0 MI
0 HMI
0 MI
CAT-1:
8972
Epochs
No PA: 0
vpl [m]
vpe [m]
Generated by EUROCONTROL/PEGASUS
Number of Points per Pixel

Table 3

The availability analysis results obtained on 02–04.04.2016

Parameter	Day	02.04.2016		03.04.2016		04.04.2016	
		Dęblin	Olsztyn	Dęblin	Olsztyn	Dęblin	Olsztyn
Availability	signal availability	1	1	1	1	1	1
	NPA operational availability	0.999697	0.999813	0.999780	0.999889	0.998588	0.998611
	APV-1 operational availability	0.999697	0.999813	0.999720	0.999876	0.996736	0.998611

The availability of EGNOS signal throughout the test period is very close to 100%. Operational availability of EGNOS NPA and APV-1 reaches the value of around 0.999 in both examined locations, which meets the official requirements of the application in the APV-1 approach (the result of better than 99%).

In performed studies continuity parameter was also examined. All discontinuity events for NPA and APV-1 were analysed. In the case of NPA variant for the calculation all measurement epochs with a NPA solution (HPL<556 m) were taken into consideration. APV-1 variant includes all the epochs for which HPL<40 m and VPL<50 m. Table 4 presents the results of analysis of the continuity of the EGNOS system in the considered period.

Table 4

The results of the continuity analysis on 02–04.04.2016

Parameter	Day	02.04.2016		03.04.2016		04.04.2016	
		Dęblin	Olsztyn	Dęblin	Olsztyn	Dęblin	Olsztyn
Continuity	All NPA discontinuity events	–	–	–	–	–	–
	All APV–1 discontinuity events	–	–	–	–	1	–
	Long NPA discontinuity events	–	–	–	–	–	–
	Long APV–1 discontinuity events	–	–	–	–	1	–

The only event of loss of continuity was observed in Dęblin in the third measurement session (04.04.2016). It concerns the use of EGNOS in the APV-1 approach only. With these results, it is advisable to perform experiments based on data from longer periods, or to perform permanent monitoring of continuity of the EGNOS system at certain location.

Conclusion

The results of performed analyses and comparisons are preliminary ones and indicate initial quality assessment of GPS/EGNOS positioning in the airfields located at Polish Air Force Academy in Dęblin and Aeroclub in Olsztyn. These analyses were possible due to the newly established GNSS/EGNOS monitoring stations equipped with proper GNSS receivers. The quality of basic positioning parameters such as: accuracy, integrity, continuity and availability was analysed in detail. Achieved, preliminary results indicate good trends of EGNOS development for the use in air navigation in eastern Europe. In the analysed period, just a few events exceeding the limit values of quality were observed, but the overall results are at a satisfactory level. Attained, good values of positioning parameters prove that the EGNOS system upgrades that were made in recent years translate into the possibility of obtaining good accuracy, integrity, availability and continuity also in the eastern Poland. However, the research carried out on the basis of just 3 days of observation in 2 locations, do not constitute a final assessment of the GPS/EGNOS quality in eastern Poland. According to the authors, there should be continuous monitoring of the EGNOS performance in the area of the eastern Poland, prior to practical implementation of procedures in accordance with APV-1 in that region.

References

2014 Federal Radionavigation Plan. 2015. Department of Defense, Department of Homeland Security, and Department of Transportation. Springfield, Virginia.

ALLIEN A., TAILLANDER C., CAPO C. 2009. *User Guide For EGNOS Application Development*. European Space Agency, Paris.

BAKUŁA M., PRZESTRZELSKI P., KAŹMIERCZAK R. 2015. *Reliable technology of centimeter GPS/GLONASS surveying in forest environments*. Geoscience and Remote Sensing, 53(2): 1029–1038.

CIEĆKO A., GRUNWALD G., ĆWIKLAK J., POPIELARCZYK D., TEMPLIN T. 2016. *EGNOS performance monitoring at newly established GNSS station in Polish Air Force Academy.* SGEM2016 Conference Proceedings, 2(2): 239–246, doi: 10.5593/SGEM2016/B22/S09.031.

ENE A. 2009. *Utilization of Modernized Global Navigation Satellite Systems for Aircraft-Based Navigation Integrity*. PhD Thesis, Department of Aeronautics, Stanford University.

EUROCONTROL – Driving excellence in ATM performance. www.eurocontrol.int/articles/pegasus (access: 2.05.2016).

FELSKI A., NOWAK A. 2013. *On EGNOS Monitoring in Local Conditions.* Artificial Satellites, 48(2): 85–92.

FELSKI A., NOWAK A., WOŹNIAK T. 2011. *Accuracy and Availability of EGNOS – Results of Observations.* Artificial Satellites, 46: 111–118.

GRUNWALD G., BAKUŁA M., CIEĆKO A., KAŹMIERCZAK R. 2016. *Examination of GPS/EGNOS integrity in north-eastern Poland.* IET Radar, Sonar & Navigation. The Institution of Engineering and Technology, 10(1): 114–121, doi: 10.1049/iet-rsn.2015.0053.

GRZEGORZEWSKI M., CIEĆKO A., OSZCZAK S., POPIELARCZYK D. 2008. *Autonomous and EGNOS Positioning Accuracy Determination of Cessna Aircraft on the Edge of EGNOS Coverage.* Proceedings of the 2008 National Technical Meeting of the Institute of Navigation – NTM, p. 407–410.

International Standards and Recommended Practices (SARPS). 2006. Annex 10 to the Convention on International Civil Aviation, Aeronautical Telecommunications, Vol. I, Radio Navigation Aids', 6th Edition, International Civil Aviation Organization (ICAO).

LI X., GE M., DAI X., REN X., FRITSCHE M., WICKERT J., SCHUH H. 2015a. *Accuracy and reliability of multi-GNSS real-time precise positioning: GPS, GLONASS, BeiDou, and Galileo*. J. Geod., 89: 607–635, doi: 10.1007/s00190-015-0802-8.

LI X., ZHANG X., REN X., FRITSCHE M., WICKERT J., SCHUH H. 2015b. *Precise positioning with current multi-constellation Global Navigation Satellite Systems: GPS, GLONASS, Galileo and BeiDou*. Scientific Reports, 5(8328): 1–14, doi: 10.1038/srep08328.

Minimum Operational Performance Standards for Airborne Equipment Using Global Positioning System/Wide Area Augmentation System. 2013. Radio Technical Committee for Aeronautics. Doc. DO-229D.

OLIVEIRA J., TIBERIUS C. 2009. *Quality Control in SBAS: Protection Levels and Reliability Levels.* The Journal of Navigation, 62: 509–522.

Safety of Life Service Definition Document. v. 3.0. 2015. GSA – European Global Navigation Satellite Systems Agency.

SALÓS ANDRÉS C.D. 2012. *Integrity monitoring applied to the reception of GNSS signals in urban environments*. PhD Thesis, Toulouse University.

TIBERIUS C., ODIJK D. 2008. *Does the HPL bound the HPE?* NAVITEC. Proceedings of NaviTec'08 workshop, ESA-Estec, Noordwijk.

Guide for Autors

Introduction

Technical Sciences is a peer-reviewed research Journal published in English by the Publishing House of the University of Warmia and Mazury in Olsztyn (Poland). Journal is published continually since 1998. Until 2010 Journal was published as a yearbook, in 2011 and 2012 it was published semiyearly. From 2013, the Journal is published quarterly in the spring, summer, fall, and winter.

The Journal covers basic and applied researches in the field of engineering and the physical sciences that represent advances in understanding or modeling of the performance of technical and/or biological systems. The Journal covers most branches of engineering science including biosystems engineering, civil engineering, environmental engineering, food engineering, geodesy and cartography, information technology, mechanical engineering, materials science, production engineering etc.

Papers may report the results of experiments, theoretical analyses, design of machines and mechanization systems, processes or processing methods, new materials, new measurements methods or new ideas in information technology.

The submitted manuscripts should have clear science content in methodology, results and discussion. Appropriate scientific and statistically sound experimental designs must be included in methodology and statistics must be employed in analyzing data to discuss the impact of test variables. Moreover there should be clear evidence provided on how the given results advance the area of engineering science. Mere confirmation of existing published data is not acceptable. Manuscripts should present results of completed works.

There are three types of papers: a) research papers (full length articles); b) short communications; c) review papers.

The Journal is published in the printed and electronic version. The electronic version is published on the website ahead of printed version of Technical Sciences.

Technical Sciences does not charge submission or page fees.

Types of paper

The following articles are accepted for publication:

Reviews

Reviews should present a focused aspect on a topic of current interest in the area of biosystems engineering, civil engineering, environmental engineering, food engineering, geodesy and cartography, information technology, mechanical engineering, materials science, production engineering etc. They should include all major findings and bring together reports from a number of sources. These critical reviews should draw out comparisons and conflicts between work, and provide an overview of the 'state of the art'. They should give objective assessments of the topic by citing relevant published work, and not merely present the opinions of individual authors or summarize only work carried out by the authors or by those with whom the authors agree. Undue speculations should also be avoided. Reviews generally should not exceed 6,000 words.

Research Papers

Research Papers are reports of complete, scientifically sound, original research which contributes new knowledge to its field. Papers should not exceed 5,000 words, including figures and tables.

Short Communications

Short Communications are research papers constituting a concise description of a limited investigation. They should be completely documented, both by reference list, and description of the experimental procedures. Short Communications should not occupy more than 2,000 words, including figures and tables.

Letters to the Editor

Letters to the Editor should concern with issues raised by articles recently published in scientific journals or by recent developments in the engineering area.

Contact details for submission

The paper should be sent to the Editorial Office, as a Microsoft Word file, by e-mail: techsci@uwm.edu.pl

Referees

Author/authors should suggest, the names, addresses and e-mail addresses of at least three potential referees. The editor retains the sole right to decide whether or not the suggested reviewers are used.

Submission declaration

After final acceptance of the manuscript, the corresponding author should send to the Editorial Office the author's declaration. Submission of an article implies that the work has not been published previously (except in the form of an abstract or as part of a published lecture or academic thesis or as an electronic preprint), that it is not under consideration for publication elsewhere, that publication is approved by all authors and tacitly or explicitly by the responsible authorities where the work was carried out, and that, if accepted, it will not be published elsewhere in the same form, in English or in any other language.

To prevent cases of ghostwriting and guest authorship, the author/authors of manuscripts is/are obliged to: (i) disclose the input of each author to the text (specifying their affiliations and contributions, i.e. who is the author of the concept, assumptions, methods, protocol, etc. used during the preparation of the text); (ii) disclose information about the funding sources for the article, the contribution of research institutions, associations and other entities.

Language

Authors should prepare the full manuscript i.e. title, abstract and the main text in English (American or British usage is accepted). Polish version of the manuscript is not required.

The file type

Text should be prepared in a word processor and saved in doc or docx file (MS Office).

Article structure

Suggested structure of the manuscript is as follows:

Title
Authors and affiliations
Corresponding author
Abstract
Keywords
Introduction
Material and Methods
Results and Discussion
Conclusions

Acknowledgements (*optional*)
References
Tables
Figures

Subdivision – numbered sections

Text should be organized into clearly defined and numbered sections and subsections (optionally). Sections and subsections should be numbered as 1. 2. 3. then 1.1 1.2 1.3 (then 1.1.1, 1.1.2, ...). The abstract should not be included in numbering section. A brief heading may be given to any subsection. Each heading should appear on its own separate line. A single line should separate paragraphs. Indentation should be used in each paragraph.

Font guidelines are as follows:
– Title: 14 pt. Times New Roman, bold, centered, with caps
– Author names and affiliations:12 pt. Times New Roman, bold, centered, italic, two blank line above
– Abstract: 10 pt. Times New Roman, full justified, one and a half space. Abstract should begin with the word Abstract immediately following the title block with one blank line in between. The word Abstract: 10 pt. Times New Roman, centered, indentation should be used
– Section Headings: Not numbered, 12 pt. Times New Roman, bold, centered; one blank line above
– Section Sub-headings: Numbered, 12 pt. Times New Roman, bold, italic, centered; one blank line above
– Regular text: 12 pt. Times New Roman, one and a half space,full justified, indentation should be used in each paragraph

Title page information

The following information should be placed at the first page:

Title

Concise and informative. If possible, authors should not use abbreviations and formulae.

Authors and affiliations

Author/authors' names should be presented below the title. The authors' affiliation addresses (department or college; university or company; city, state and zip code, country) should be placed below the names. Authors with the same affiliation must be grouped together on the same line with affiliation information following in a single block. Authors should indicate all affiliations with a lower-case superscript letter immediately after the author's name and in front of the appropriate address.

Corresponding author

It should be clearly indicated who will handle correspondence at all stages of refereeing and publication, also post-publication process. The e-mail address should be provided (footer, first page). Contact details must be kept up to date by the corresponding author.

Abstract

The abstract should have up to 100-150 words in length. A concise abstract is required. The abstract should state briefly the aim of the research, the principal results and major conclusions. Abstract must be able to stand alone. Only abbreviations firmly established in the field may be eligible. Non-standard or uncommon abbreviations should be avoided, but if essential they must be defined at their first mention in the abstract itself.

Keywords

Immediately after the abstract, author/authors should provide a maximum of 6 keywords avoiding general, plural terms and multiple concepts (avoid, for example, 'and', 'of'). Author/authors should be sparing with abbreviations: only abbreviations firmly established in the field may be eligible.

Abbreviations

Author/authors should define abbreviations that are not standard in this field. Abbreviations must be defined at their first mention there. Author/authors should ensure consistency of abbreviations throughout the article.

Units

All units used in the paper should be consistent with the SI system of measurement. If other units are mentioned, author/authors should give their equivalent in SI.

Introduction

Literature sources should be appropriately selected and cited. A literature review should discuss published information in a particular subject area. Introduction should identify, describe and analyze related research that has already been done and summarize the state of art in the topic area. Author/authors should state clearly the objectives of the work and provide an adequate background.

Material and Methods

Author/authors should provide sufficient details to allow the work to be reproduced by other researchers. Methods already published should be indicated by a reference. A theory should extend, not repeat, the background to the article already dealt within the Introduction and lay the foundation for further work. Calculations should represent a practical development from a theoretical basis.

Results and Discussion

Results should be clear and concise. Discussion should explore the significance of the results of the work, not repeat them. A combined Results and Discussion section is often appropriate.

Conclusions

The main conclusions of the study may be presented in a Conclusions section, which may stand alone or form a subsection of a Results and Discussion section.

Acknowledgements

Author/authors should include acknowledgements in a separate section at the end of the manuscript before the references. Author/authors should not include them on the title page, as a footnote to the title or otherwise. Individuals who provided help during the research study should be listed in this section.

Artwork
General points

– Make sure you use uniform lettering and sizing of your original artwork
– Embed the used fonts if the application provides that option

– Aim to use the following fonts in your illustrations: Arial, Courier, Times New Roman, Symbol
– Number equations, tables and figures according to their sequence in the text
– Size the illustrations close to the desired dimensions of the printed version

Formats

If your electronic artwork is created in a Microsoft Office application (Word, PowerPoint, Excel) then please supply 'as is' in the native document format

Regardless of the application used other than Microsoft Office, when your electronic artwork is finalized, please 'Save as' or convert the images to one of the following formats (note the resolution requirements given below):

EPS (or PDF): Vector drawings, embed all used fonts

JPEG: Color or grayscale photographs (halftones), keep to a minimum of 300 dpi

JPEG: Bitmapped (pure black & white pixels) line drawings, keep to a minimum of 1000 dpi or combinations bitmapped line/half-tone (color or grayscale), keep to a minimum of 500 dpi

Please **do not**:
– Supply files that are optimized for screen use (e.g., GIF, BMP, PICT, WPG); these typically have a low number of pixels and limited set of colors
– Supply files that are too low in resolution
– Submit graphics that are disproportionately large for the content

Color artwork

Author/authors should make sure that artwork files are in an acceptable format (JPEG, EPS PDF, or MS Office files) and with the correct resolution. If, together with manuscript, author/authors submit color figures then Technical Sciences will ensure that these figures will appear in color on the web as well as in the printed version at no additional charge.

Tables, figures, and equations

Tables, figures, and equations/formulae should be identified and numbered consecutively in accordance with their appearance in the text.

Equations/mathematical and physical formulae should be presented in the main text, while tables and figures should be presented at the end of file (after References section). Mathematical and physical formulae should be presented in the MS Word formula editor.

All types of figures can be black/white or color. Author/authors should ensure that each figure is numbered and has a caption. A caption should be placed below the figure. Figure must be able to stand alone (explanation of all symbols and abbreviations used in figure is required). Units must be always included. It is noted that figure and table numbering should be independent.

Tables should be numbered consecutively in accordance with their appearance in the text. Table caption should be placed above the table. Footnotes to tables should be placed below the table body and indicated with superscript lowercase letters. Vertical rules should be avoided. Author/authors should ensure that the data presented in tables do not duplicate results described in figures, diagrams, schemes, etc. Table must be able to stand alone (explanation of all symbols and abbreviations used in table is required). Units must be always included. As above, figure and table numbering should be independent.

References

References: All publications cited in the text should be presented in a list of references following the text of the manuscript. The manuscript should be carefully checked to ensure that the spelling of authors' names and dates of publications are exactly the same in the text as in the reference list. Authors should ensure that each reference cited in the text is also present in the reference list (and vice versa).

Citations may be made directly (or parenthetically). All citations in the text should refer to:

1. Single author

The author's name (without initials, with caps, unless there is ambiguity) and the year of publication should appear in the text

2. Two authors

Both authors' names (without initials, with caps) and the year of publication should appear in the text

3. Three or more authors

First author's name followed by et al. and the year of publication should appear in the text

Groups of references should be listed first alphabetically, then chronologically.

Examples:

"... have been reported recently (ALLAN, 1996a, 1996b, 1999; ALLAN and JONES, 1995). KRAMER et al. (2000) have recently shown..."

The list of references should be arranged alphabetically by authors' names, then further sorted chronologically if necessary. More than once reference from the same author(s) in the same year must be identified by the letters "a", "b", "c" etc., placed after the year of publication.

References should be given in the following form:

KUMBHAR B.K., AGARVAL R.S., DAS K. 1981. *Thermal properties of fresh and frozen fish*. International Journal of Refrigeration, 4(3), 143–146.

MACHADO M.F., OLIVEIRA F.A.R., GEKAS V. 1997. *Modelling water uptake and soluble solids losses by puffed breakfast cereal immersed in water or milk*. In Proceedings of the Seventh International Congress on Engineering and Food, Brighton, UK.

NETER J., KUTNER M.H., NACHTSCHEIM C.J., WASSERMAN W. 1966. *Applied linear statistical models* (4th ed., pp. 1289–1293). Irwin, Chicago.

THOMSON F.M. 1984. *Storage of particulate solids*. In M. E. Fayed, L. Otten (Eds.), Handbook of Powder Science and Technology (pp. 365–463). Van Nostrand Reinhold, New York.

Citation of a reference as 'in press' implies that the item has been accepted for publication.

Note that the full names of Journals should appear in reference list.

Submission checklist

The following list will be useful during the final checking of an article prior to the submission. Before sending the manuscript to the Journal for review, author/authors should ensure that the following items are present:

– Text is prepared with a word processor and saved in DOC or DOCX file (MS Office). One author has been designated as the corresponding author with contact details: e-mail address

– Manuscript has been 'spell-checked' and 'grammar-checked'

– References are in the correct format for this Journal

– All references mentioned in the Reference list are cited in the text, and vice versa

– Author/authors does/do not supply files that are too low in resolution

– Author/authors does/do not submit graphics that are disproportionately large for the content.